Study on conservation of archaeological - waterlogged wood in Vietnam

Thanh Duc Nguyen

2018

Contents

List of Abbreviations

ASE	Anti-shrink/swell efficiency
D	Diffusion coefficient
HSQC	Heteronuclear single quantum coherence
ML	Middle lamella
NMR	Nuclear magnetic resonance spectroscopy
PAANa	Sodium polyacrylate
PEG	Polyethylene glycol
ρ	Basic density
SEM	Scanning electron microscopy
TAPPI	Technical Association of the Pulp and Paper Industry
TEM	Transmission electron microscopy
U_{max}	Maximum moisture content
WW	Waterlogged wood

Chapter 1. General introduction

1.1. Conservation of archaeological waterlogged wood

1.1.1. Characteristic of archaeological waterlogged wood

Wood is organic material and it will normally be decomposed organism and eventually disappear (Kohdzuma, 2004). Archaeological waterlogged wood (WW) are generally survived over the centuries because it was buried in a special environment where the deterioration process was limited (Kohdzuma, 2004; Pearson, 1987; Rowell and Barbour, 1990; Unger et al., 2001). Wooden objects remaining from historical sites provides interesting image of the skills and creativity of past generations (Nilsson and Rowell, 2012). Moreover, the changes in wood structure reflects the environmental changes in the passage of time (Blanchette, 2000; Nilsson and Rowell, 2012). There are a several types of natural environment where archaeological WW can be discovered: sea, wet ground, pits, ditches, clay soils, ice, peat bogs, lake bottom, river bottom (Kohdzuma, 2004; Morgós et al., 2015; Pearson, 1987; Rowell and Barbour, 1990; Unger et al., 2001).

Trees are classified into three categories: monocotyledons, hardwoods (angiosperms), and softwoods (gymnosperms). Most archaeological relics are made of hardwoods or softwoods, though monocotyledons such as palm and bamboo were used in the tropics (Rodgers, 2004). The wood consists of cells arranged longitudinally except for the ray cells (Fig. 1.1c). Wood cells are mainly made of complex carbohydrate molecules of cellulose, hemicellulose and lignin. In addition to those three main components, several percent of ash and extractives are included (Koshijima and Watanabe, 2003; R. Thompson, 2005; Sjostrom and Alen, 1999). Wood cells

contain a primary cell wall and the secondary cell wall. The secondary cell wall is structured in three distinct layers S_1, S_2, and S_3 (Fig. 1.1a). The secondary wall is responsible for most of wood's strength (Goodell et al., 2003; Koshijima and Watanabe, 2003).

a: Cell Wall Anatomy with Fiber Orientation
- 1 Warty Layer
- 2 S3
- 3 S2
- 4 S1
- 5 Primary Wall

b: Wood Cell Orientation

c: Gross Anatomy
- 1 Ray
- 2 Outer Bark
- 3 Annual Ring
- 4 Phloem & Cambium
- 5 Heartwood (xylem)
- 6 Sapwood (xylem)
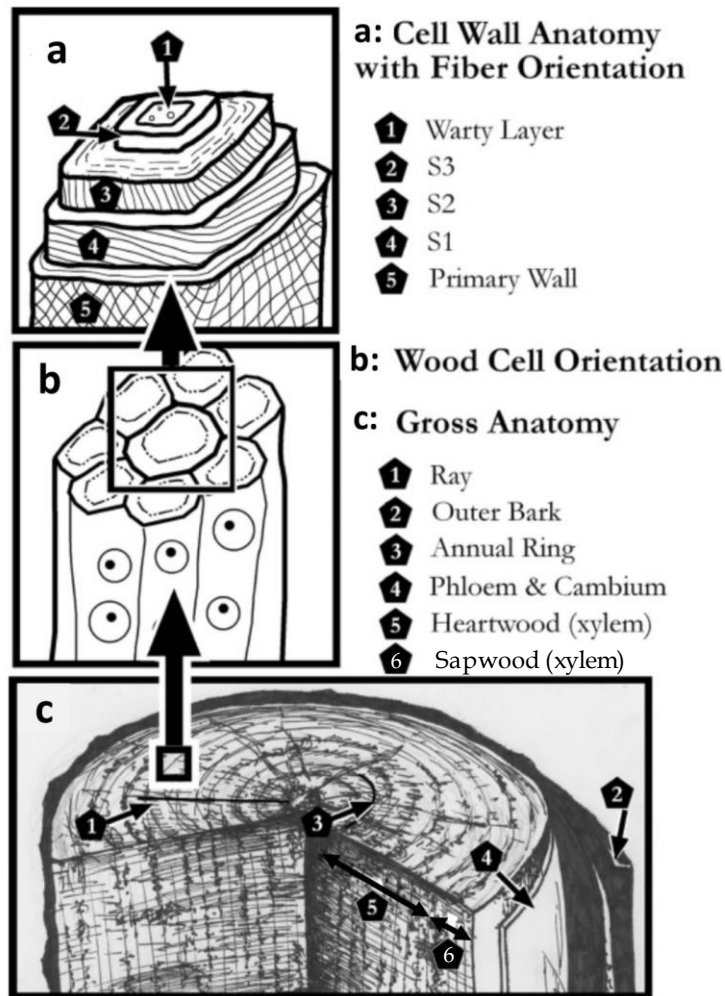
Fig. 1.1 Structure of wood. Micro-fiber directions in the secondary cell wall (S_1, S_2, S_3) are responsible for the overall drying behavior (modified from Rodgers, 2004).

In aquatic environments, anaerobic bacteria are primarily responsible for the depletion of wood carbohydrates, leaving a porous and unstable residual structure mainly consisting of lignin (Blanchette, 2000; Rowell and Barbour, 1990). Previous studies shown that the decomposition in WW generally starts with the hemicelluloses,

followed by cellulose (Pearson, 1987; Rowell and Barbour, 1990; Smith, 2003; Unger et al., 2001) (Fig. 1.2). Lignin is the most resistant and therefore the amount of lignin in wood increases during decomposition (Pearson, 1987; Rowell and Barbour, 1990; Unger et al., 2001). However, if wood constituent is expressed on the basis of volume percentage, the lignin content remains relatively constant with rising decomposition of hemicellulose and cellulose as indicated by growing of maximum moisture content values (Hoffmann, 1986).
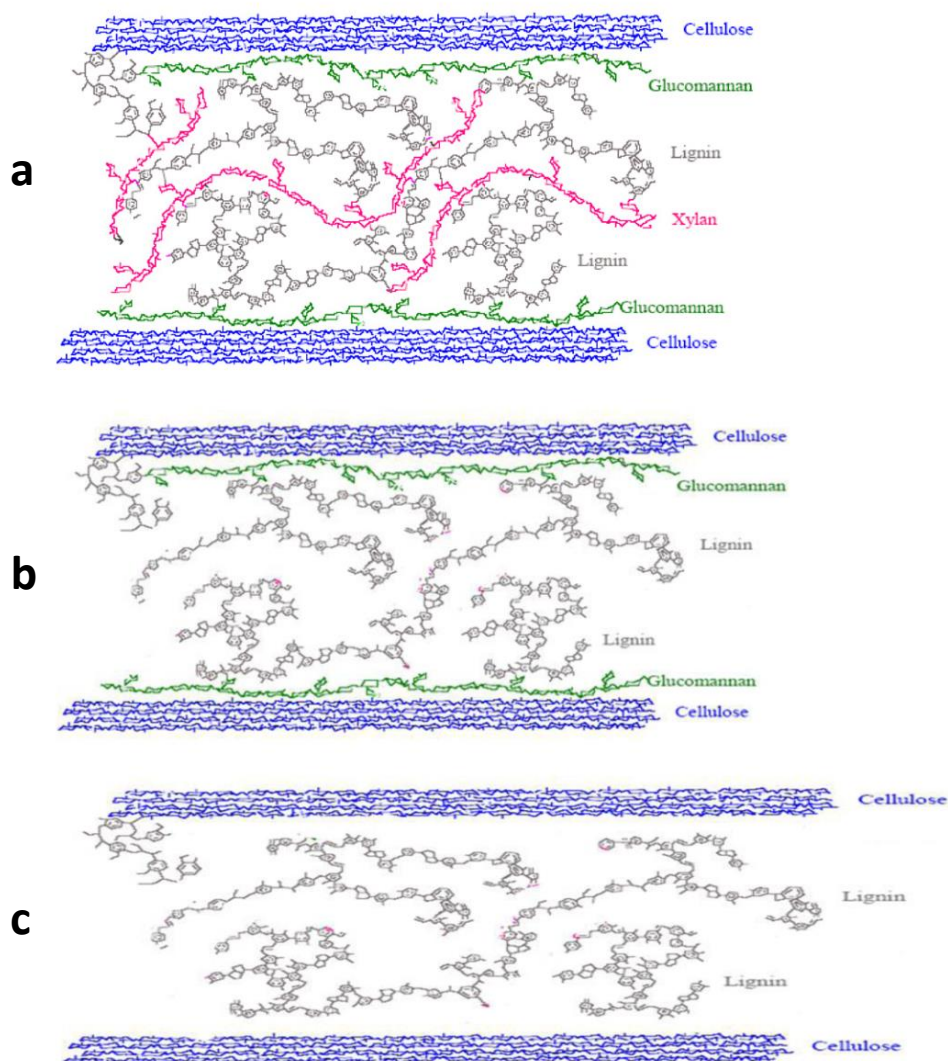
Fig. 1.2 Different stages of wood cell wall degradation (Nilsson and Rowell, 2012); a: non-degradation, b: loss of some hemicelluloses, c: loss of all carbohydrate polymers

Within the wood cells, the cellulose of the S_2 and S_3 layers is attacked either from the lumen or the borders between the S_1 and S_2 layers because of the acid hydrolysis of the hemicelluloses (Rowell and Barbour, 1990). After a breakup of the crystalline structure, the cellulose chain molecules are depolymerized and dissolved (Salanti et al., 2010; Unger et al., 2001; Uzielli, 2009). The S_2 layers are almost completely destroyed by biological degradation and detached from the S_1 layer (Fig. 1.3). Finally, the S_1 layer also decomposes, leaving only the intact middle lamella (ML). (Rodgers, 2004; Rowell and Barbour, 1990). Resistance of ML to the erosion under waterlogged situations is likely to be due to its high lignin concentration (Kim et al., 2008) and the composition of lignin in ML is also different from the secondary cell walls (Faix, 1991; Fengel and Wegener, 1984).
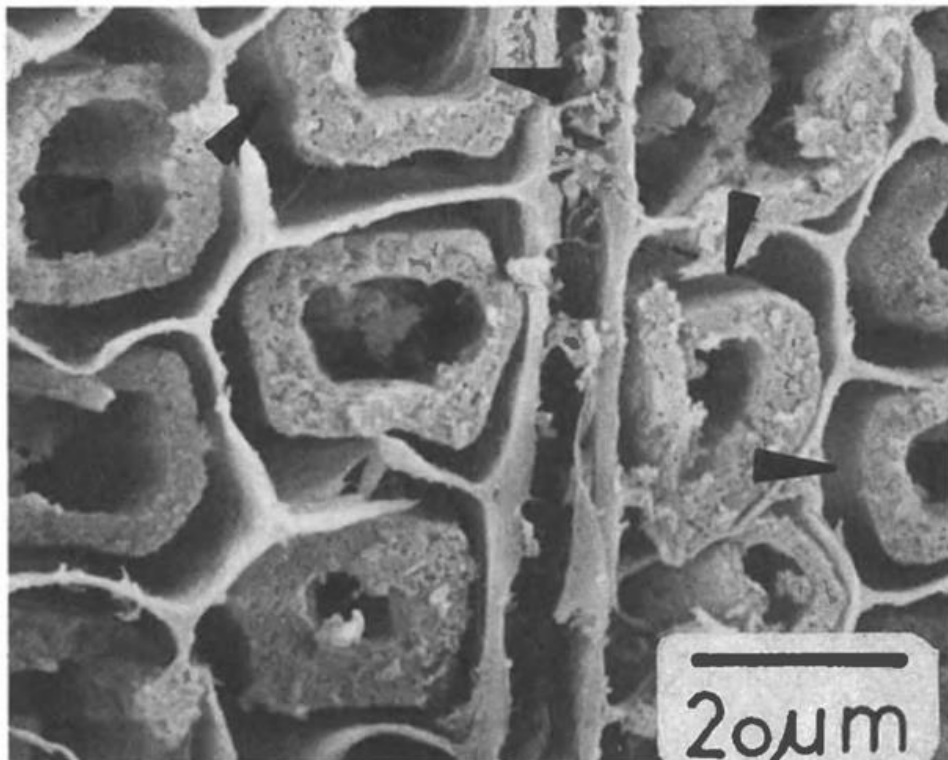
Fig. 1.3 The heavily degraded Spruce wood. Arrows: The S_2 layer was detached from smooth ML (Rowell and Barbour, 1990)

The loss of wood substance causes a decrease of density and a growing microporosity and permeability. Therefore, the wood is bulked by water. WWs often subject to dramatic dimensional changes and distortions upon drying. The dimensional changes of WW results from two different actions, shrinkage and collapse (Rowell and Barbour, 1990). Shrinkage in heavily degraded WW is isotropic and may occur in radial, tangential and longitudinal cracks that cause cuboidal cracks. Collapse is expressed by longitudinal cracks oriented radially or tangentially, and by depressions and distortions (Bugani et al., 2009; Kohdzuma, 2004; Morgós et al., 2015). The decrease in mechanical properties of WW was also investigated (Rowell and Barbour, 1990). The conservation treatments often involve the replacement of water by filling the microporosities of the cell walls or all the microcavities of the wooden structure including the cell lumina with appropriate consolidation materials (Bugani et al., 2009). Depending on the degree of wood decay, the appropriate conservation treatment for WW will be applied.

1.1.2. Conservation treatment of waterlogged wood

The conservation of cultural heritage is fundamental for conveying to future generations our culture, traditions, and ways of thinking and behaving. Conservation has an impressive impact on society from a political, sociological and anthropological points of view. The conservation treatments aim to prolong the life of cultural properties, without impairing the information and value they contain (Rodgers, 2004; Takayasu, 2004). The conservation treatments have been developed to prevent the dramatic dimensional changes caused by cell collapse and cell wall shrinkage during drying. Impregnation and bulking involves replacing the water filling WW with an appropriate chemical to prevent collapse and loss of shape during drying (Broda and Mazela, 2017; Pearson, 1987; Rowell and Barbour, 1990).

The recovery of the first large objects of WW with alum salt, $KAl(SO_4)_2 \cdot 12H_2O$, was routinely applied in Sweden in 1861 (Christensen et al., 2006; Kohdzuma, 2004). This method became the National museum's standard treatment for WW for the next hundred years. However, after nearly 100 years had passed, objects treated with this method were found to have developed serious problems. The alum-treated wood becomes brittle because of the elevated acidity of the wood, which leads to acid hydrolysis (Braovac and Kutzke, 2012). The potassium alum treatment has therefore not been used since the middle of the twentieth century (Kohdzuma, 2004).

Currently, the most widely used consolidation is polyethylene glycol (PEG) which is freely soluble in alcohols (ethanol, methanol and isopropanol) as well as in water. The PEG method was pioneered in the late 1960s and early 1970s by the National Museum of Denmark with the Skuldelev Viking ships, and by Barkman with the Vasa sunken ship in Sweden (Hocker et al., 2012; Rodgers, 2004; Tejedor, 2010). High molecular weight PEG is more suitable for more degraded wooden objects (Babiński, 2015; Broda and Mazela, 2017), while low molecular weight PEG is often applied for conservation of less deteriorated WW. The PEG can penetrate wood tissue, replace water molecules and reinforce its structure, thus improving its dimensional stability (Broda and Mazela, 2017; Rowell and Barbour, 1990). PEG treatments are so commonly used because of the low cost for materials and equipment as well as the satisfactory results could be obtained (Broda and Mazela, 2017). For small objects, an impregnation tank is often used to conduct the treatment, while the large wooden objects such as ships which could not feasibly be placed in tanks, a PEG solution was sprayed onto the wood. However, the impregnation of PEG is time consuming; the treatment process needs decades for large objects. Moreover, in PEG-treated wood, the levels of formic acid increase because of PEG degradation (Hocker et al., 2012; Mortensen, 2009; Sandström et al., 2002; Unger et al., 2001). This phenomenon may cause acid-induced hydrolysis and further weakening and stability loss.

Recently, the use of carbohydrates as a conservation treatment has been investigated (Babiński, 2015; Babiński et al., 2017; Horie, 2010; Morgós et al., 2015; Unger et al., 2001). Carbohydrates are organic compounds made up of combinations of saccharides organized in a ring structure. Carbohydrates have many advantages such as non-toxic, non-corrosive, have low hygroscopic in normal air humidity. The conservation of WW with sucrose, mannitol and recently lactitol and trehalose has been being investigated (Babiński, 2015; Babiński et al., 2017; Morgós et al., 2015; Unger et al., 2001). Impregnation of WW can be completed with or without heating. This is due to small molecular size of sucrose, lactitol and trehalose which enhances chemicals penetrate easily into the WW. Treated wooden objects have a natural color and can be cleaned and glued easily. Carbohydrates can also be easily extracted from treated artefacts by water so conservation treatment can be reversed if necessary (Morgós et al., 2015).

Additionally, various alternative treatments for excavated wood have been also investigated. The treatment method using higher alcohol, which has a low molecular weight, is under development (Kohdzuma, 2004). Higher alcohol can reduce the impregnation time considerably. Higher alcohols do not dissolve in water, hence the artifacts treated with the higher alcohol method have high resistance to moisture (Kohdzuma, 2004; National Research Institute of Cultural Heritage, 2012).

Melamine-formaldehyde resins have been used for archaeological WW preservation for decades (Wittköpper, 1998). Recently, Kauramin 800 (a melamine-formaldehyde resin) has been extensively used in conservation of WWs (Cesar et al., 2016; Unger et al., 2001). Kauramin 800 is well-suited for the conservation of WW due to its good solubility in water, small molecular size, and therefore it allows for good penetration into the wood (Christensen et al., 2012). However, it is difficult to

remove the excess polymer from the surfaces of treated objects and additional treatment is required to improve color tone (Wittköpper, 1998). Additionally, the polymer fills almost completely the wood voids, leaving no space for future retreatment. These features are the drawbacks of the method because the reversibility is one of conservation requirements. Silicon-containing polymers have been examined with relatively good results (Smith, 2003). Consolidation treatment with dicarboxylic acids also showed good achievement because of its far penetration into wood (Chaumat et al., 2007). However, more thorough data on stability and degradation is still needed before the effectiveness of these polymers can be properly evaluated (Christensen et al., 2012). There has been an increased interest over the past decade in green materials for consolidation such as keratin (Endo et al., 2008; Kawahara et al., 2002), isoeugenol (Mchale et al., 2017) and so on.

The efficiency of WW treatment is not only depending on impregnation process but it also depends on method of its drying. Currently, the main drying methods used by conservators are slow air drying and freeze drying (Schindelholz et al., 2009). Slow air drying is an inexpensive drying method. The controlled air drying can reduce the drying stresses, therefore reduce shrinkage of the outer surfaces of the wood. Controlled air drying of WW has been performed with satisfactory results (Schweizer et al., 1984). Beside, freeze-drying is one of the most effective methods of conservation for WW (Rowell and Barbour, 1990). Compared with other drying methods, water is removed by the ice sublimation instead of liquid evaporation, the capillary effects of fluid flow that may bring cell collapse can be avoided, and therefore the dimensional stability of the wooden object can be preserved (Shaozhi et al., 2016). However, a pre-treatment process, such as PEG impregnation, is often required to prevent damage to the cells during freezing (Babiński, 2015, 2011; Schindelholz et al., 2009). Generally, freeze drying gave the successful conservation treatment results with

lower chemical uptake, while, an extensive uptake of chemicals is required for air-drying method (Babiński, 2015, 2012; Schindelholz et al., 2009). As less chemical is used, the wood is lighter both in color and weight (Hocker et al., 2012). The increased energy costs of freeze-drying may be offset by reduced treatment times. The major limitation for treating large artifacts, obviously, is the size of the freeze-drying chamber.

There were complex problems caused by historical conservation treatments such as darkening the wood, filling all wood voids so that further work is impossible, or releasing toxic reactants, etc. Therefore, to develop preservation strategy in the future, we must first look to the past and propose new strategies without the limitations of previous preservation problems. Even the good dimensional stabilization can be achieved, a future retreatment must be considered.

1.2. Imperial Citadel of Thang Long

1.2.1. Overview of the Imperial Citadel of Thang Long

Thang Long is the former name of Hanoi, the capital city of Vietnam. In the 11th century, Ly Cong Uan, the founder of the Ly Dynasty, moved the capital from Hoa Lu to the Dai La Citadel, and then renamed Thang Long, marking the establishment of the independent of the Dai Viet. The city played as the political and economic center through the Ly Dynasty (1009-1225), Tran Dynasty (1225-1400), early Le Dynasty (1428-1527), Mac Dynasty (1527-1592) and restored Le Dynasty (1592-1789). Although during the Nguyen Dynasty (1802-1945) the imperial capital was moved to Hue, Thang Long, later renamed Hanoi, still remained an important political center in Northern Vietnam (Chau, 2005; Labbé, 2011; Phuong and Groves, 2004; UNESCO, 2013). The Thang Long Imperial Citadel site is one of the most

important heritage sites in Vietnam and it was named on the World Heritage List by UNESCO's World Heritage Committee in 2010 (Tri and Tin, 2010; UNESCO, 2013).

The Imperial Citadel of Thang Long is divided into two parts, the central axis of the Nguyen Dynasty's Hanoi Ancient Citadel and the Archaeological Site at 18 Hoang Dieu. The Imperial Citadel buildings and the remains in the 18 Hoang Dieu Archaeological Site reflect a unique South-East Asian culture specific to the lower Red River Valley, at the cross roads between influences coming from China in the north and the ancient Kingdom of Champa in the south (Phuong et al., 2009; Tri, 2005; Vuong and Long, 1977).

The Imperial Citadel of Thang Long is the complexity of the successive historical and cultural events, and philosophical and religious ideas associated with the site (Labbé, 2011; Phuong and Groves, 2004; UNESCO, 2013). While architectural remains and artifacts reveal the history of the Citadel stretching over 1.000 years, many of its structures have yet to be discovered (Tri and Tin, 2006; UNESCO, 2013). The excavation revealed evidence of the complexity of ancient structures from different historical periods, such as the establishment of the Kinh Thien Palace, Doan Mon and Bac Mon, built during the Le Dynasty, or other architectural structures built during and after the French's colonization period (Fig. 1.4) (Thang and Tri, 2016; Tri and Tin, 2010, 2006; UNESCO, 2013).
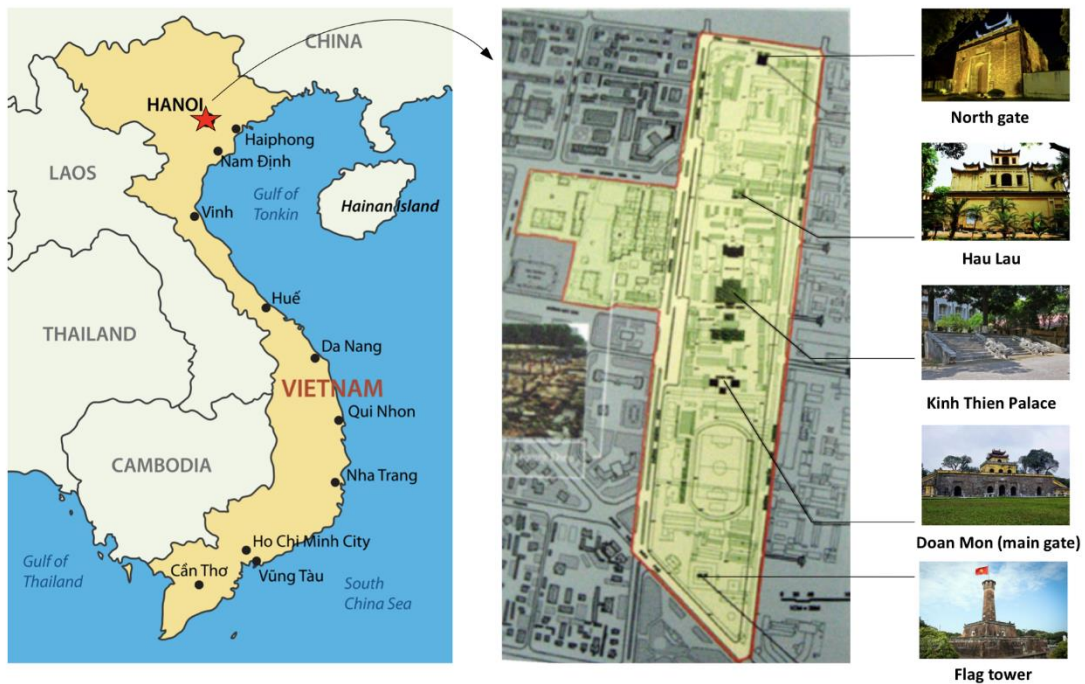
Fig. 1.4 The Central sector of the Imperial Citadel of Thang Long – Hanoi

The challenges in preservation and promotion of the values of Thang Long Imperial Citadel are to protect the integrity of the properties include the lack of a full understanding about the heritage values of different structures and multiple layers of cultures existing at the site, balancing the stress of socio-economic development in Hanoi with heritage preservation and the need to better promote the outstanding universal values of the site to the public (Tri, 2005; Tri and Tin, 2010; UNESCO, 2013). This indicates that massive challenges to the further study, as well as the protection, conservation and promotion of the Citadel.

1.2.2. Conservation activities in the Imperial Citadel of Thang Long

In 2002, archaeological relics were exposed during the preparations for the construction of the new National Assembly Hall at 18 Hoang Dieu. As results of the finding, construction work was postponed to allow for further archaeological investigation. During the excavation from 2002 to 2004, many artifacts and items from

the 6th to the 20th century belonging to the Ly, Nguyen, Tran, Le periods were found (Chau, 2005; Tri, 2005).

In 2007, the Japan-Viet Nam Cooperation Committee on the preservation of the Cultural Heritage Complex of Thang Long was established. Discussions between international and national experts during the missions emphasized the importance value of the location, conservation procedures, a comprehensive management plan and capacity building for Thang Long management staffs (Thang and Tri, 2016; UNESCO, 2013).

In January 2010, the UNESCO/Japanese Funds-in-Trust project "Preservation of the Cultural Heritage Complex of Thang Long-Hanoi" officially started. Major counterparts such as Thang Long-Hanoi Heritage Conservation Center, the National Research Institute for Cultural Properties, Tokyo (NRICPT) and the UNESCO Hanoi Office have jointly implemented project activities including the value assessment, conservation research and management plan development (Labbé, 2011; Thang and Tri, 2016; UNESCO, 2013).

From 2010 to 2013, the archaeologists excavated various artifacts dated to different dynasties such as a two-meter long water drainage and brick pillar foundation from the Nguyen Dynasty, the foundation of the Royal Path and Dan Tri yard from the Le Dynasty, brick walls and a large water drainage from the Tran Dynasty, mud foundation from the Ly Dynasty and roof tiles and pottery dated to the Dinh, early-Le and Dai La periods. Noticeably, the large-scale archaeological excavations in 2011-2013 revealed pillar foundations of the Ly Dynasty in the surrounding area of Kinh Thien Palace. This indicates the potential for discovering more remains of architectural

structures of the Ly Dynasty in the Central Axis (Bich et al., 2013; Labbé, 2011; Thang and Tri, 2016; UNESCO, 2013).
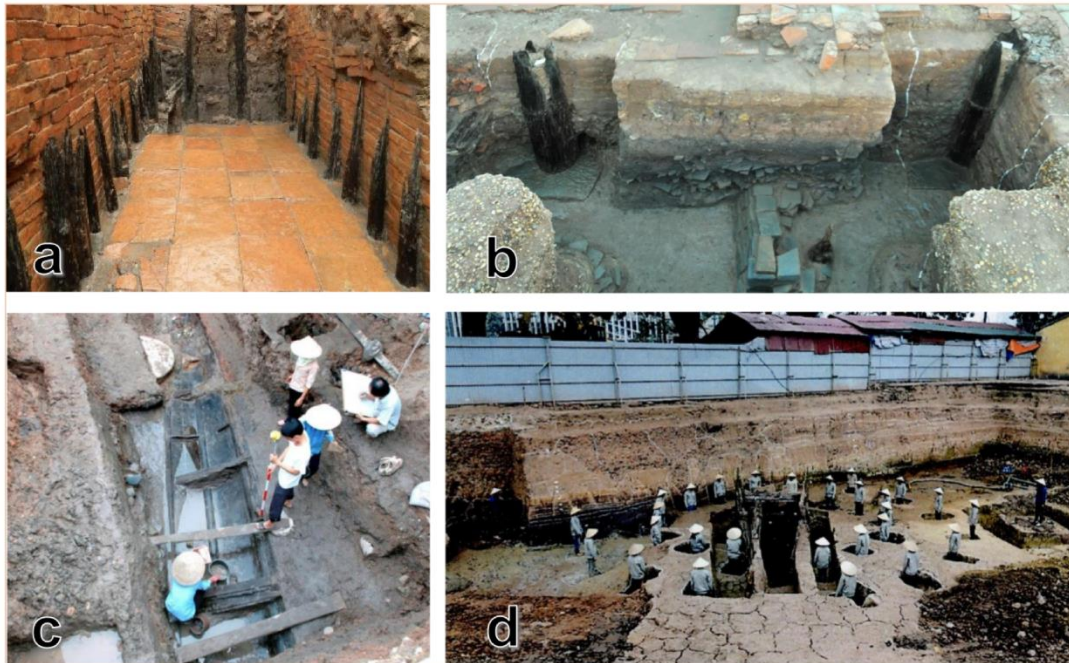
Fig. 1.5 Archaeological excavation at the Imperial Citadel of Thang Long – Hanoi site; a: large water drainage from the Tran Dynasty, b: building basement, c: shipwreck, d: a special spiritual relic

Among the findings, wooden artifacts accounted a large proportion of archaeological objects excavated at the Thang Long heritage site. Some of them remain buried *in-situ* while others were salvaged from the site (Fig. 1.5). These cultural properties are continually threatened by environmental impacts since the long-term protections are not implemented. In general, a total of 3291 wooden artifacts have been excavated between 2002-2009 with varied shapes and size (Tri and Tin, 2006; UNESCO, 2013). The excavated wooden objects are classified into 6 main groups based on their functions and shapes:

- Group 1: Wooden artifacts related to the construction of buildings, walls, drainage system (pile, wooden foundation, wooden panels, etc.)

- Group 2: Wooden artifacts related to components of architectural structures (columns, rafters, tips, shuttering, strings, door railing, stairs, etc.)

- Group 3: Wooden objects related to woodworking or masonry tools (plane, chisel, clod-breaker, hoes, spade, etc.)

- Group 4: Wooden artifacts used in daily life (box, jar, bucket, water bucket, palanquin, lacquer trays, shuttle, wooden clogs, boat, etc.)

- Group 5: Natural wood such as tree trunks, branches (twig types, bamboo stump, flexible plants, etc.)

- Group 6: artifacts with undefined functions.

At the moment, two conservation methods are applying for wooden artifacts including *in-situ* conservation and temporary storage preservation such as immersing them in water tanks or special storage facilities (Fig. 1.6) (Bich et al., 2013; Phuong et al., 2009; UNESCO, 2013). Investigation on the characteristic of the wooden artifacts saved in water tanks revealed that they were in relatively good preservation conditions. However, many problems were observed on *in-situ* preservation of artifacts (Thang and Tri, 2016; Tri and Tin, 2006; UNESCO, 2013). The observation on exposed wooden artifacts at the archaeological site revealed that shrinkage and collapse of WWs due to the changing moisture level in Hanoi and termite attacks occurred. This poses considerable threats to the protection of wooden artifacts for moisture changes and termites can lead to irreversible deterioration of wood (Bich et al., 2013, 2011; UNESCO, 2013). It is essential that long-term conservation treatments are required to prevent further deterioration of the remains (Bich et al., 2013; Phuong et al., 2009; Thang and Tri, 2016; UNESCO, 2013).
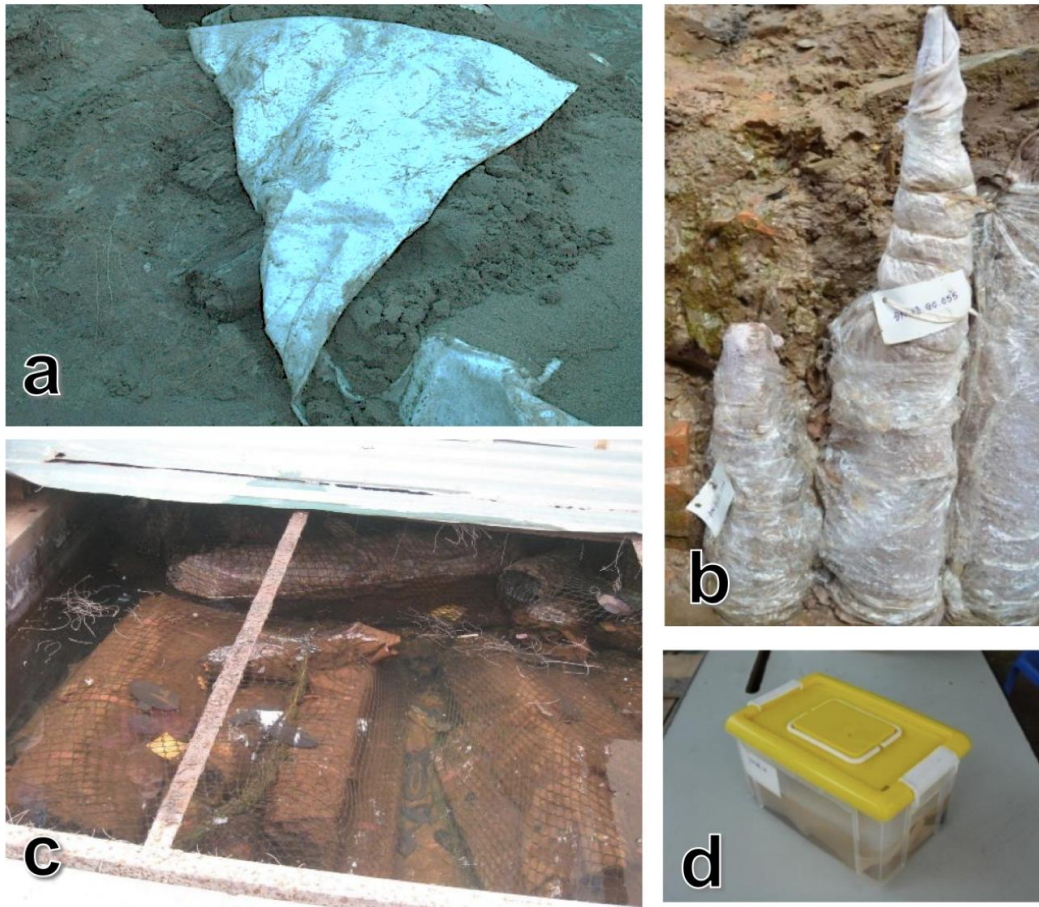
Fig. 1.6 Temporary storage of WW at the Imperial Citadel of Thang Long –
Hanoi; a: burying under a very thin layer of sand, b: wrapping by fabric & plastic,
c: soaking in the water tanks, d: stored in sealed box

1.3. Objectives of the thesis

Conservation of cultural relics at Thang Long Imperial Citadel site is one of
the important plans put forth by the Government of Vietnam. The current situation of
the *in-situ* preservation of artifacts requires urgent conservation treatment. These
cultural properties are continually threatened by environmental impacts given that no
long-term protective procedures are implemented. Furthermore, archaeological woods
stored in water tanks for a long time, can suffer from microorganism-induced erosion
that is not visible from the exterior. Given the current condition of heritage, it is
recommended that the immediate conservation treatment should be taken into account

for preserving these artifacts. However, there are limited reports on the conservation of Vietnamese archaeological wood.

The major purpose of this study is to establish suitable conservation treatments for some archaeological woods obtained from Thang Long Imperial Citadel site. In Chapter 2, species identification and physicochemical properties of 15 WWs were determined to reveal traditionally wood selection and to understand the deterioration degree of these WWs. In Chapter 3, the natural durability of the culturally and historically important timber *Erythrophleum fordii* Oliv. wood was investigated to illustrate well preservation of this wood buried in soil for centuries, even for a millennium. In Chapter 4, general WW conservation methods using PEG, trehalose and keratin was performed. The comparison of chemical treatments on dimensional stability of WWs was discussed to find out the most effective chemical agent. In Chapter 5, a preliminary examination on diffusivity of PEG, trehalose and keratin into WWs was conducted. The diffusion coefficients calculated in this study together with the measured dimensions of WWs of the same species, can be used to estimate treatment time. In Chapter 6, the *in-situ* polymerization of hydrophilic polymer was developed to enhance the recoverability of WWs, which is very important to avoid hornification of the WW cell wall upon drying.

Chapter 2. Characterization of some archaeological waterlogged woods at Thang Long Imperial Citadel site

2.1. Introduction

When dealing with conservation of WW, it is necessary to determine wood species and its state of degradation (Jensen and Gregory, 2006; Rowell and Barbour, 1990). The identification of wood is needed to understand their historical value and because of their importance from a technological point of view, mainly to understand wood selection and its utilization. Whereas, the chemical and physical characteristics of archaeological WW are determined for understanding the process of degradation and development of a reasonable preservation treatment to stabilize the WW (Pearson, 1987; Rowell and Barbour, 1990; Unger et al., 2001).

At the present, a large quantity of wooden objects has been excavated in Thang Long Imperial Citadel site. However, there are little reports on the identification of these wooden findings. Therefore, wood identification by scientific methods is needed to highlight the high capacity achieved by Vietnamese ancient artisans in wood technology and the ancient timber selection, in addition to the other archaebotanical data.

In many publications, physical factors such as water content and density is regularly selected to evaluation of the state of deterioration of WW (Broda and Mazela, 2017; Rowell and Barbour, 1990). This is because it is simple investigation technique and considerable repeatability of the results can be achieved. Additionally, the measurement of shrinkage/swelling of wood allows the estimation of the possible movement of wood without any conservation treatment (Babiński et al., 2014; Macchioni, 2003).

However, degradation assessment of WW cannot be based only on one type of measurement. According to previous study (Macchioni, 2003), high ash content in WW samples affected to measurement of shrinkage of WW, giving an incorrect image of the state of WW preservation. Therefore, other examination such as microscopy or chemical analysis should be implemented (Broda and Mazela, 2017; Giachi et al., 2003; Zoia et al., 2015).

This chapter aimed to determine wood species and physicochemical properties of 15 WW samples obtained from Thang Long Imperial Citadel site. The physical and chemical characterizations will be used to evaluate the decay level of wood, and to define the consolidation strategies for the conservation of those wooden objects.

2.2. Materials and methods

2.2.1. Materials

Fifteen wood samples were collected from Thang Long Imperial Citadel site. For chemical analysis, WWs were cut into small pieces and then dried in an oven at 70 ºC overnight. The wood chips were powdered in a coffee grinder and the wood powder's size between 150 and 250 μm was collected for further chemical examination. For physical properties examination, the specimens were cut into 20 × 20 × 10 mm blocks (radial × tangential × longitudinal dimensions). The samples were cut from same block of WW and decayed parts were removed to give samples with similar properties.

2.2.2 Anatomical characterization

Small specimens, 5 × 5 × 5 mm blocks (radial × tangential × longitudinal dimensions), were embedded in PEG1500 to fix the wood cell walls. Then, 20–30 μm radial, tangential, and longitudinal sections were cut from each sample using a microtome (TU-213, Yamato Scientific Co., Ltd., Japan). The sections were immersed in water at 60 °C for 6 h to remove the PEG. The sections were then stained in 1% safranin for 2 h and then dehydrated using ethanol solutions of increasing concentration. After dehydration, the sections were mounted on glass slides and observed using an optical microscope (BX51; Olympus, Tokyo, Japan) under 5×, 10×, and 20× magnifications. Identification was performed with the help of the literature and reference databases from Xylarium, RISH, Kyoto University, and the Vietnamese Academy of Forest Sciences.

2.2.3. Physical properties

Physical parameters such as density and moisture content can be measured to evaluate the state of degradation of WWs (Babiński et al., 2014). The maximum moisture content of wood (U_{max}) was determined by wood mass measurement for samples were repeatedly saturated with water under low pressure and then oven-dried up to constant weight for 24 h at 105^0C (m_{max}) compared to the mass of dry wood (m_0), according to Eq. (2.1):

$$U_{max} = \frac{m_{max} - m_0}{m_0} x100 \qquad (2.1)$$

Basic wood density (ρ) is a parameter that is typically used by archaeologists and conservators to quantify the amount of wood degradation (Macchioni, 2003; Rowell and Barbour, 1990). It was calculated as the ratio of the weight of an absolutely

dry wood sample (m_0) to its volume in the state of maximum water saturation (V_{max}) according to Eq. (2.2):

$$\rho = \frac{m_0}{V_{max}}$$ (2.2)

Linear wood shrinkage/swelling in tangential, radial and longitudinal directions was calculated using the Eq. (2.3):

$$\beta = \frac{l_0 - l_1}{l_0} x 100$$ (2.3)

β: linear wood shrinkage/swelling [%]; l_0: initial sample dimension (at the maximum moisture content, waterlogged) [mm]; l_1: final sample dimension (after drying and seasoning) [mm].

2.2.4. Chemical analysis

In order to evaluate the state of degradation of WWs, the percentage content of main wood components (extractives, lignin, holocellulose and α-cellulose) was determined were determined in triplicate by chemical analysis. Solvent extractive components were measured according to TAPPI standards (TAPPI, 1999; 2007). Lignin content was measured according to the TAPPI standard (TAPPI, 1998). Holocellulose content was determined according to the procedure described (TAPPI, 2011) using an acid solution of sodium chlorite. Alpha-cellulose was calculated according to the TAPPI standard by using sodium hydroxide solution (TAPPI, 1999b). The acid soluble lignin (ASL) is measured by conventional UV spectrophotometric method using the absorption at 205 nm (UV-1800, Shimadzu, Japan).

2.3. Results and discussion

2.3.1. Wood identification

The microscopic images of 15 samples are presented in Table. 2.1. Based on the diagnostic anatomical features, a total of 15 samples were identified as shown in Table 2.2. The results showed that all samples come from 10 different genus: *Afzelia* sp., *Albizia* sp., *Bouea* sp., *Dysoxylum* sp., *Elaeocarpus* sp., *Erythrophleum fordii* Oliv., *Garcinia* sp., *Sterculia* sp., *Syzygium* sp. and *Vatica tonkinensis* A. Chev. The identification commonly reaches in general the genus level, but the historical period and traditional wood selection suggest in several cases at the species level, i.e., *E. fordii* and *V. tonkinensis*. Because of high quality timber, these woods have been used for multiple purposes such as furniture, building constructions, ship building, household items, and so on.

2.3.2. Wood characterization

The relationship between U_{max} and basic density of WWs is shown in Fig. 2.1. All the samples from different species show the same behavior. The higher water content is associated with lower basic density of WW. Degradation of WW involves loss of wood substance, mainly polysaccharides: cellulose and hemicellulose. The losses appearing in wood are immediately filled with water. Therefore, the increase of maximum wood moisture content (U_{max}) as well as the decrease of the basic density indicate an increasing grade of wood degradation (Broda and Mazela, 2017; Rowell and Barbour, 1990). The U_{max} ranged from 55% to 864%, while basic density of WWs was between 0.11 and 0.84 g/cm^3. Among the species evaluated, *E. fordii* and *V. tonkinensis* wood have low water content as well as high basic density which were about 60% and 0.8 g/cm^3, respectively. This indicates that both *E. fordii* and *V.*

tonkinensis were relatively intact and their characteristics were similar to those of sound wood.
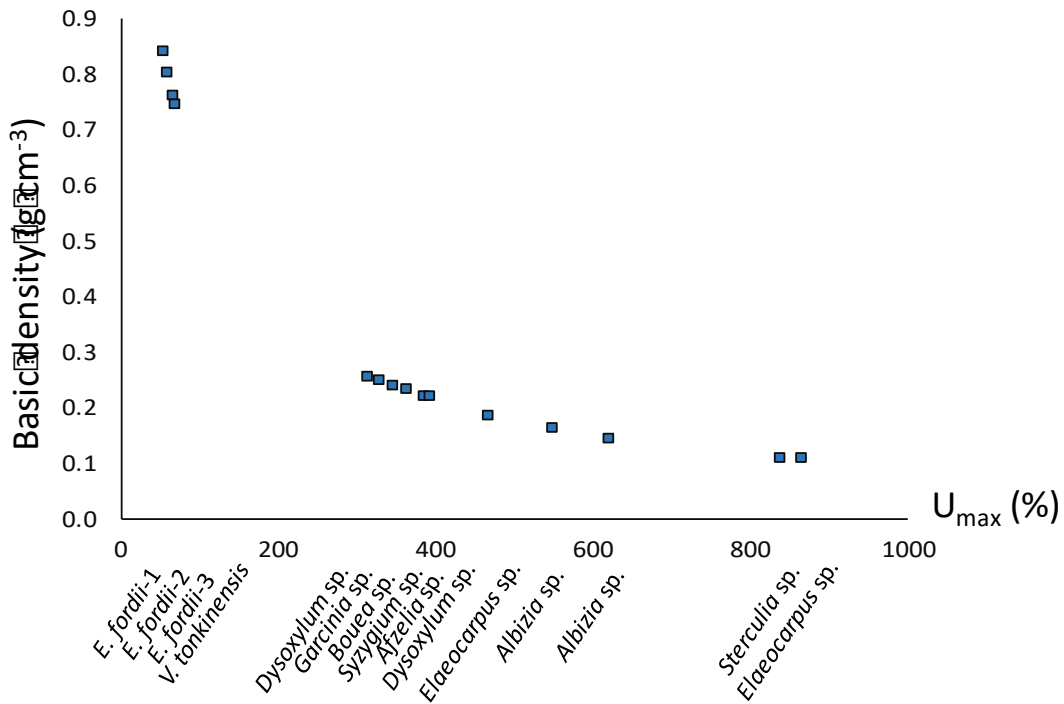
Fig. 2.1 Relationship between U_{max} and ρ for all examined WWs

The shrinkage of WWs is presented in Fig 2.2. Naturally, the more degraded WWs, the higher shrinkage occurred. The shrinkage of heavily degraded WWs was observed between 36.3% and 68.6% in tangential direction, 18.1% and 35% in radial direction. The highest shrinkage value in longitudinal direction was 15.6%. This extreme radial, tangential, and longitudinal shrinkage could suggest that the cellulose underwent severe degradation (Berti et al., 2002). However, little dimensional changes were observed in the case of *E. fordii* and *V. tonkinensis* woods. The tangential shrinkage of these woods ranged between 9% and 12.7%, shrinkage value in radial direction was 6.5% and 8.4% and 0.5% and 1.6% in fiber direction. These values were similar to sound wood which accounted about 15% in tangential direction, 7% in radial direction and 1% in fiber axes (Rowell, 2005).
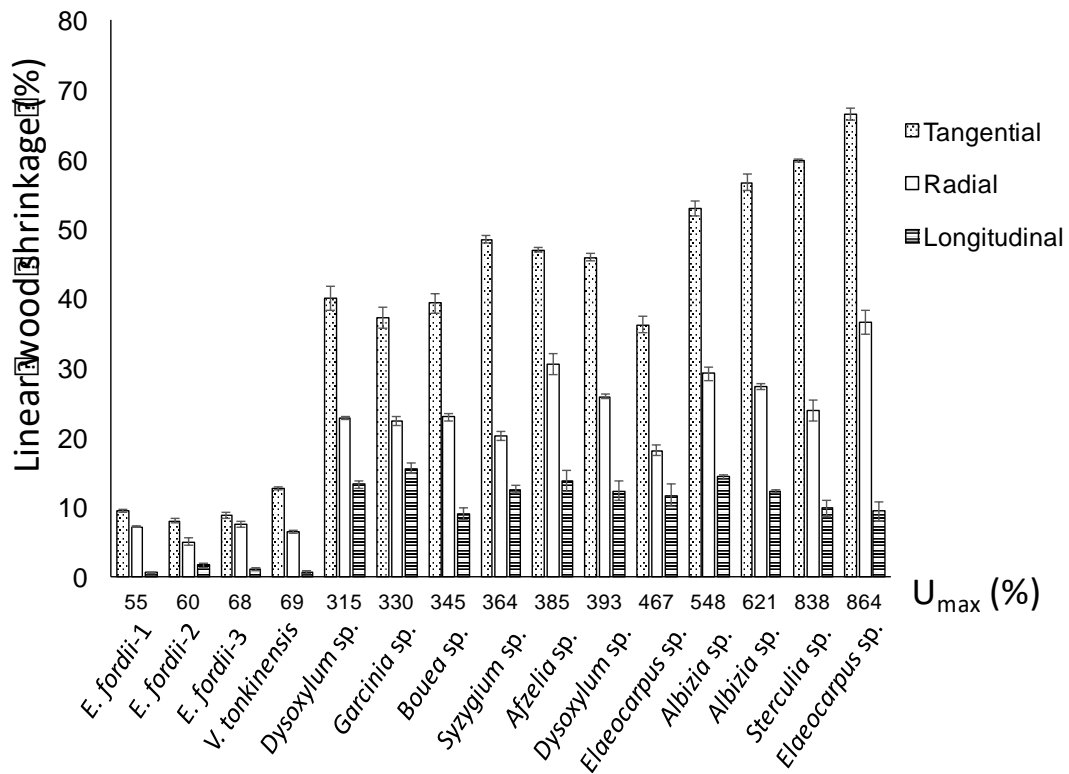
Fig 2.2 Mean values of linear wood shrinkage of untreated WWs

The ratio of shrinkage anisotropy of degraded WWs (U_{max} more than 300%) is considerably reduced. In particular, the ratio of tangential to longitudinal shrinkage of WWs was about 5, while a factor of about 20 has been found for normal wood. These observations are in agreement with the loss of cellulose and the decrystallization of remaining cellulose.

Furthermore, an evaluation of chemical composition is valuable to assess the wood degradation (Fig. 2.3). The holocellulose content of WWs (U_{max} more than 300%) was considerably reduced to around 20%, while the lignin content raised to merely 80%. According to previous studies, the degradation of WW mainly involves the deterioration of hemicellulose and cellulose. The low content of holocellulose

suggests that cellulose and hemicellulose have been severely destroyed (Jingran et al., 2014).
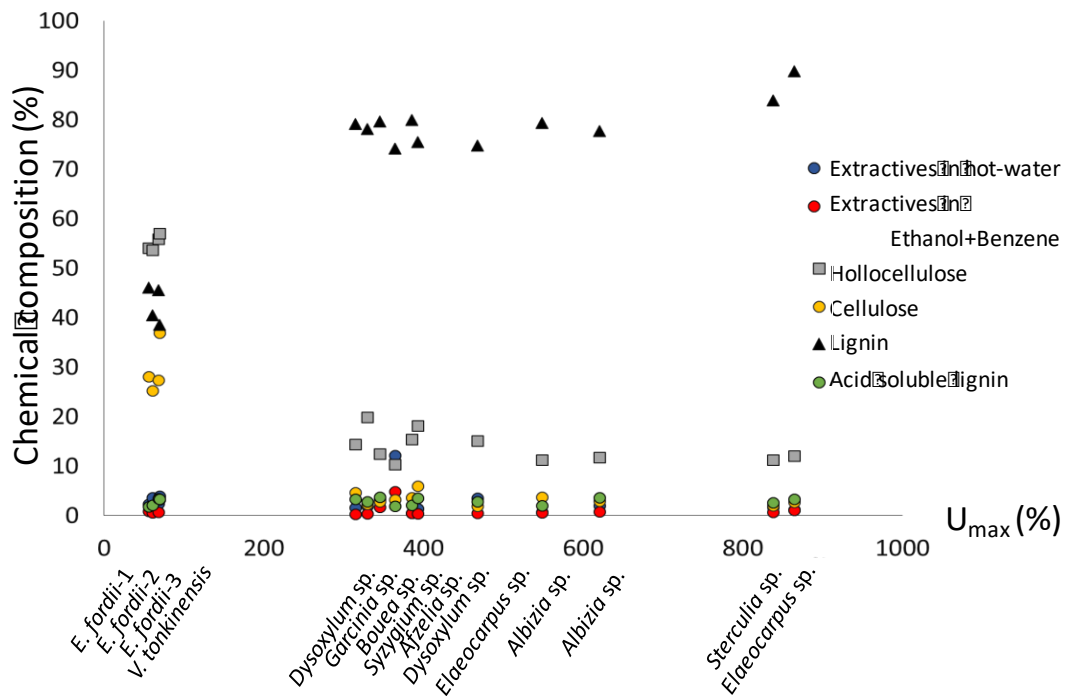
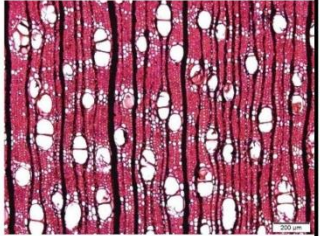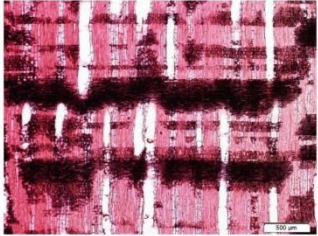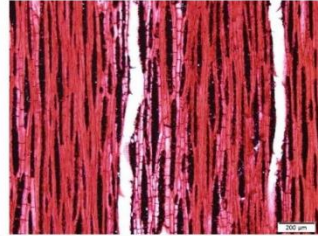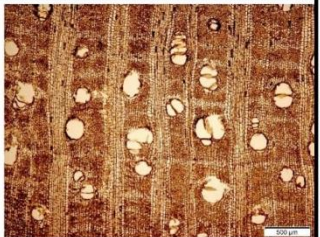**Fig. 2.3** Chemical composition of all WWs evaluated
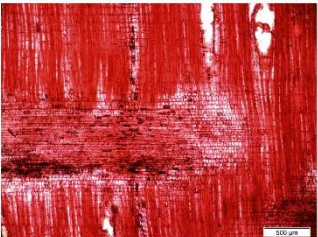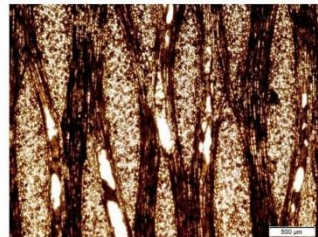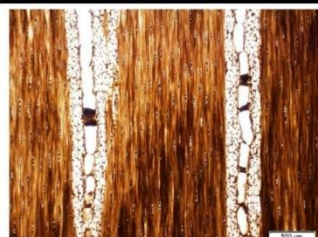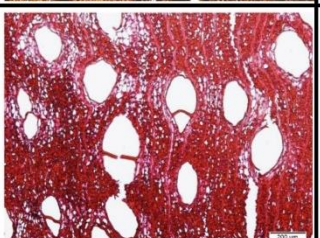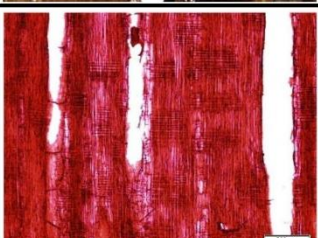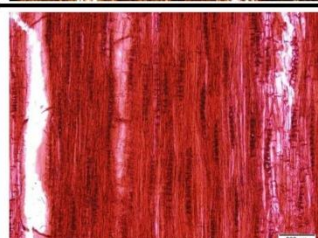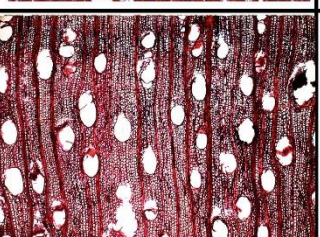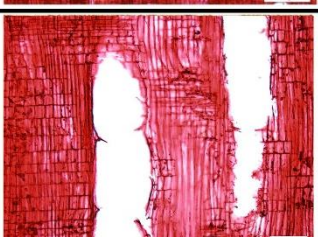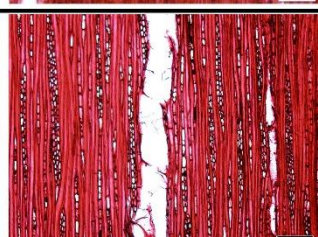
The cellulose content of these WWs was considerably reduced to between 2 and 6%, while, about 40% cellulose has been found in non-degraded wood (Rowell, 1984). These results indicate the extensive decay of WWs evaluated. Interestingly, holocellulose and lignin content in *E. fordii* and *V. tonkinensis* wood were about 60% and 40%, respectively. The results indicated that both *E. fordii* and *V. tonkinensis* were relatively in good condition and its characteristics were relatively similar to sound wood. Total extractives content in WWs ranged from 2% to 5%, except for *Syzygium* sp., which was about 17%. The high soluble materials contents in this species may limit the penetration of conservation agent.

2.4. Summary

Total 15 WW samples were characterized and classified into 10 taxa. The wood identification reaches in common the genus level. However, the *E. fordii* and *V. tonkinensis* were identified to species level because of its commonly selected wooden materials in the past. The measurements on physical and chemical characteristics of WW showed different classes of wood degradation. The heavy decay of wood samples revealed in a very low basic density (average value less than 0.2 g/cm^3) and the high value of water content (more than 300%). Chemical analysis also confirms the degree of wood degradation. The high lignin content was determined in wood with U_{max} from 315% to 864%. On the other hand, the cellulose content of degraded WWs dropped to around 10%. Among species evaluated, *E. fordii* and *V. tonkinensis* have similar properties comparing to those of modern woods. The heavily degraded wooden objects need to be treated to keep its original structure, while the excavated *E. fordii* and *V. tonkinensis* wood are sometimes intact and do not need to be preserved.
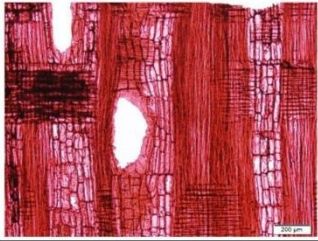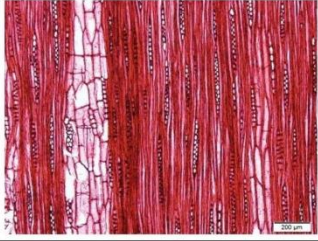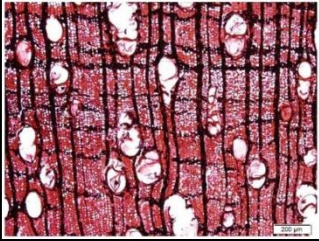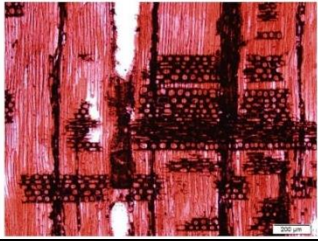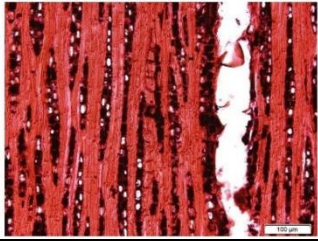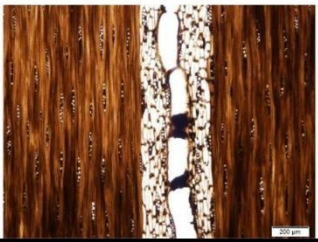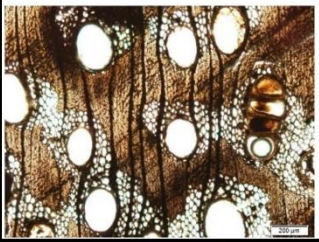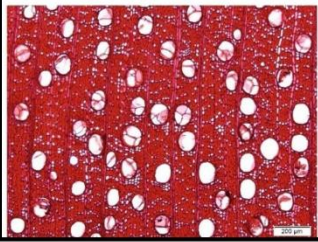
Figure captions

Table 2.1 Typical sections of WWs (1/3)

	Cross-section	Radial section	Tangential section
048			
052			
066			
104			
108			
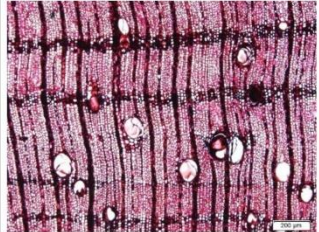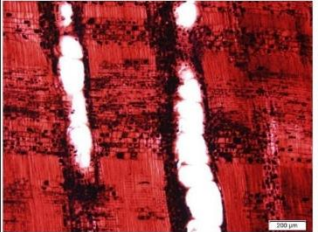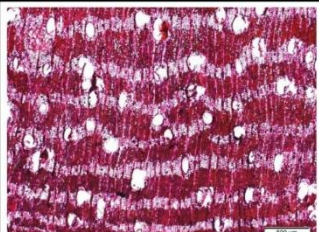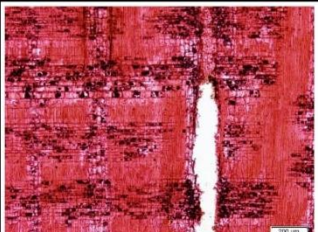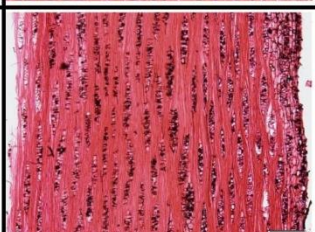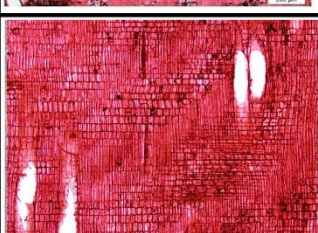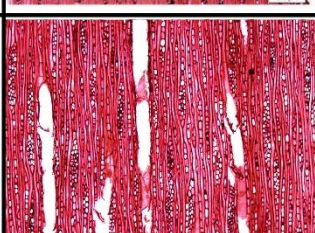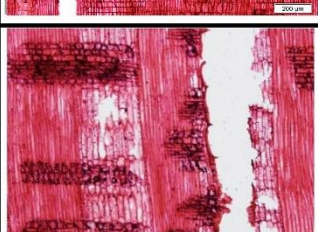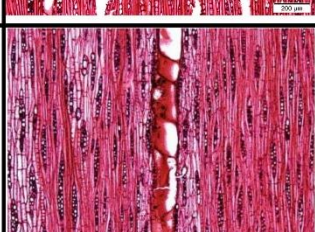
Table 2.1 Typical sections of WWs (2/3)

	Cross-section	Radial section	Tangential section
137			
138			
181			
182			
235			

Table 2.1 Typical sections of WWs (3/3)

	Cross-section	Radial section	Tangential section
257			
258			
260			
270			
357			

Table 2.2 Anatomical features of WWs

Samples code	Cross section	Radial section	Tangential section	Taxa
048	Wood diffuse porous, growth rings absent. Tangential diameter of solitary vessel 76 (42 - 110) μm. Axial parenchyma confluent.	Simple perforation plates. Intervessel pits alternate. Body ray cells procumbent with 2-4 rows of square marginal cells. All rays stored	Narrow rays, generally 2 to 3 cells. Ray width 26(18 – 34) μm. Ray height 447 (225-483) μm	*Syzygium* sp.
052	Diffuse porous, growth rings absent. Tangential diameter of solitary vessel 148 (78 - 198) μm. Axial parenchyma diffuse-in-aggregates. Axial parenchyma in seemingly marginal bands	Perforation plates simple. Intervessel pits alternate. Rays heterogeneous. Body ray cells procumbent with 2-4 rows of square marginal cells.	Large rays, commonly > 10 seriate. Rays of two distinct sizes. Ray height 1466 (1077-2390) μm.	*Sterculia* sp.
066 181 182	Vessel diffuse porous, growth rings present. Tangential diameter of solitary vessel 106 (22 - 216) μm. Gums and other deposits in vessels. Axial parenchyma aliform, confluent. Very thicked-wall fibers and narrow fibers lumina.	Vessel-ray pits, round, oval or elongated horizontally. Rays homocellular, procumbent cells. Perforation plates simple.	Narrow rays, generally 1-2 cells. Vessel-vessel pits alternate. Maximum height 288(67-769) μm and wide 31(12-51) μm	*Erythrophleum fordii* Oliv.
104	Diffuse porous, growth rings present. Tangential diameter of solitary vessel 116 (47 - 248) μm. Axial parenchyma aliform	Perforation plates simple. All ray cells procumbent. Vessel-ray pits alternate.	Narrow rays, generally 1-2 cells. Ray height 321 (213 – 544) μm	*Afzelia* sp.

108	Growth rings absent. Vessel diffuse-porous. Vessels in radial multiples of 4 or more common. Tangential diameter of solitary vessel 166 (118 - 255) μm. Fibers very thin-walled. Axial parenchyma absent.	Simple perforation plates. Intervessel pits alternate. Vessel-ray pits with distinct borders; similar to intervessel pits. Body ray cells procumbent with mostly 2-4 rows of square marginal cells	Narrow rays, generally 1-3 cells. Ray height 886 (544 - 1327) μm.	*Elaeocarpus* sp.
137	Diffuse porous, growth rings absent. Tangential diameter of solitary vessel 186 (78 – 276) μm. Axial parenchyma aliform	Simple perforation plates. Intervessel pits alternate. Rays homocellular, procumbent cells. Vessel-ray pits alternate.	Narrow rays, generally 1-2 cells. Ray height 317 (198 - 438) μm.	*Albizia* sp.
138	Semi-ring porous, growth rings present. Tangential diameter of solitary vessel 68 (27 - 99) μm. Axial parenchyma in narrow bands or lines up to three cells wide	Simple perforation plates. Intervessel pits alternate. Body ray cells procumbent with 2-4 rows of square marginal cells. Gums and other deposits in ray cells.	Narrow rays, generally 1-2 cells. Ray height 350 (263 - 439) μm. Prismatic crystals in chambered axial parenchyma cells	*Garcinia* sp.
235	Growth rings present. Vessel diffuse-porous. Tangential diameter of solitary vessel 85 (33 - 135) μm. Vessels occasional with tyloses. Fibers very thick-walled Axial canals diffuse.	Simple perforation plates. Vessel-ray pits simple to irregularly narrowly bordered, and round to oval horizontally. Prismatic crystals present	Ray 1-2 to 3-4 seriate, with a tendency to 2 sizes, maximum height 356(80-1129) μm. The form of ray cells is heterogeneous. Crystals often present in ray cells. Vessel-vessel pits alternate.	*Vatica tonkinensis* A. Chev.
257	Growth ring absent. Vessel diffuse-porous. Tangential diameter of solitary vessel 70 (32 - 99) μm. Axial parenchyma in narrow bands.	Vessel-ray pits with distinct borders; similar to intervessel pits in size and shape. Simple perforation plates. Rays	Narrow rays, generally 1 - 3 cells wide. Ray height 319 (249 - 424) μm.	*Bouea* sp.

		heterocellular. Prismatic crystals present in rays		
258 260	Diffuse porous, growth rings distinct. Tangential diameter of solitary vessel 113 (76 – 153) μm, radial diameter of solitary vessel 151 (110 - 247) μm. Fibers thin- to thick-walled. Axial parenchyma bands more than three cells wide	Simple perforation plates. Intervessel pits alternate. Body ray cells procumbent with mostly 2-4 rows of upright cells	Narrow rays, generally 1-2 cells. Ray height 305 (213 - 451) μm. Vessel-ray pits alternate.	*Dysoxylum* sp.
270	Growth rings absent. Vessel diffuse-porous. Vessels in radial multiples of 4 or more common. Tangential diameter of solitary vessel 72 (22 - 104) μm. Fibers very thin-walled. Axial parenchyma absent.	Simple perforation plates. Intervessel pits alternate. Vessel-ray pits with distinct borders; similar to intervessel pits. Body ray cells procumbent with mostly 2-4 rows of square marginal cells	Narrow rays, generally 1-3 cells. Ray height 523 (367 - 819) μm.	*Elaeocarpus* sp.
357	Diffuse porous, growth rings absent. Tangential diameter of solitary vessel 123 (44 – 154) μm, radial diameter of solitary vessel 147 (75 - 207) μm. Axial parenchyma aliform	Simple perforation plates. Intervessel pits alternate. Rays homocellular, procumbent cells. Vessel-ray pits alternate.	Narrow rays, generally 1-2 cells. Ray height 287 (181 - 420) μm.	*Albizia* sp.

Chapter 3. Natural durability of the culturally and historically important timber - *Erythrophleum fordii* wood against white-rot fungi

3.1. Introduction

Erythrophleum fordii Oliv. is a precious hardwood tree species of Caesalpiniaceae and naturally distributed in Vietnam and South China. It is known by the name "Gemu" and is used by native Chinese people as an agent promoting invigoration and circulation (Du et al., 2010; Nan et al., 2004). Moreover, *Ganoderma lucidum* (Curtis) P. Karst, which has high medicinal value, can be found in natural forests and plantations of this species when stumps decay. The *E. fordii* has important medicinal value and toxic properties (Cheng and Zhen, 1987). Alkaloids, triterpenoids, diterpenoids, and diterpenoid dimers have been isolated and identified from seeds, bark, and leaves (Du et al., 2010; Nan et al., 2004; Ha et al., 2017; Hung et al., 2014; Qu et al., 2006; Tsao et al., 2008). The biological effects of alkaloids present in *E. fordii* have been reported (Du et al., 2010; Hung et al., 2014; Qu et al., 2006; Tsao et al., 2008). The *E. fordii* also has important health and ecological benefits (Zhigang et al., 2012)

The *E. fordii* is indeed a valuable timber tree species in tropical and subtropical regions with a clear distinction between heartwood and sapwood. The *E. fordii* tree produces quite hard, heavy, and durable wood, commonly called as 'iron wood', which is generally used for the production of ships, high-grade furniture, flooring, sculpture, and crafts (Chen, 1988; Fang and Fang, 2007). Because of its superior wood, the *E. fordii* was classified in the most durable wood group in Vietnam (QD 2198-CN, 1997). It has been used as traditional timber in many historical buildings in Vietnam.

Recently, wooden artifacts excavated from archaeological sites in Vietnam, such as Thang Long imperial citadel, Hanoi, Bach Dang stake yard, Quang Ninh, were identified as *E. fordii*. Interestingly, despite those artifacts being buried for hundreds of years, the degree of degradation of *E. fordii* wood was limited. The degradation of the wood's surface layer was limited to a depth of approximately 1 to 2 cm. Below the outer surface layer, microscopic observation, chemical analyses and mechanical tests revealed no significant differences between excavated and modern wood (Bich et al., 2011). Considering the medicinal and antifungal properties of different parts of the plant, it is considered that *E. fordii* wood would exhibit these properties. However, there are limited reports on natural durability of *E. fordii* wood.

Various organisms can induce wood to deteriorate, and the greatest level of deterioration is caused by fungi. White rot fungi are among the most efficient degraders of plant fiber (lignocellulose), and are capable of degrading cellulose, hemicellulose, and lignin. They commonly cause rotten wood to feel moist, soft, spongy, or stringy, and to appear white or yellow (Mtui and Nokes, 2014; Mahajan, 2011; Jones and Brischke, 2017). Wood undergoes a number of changes during the decay process, including reductions in mass and strength (Bari et al., 2015; Blanchette, 1984a; Blanchette, 1984b). Significant changes occur in the chemical composition of the cell wall during the fungal attack (Bari et al., 2015). Attack of fungi causes a decrease in mechanical and physical properties of wood, influencing its moisture content, electrical conduction, acoustics, elasticity, and plasticity (Cowling, 1961; Schmidt, 2006).

The degradation of wood by white-rot fungi has been investigated with different methods, including microscopy techniques (Anagnost, 1998; Takano et al., 2009; Pelit and Yalçın, 2017; differential scanning calorimetric (Tsujiyama, 2001); X-

ray diffraction (Kim, 2005); Gas chromatography - mass spectrometry (GC–MS) spectroscopy, chemical analysis (Nishimura et al., 2012; Zabell and Morrell, 1992), Nuclear magnetic resonance (NMR) and Fourier - transform infrared spectroscopy (Martínez et al., 2011; Nishimura et al., 2017; Pandey and Pitman, 2003; Kim et al., 2008). Two-dimensional nuclear magnetic resonance spectroscopy (2D NMR) techniques in the cell wall and lignin research have improved over the past decade (Eriksson et al., 1990; Ralph et al., 1999). Among various 2D NMR spectroscopic techniques available, Heteronuclear single quantum coherence (HSQC) is the most common. Solution-state 2D NMR provided an interpretable structural fingerprint of the lignin and carbohydrates of the cell wall, without further structural modification applied during the ball milling and ultra-sonication step (Kim et al., 2008; Rencovet et al., 2009).

In this chapter, microscopic observations and chemical analyses were performed to illustrate the structural and chemical changes of the *E. fordii* wood degraded by white rot fungi *Phanerochaete chrysosporium* Burdsall and *Phanerochaete sordida* (P. Karst.) J. Erikss. & Ryvarden. The deterioration of *E. fordii* wood will be discussed and compared with *Fagus crenata* Blume (Japanese beech) wood. Investigation of natural resistance of *E. fordii* wood to wood decay fungi is essential for better understanding the characteristics of this wood, and for determining appropriate procedures to conserve archaeological waterlogged *E. fordii* wood.

3.2. Materials and methods

3.2.1. Materials

Samples of *Erythrophleum fordii* Oliv. and *Fagus crenata* Blume (Japanese beech) wood, 20 × 20 × 5 mm (radial × tangential × longitudinal dimensions), were cut from defect-free heartwood parts and used for further testing. The *E. fordii* wood was obtained from woods collection of Vietnamese Academy of Forest Sciences, Vietnam, while beech wood was received from Xylarium, RISH, Kyoto University, Japan.

Sulfuric acid was purchased from Wako Pure Chemical Industries, Ltd., Japan. Dimethyl sulfoxide-d_6 (DMSO-d_6) was obtained from Sigma Aldrich, USA.

3.2.2. Wood decay testing

Fungal cultivation

The 3.8% potato dextrose agar (PDA) aqueous solution was steam-sterilized at 120°C for 20 min. In the next step, about 20 ml of PDA medium was poured into a 90 mm Petri dish. Fungi were cultivated in Petri dishes on PDA medium. After inoculation, Petri dishes were held at 28 °C and 70% relative humidity to enable the fungi to spread over the entire dish.

Extractives test

The air-dried powdered *E. fordii* wood (~10g) was extracted with 100 distilled water prior to methanol (MeOH). The water/MeOH extracts were evaporated under

reduced pressure (EYELA rotary evaporator N-1000, Tokyo Rikakikai Co., Ltd., Japan). The steam-sterilized filter papers were impregnated with 1%, 5% and 10% of each extract. The treated filter papers were exposed to two white rot fungi *P. sordida* ATCC 90872 and *P. chrysosporium* ATCC 34541 for 2 weeks.

Wood samples test

The wood samples were oven-dried at 103 °C for 24 h and weighed prior to fungal exposure. The specimens (*n*=3 for each fungus) were steam-sterilized under the same conditions and then placed on the medium. Wood samples were exposed to two white rot fungi *P. sordida* and *P. chrysosporium*. After 4 weeks of incubation, the mycelia covering the blocks were removed carefully, and the blocks were oven-dried to constant mass. The mass loss (*W*) of individual samples was calculated from the oven-dried mass before and after fungal test, and used to calculate mean percentage of mass losses:

$$\% W = [(W_0 - W_f)/W_0] \times 100$$

Where: W_0 is oven dry mass of sample prior to exposure and W_f is the oven dry mass following exposure to fungus.

3.2.3. Light and scanning electron microscopy

Optical microscopy

Small wood blocks, $2 \times 2 \times 2$ mm (radial $\times$ tangential $\times$ longitudinal dimensions), were prepared from the control and biodegraded wood specimens. The specimens were dehydrated in a series of increasing concentration of acetone baths and embedded in Spurr resin (Spurr, 1969). The embedded specimens were cut at

approximately 1 μm thicnkness with a semithin microtome (Leica RM2145, Solms, Germany) equipped with a diamond knife. The sections were stained with toluidine blue for 3 min and then washed with distilled water for 1–3 min. The sections were observed using an optical microscope (BX51; Olympus, Tokyo, Japan) to investigate patterns of hyphal and decay of wood tissue.

Scanning electron microscopy observation

The control and biodegraded specimens were prepared from internal part of samples. The clear wood surfaces were prepared using a microtome (TU-213, Yamato Scientific Co., Ltd., Japan). The specimens were freeze-dried for 2 days and then coated with platinum using an auto fine coater (JFC-1600, JEOL, Japan) operated at 30 mA for 90 s. Field emission scanning electron microscopy (SEM, JSM-7800F prime, JEOL, Japan) was operated at an accelerating voltage of 1.5 kV.

3.2.4. Chemical analysis

Lignin content

Klason lignin content was determined in samples before fungal exposure. The control wood was powdered in a coffee grinder. The measurement was carried out on sieved material (in the range 60-100 mesh, corresponding to 0.15-0.25 mm). The lignin content was determined in triplicate following the TAPPI method (Tappi, 1998), which is based on the isolation of Klason lignin after the hydrolysis of the polysaccharides (cellulose and hemicellulose). The wood powder was immersed in concentrated sulfuric acid (72%) for 4 h. In the next step, the solution was transferred to an Erlenmeyer flask and diluted to 3% acid concentration with distilled water. These

samples were boiled for 4 h. The acid-insoluble lignin was then filtered off, oven-dried, and weighed.

2D HSQC NMR analysis

To provide more detailed structural information, 2D HSQC NMR experiments were performed on control and degraded samples. The selected samples were grinded using laboratory-scale Mixer Mill MM301 (Retsch, Germany) for 5 min. The extracted wood powder was finely ball-milled in a Mono Mill P-6 (Fritsch, Japan) centrifugal ball at 550rpm for 3h. Approximately 0.4 g of finely ball-milled wood powder was suspended in 2.8 ml DMSO-d_6 in a plastic tube and sonicated in an ultrasonic cleaning bath for 30 min. In the next step, the diluted solution was moved to a NMR tube. The 2D-NMR spectra were recorded using a Bruker AVANCE III 600 MHz UltraShield instrument (Bruker, Germany) operated at 600 MHz. Bruker pulse program hsqcedetgpsp.3 was used for the HSQC experiments. The spectral widths were 16 ppm (9615 Hz) and 100 ppm (15091 Hz) for the $^1H(\delta_H)$- and $^{13}C(\delta_C)$-dimensions, respectively. The number of points (TD) was 2048 for the ^1H-dimension with a recycle delay of 1.2 s. The number of transients was 12, and 256-time increments were recorded in the ^{13}C-dimension. The optimal direct coupling ($^1J_{CH}$) used was 145 Hz.

A semi-quantitative analysis of the integrals of the HSQC cross-signal was conducted using Bruker Topspin 3.5 NMR software, and calculated based on the number of 100 aromatic units.

(S+S′)/2 + G+G′ = total integral of aromatics.

Relative integral value of the specific signal X per 100 aromatic units = 100 × (Integral-X)/(total integral of aromatics)

Where: S: syringyl lignins; G: guaiacyl lignins; S, S′ is the integration of $S_{2,6}$, $S'_{2,6}$, respectively. G, G′ is the integration of G_2, G'_2, respectively.

3.3. Results and discussion

3.3.1. Extractives test

Natural resistance to decay is one of the most important properties of wood, and is affected by the combination of wood density and the content and composition of lignin and extractives (Nuopponen et al., 2006; Oliveira et al., 2010; Onuorach, 2000). The antifungal test of *E. fordii* wood extractives were also performed. The results showed that *E. fordii* extractives were unable to inhibit the growth of fungi (Fig. 3.1). Therefore, the lignin structure is thought to be critical for resistance to degradation.
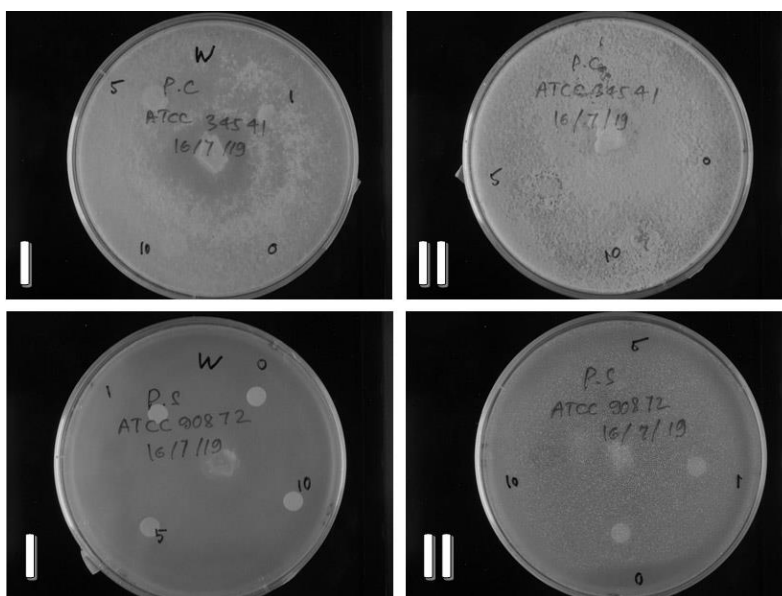
Fig. 3.1 Antifungal test of *E. fordii* wood extractives
I: Anti-fungal test of cold-water extract; II: Anti-fungal test of MeOH extract
P.C: *P. chrysosporium*; P.S: *P. sordida*; Number 0, 1, 5, 10: concentration of extractives (%)

3.3.2. Mass losses

All wood specimens were completely colonized by external mycelia after 4 weeks of incubation. The mean percentage mass losses of two wood species caused by different white rot fungi are shown in Fig. 3.2. The mean mass loss of *E. fordii* wood caused by *P. chrysosporium* and *P. sordida* was only 2%. However, these values for beech wood were 12 and 14%, respectively. After exposure to these fungi, the tested samples were subjected to further microscopic observations and chemical analyses.
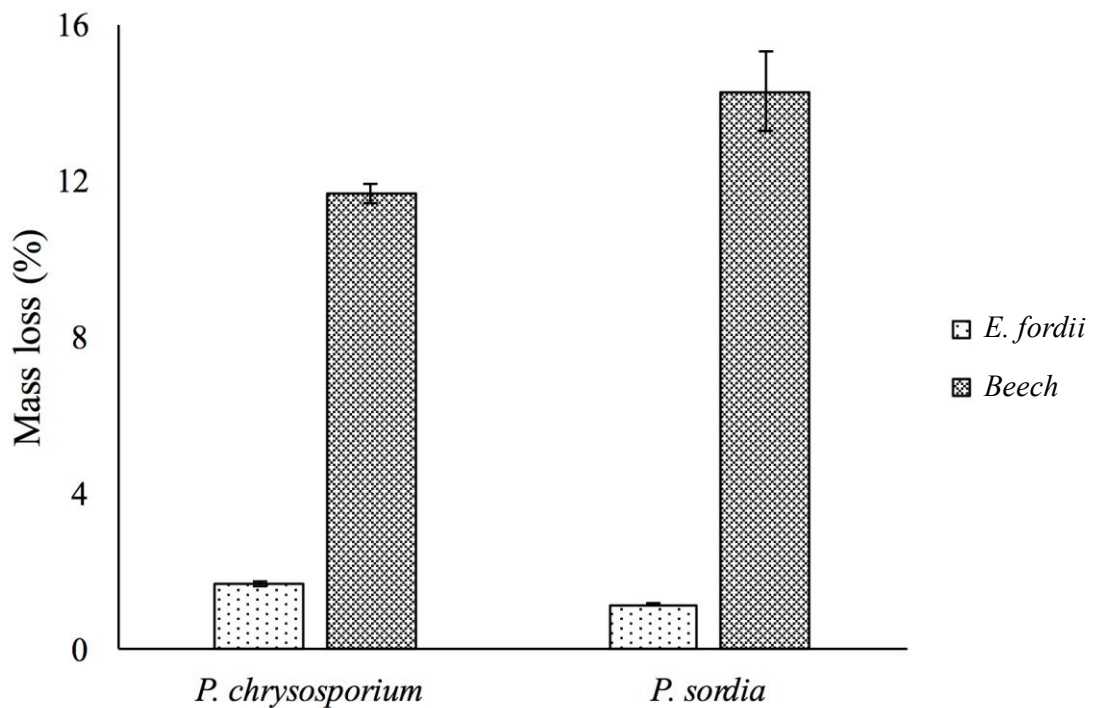
Fig. 3.2. Mean percentage mass loss in *E. fordii* wood and beech wood after 4 weeks of exposure to two white rot fungi. Error bars represent the standard error.

Light and SEM microscopic observations

Microscopic examinations of the woody biomass revealed different patterns of degradation between *E. fordii* wood and beech wood (Fig. 3.3 and 3.4). Little degradation was observed in the vessel and parenchymal cells of *E. fordii* wood (Fig. 3.3a_1 and 3.3a_2), while vessels and fiber cells of beech wood were deeply eroded by *P. chrysosporium* (Fig. 3.3c_1 and 3.3c_2). *Phanerochaete sordida* caused defibrillation through dissolution of the ML in some parenchyma of *E. fordii* wood, while fiber areas were still intact (Fig. 3.3b_1 and 3.3b_2). Besides, the defibrillation process occurred in several beech wood tissues (Fig. 3.3d_2). The *E. fordii* wood had very thick-walled fibers with the fiber lumina almost completely closed (Fig. 3.3a_1). Because of the uniqueness of fiber structure, there was little space for the development of hypha, hence limited the fungal degradation process.
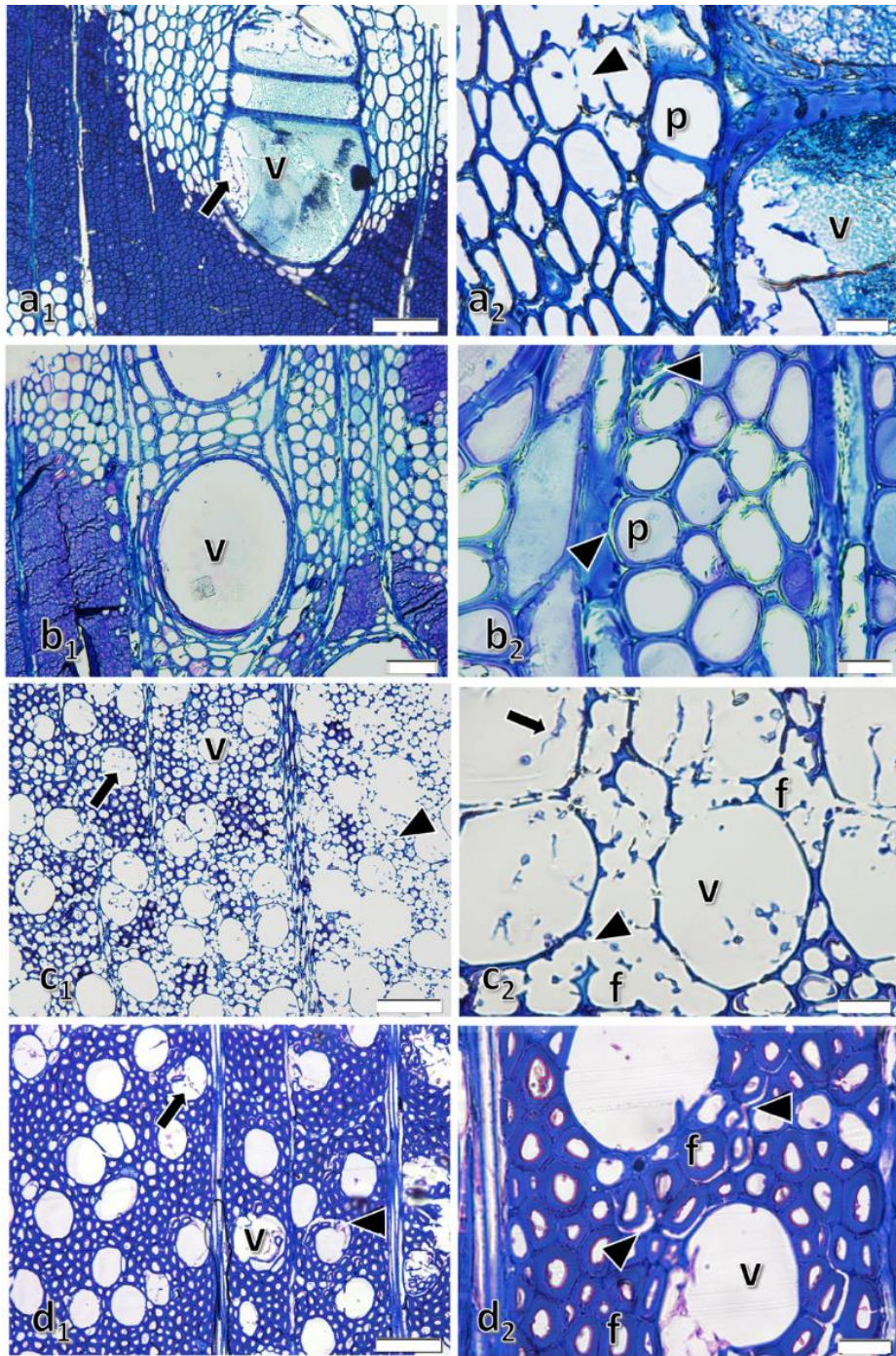
Fig. 3.3 Cross-sections of *E. fordii* wood and beech wood after 4-weeks exposure to white rot fungi: (a₁–a₂) *E. fordii* wood *exposed* to *P. chrysosporium*; (b₁–b₂) *E. fordii* wood *exposed* to *P. sordida*; (c₁–c₂) beech wood *exposed* to *P. chrysosporium*; (d₁–d₂) beech wood *exposed* to *P. sordida*. Hyphal colonization in vessels lumina (v), axial parenchymas (p), and fibers (f) (arrows), especially vessels (arrow). Erosion and rupture in cell walls and defibrillation (arrowheads). a₁, c₁ and d₁: bar 100 µm; b₁: bar 50 µm; a₂, b₂, c₂, d₂: bar 20 µm.
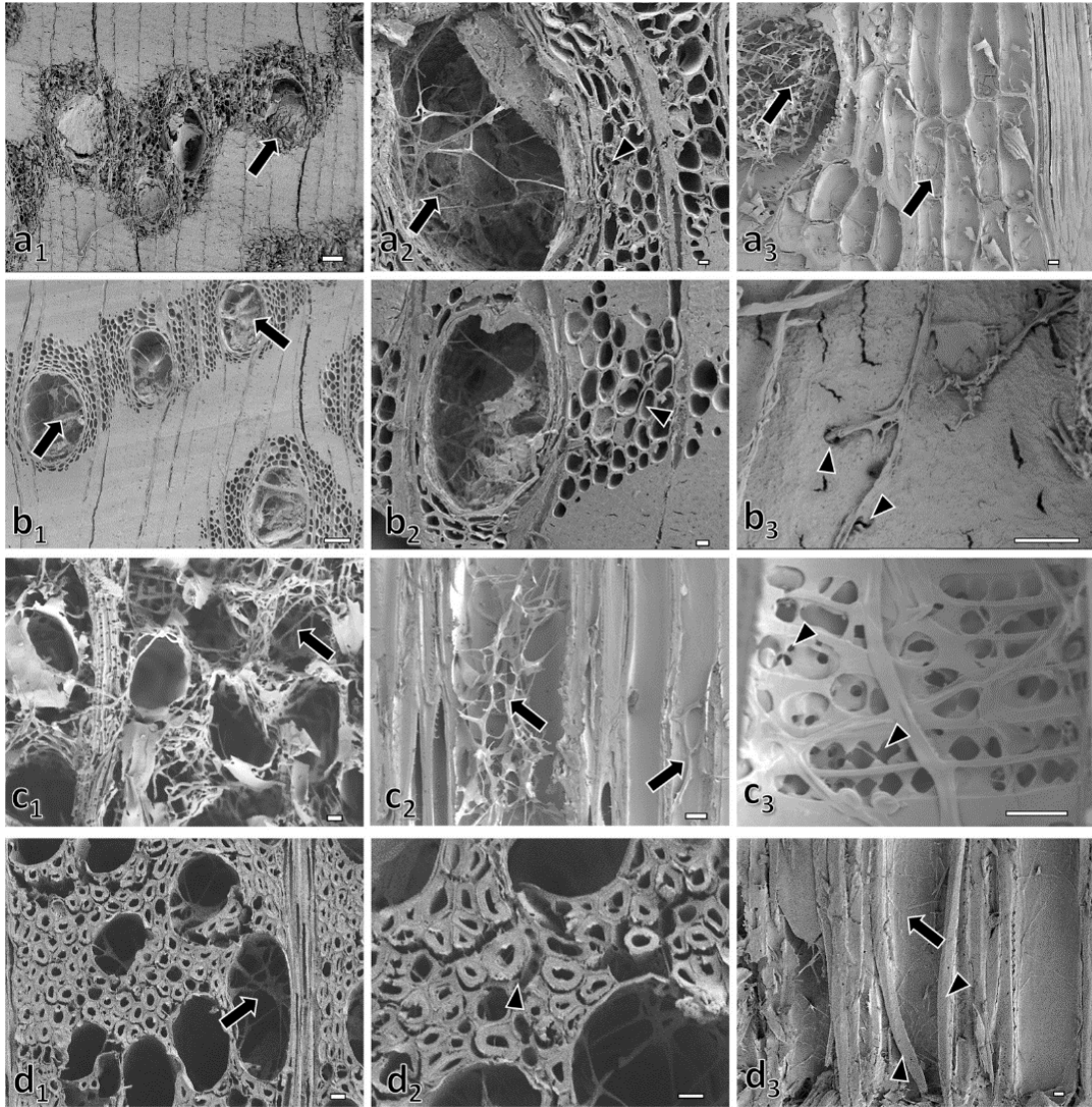
Fig. 3.4 SEM micrographs of *E. fordii* and beech wood samples: (a$_1$–a$_3$) *E. fordii* wood *exposed* to *P. chrysosporium*; (b$_1$–b$_3$) *E. fordii* wood *exposed* to *P. sordida*; (c$_1$–c$_3$) beech wood *exposed* to *P. chrysosporium*; (d$_1$–d$_3$) beech wood *exposed* to *P. sordida*; a$_1$-a$_2$, b$_1$-b$_2$, c$_1$-c$_2$ and d$_1$-d$_2$: cross-sections: Colonization of hyphae in the lumen of vessels and fibers (arrows), deterioration of parenchyma (a$_2$: arrowhead) and defibrillation of wood tissue (b$_2$, d$_2$: arrowheads). a$_3$, b$_3$, c$_2$-c$_3$ and d$_3$: radial sections: the presence of hyphae in the lumen of vessels and parenchymal cells (a$_3$) or vessels and fibers (c$_2$); b$_3$, c$_3$: hyphae penetration in vessel pits and bore holes in vessel walls (arrowheads). a$_1$andb$_1$: bar 100 µm; a$_2$-a$_3$, b$_2$-b$_3$, c$_1$-c$_3$ and d$_1$-d$_3$: bar 10 µm.

During the decay process, changes in the structure of wood were hard to observe using light microscopy, while SEM clearly showed how the cell lumina were occupied by fungal hyphae. Hyphae were only observed in the lumen of vessels and parenchymal cells of *E. fordii* wood, while the fibers remained undamaged (Fig. $3.4a_1$ and $3.4b_1$). Conversely, the hyphae were extended over whole tissues in beech wood (Fig. $3.4c_1$ and $3.4d_1$).

The difference in decay mechanism of *P. chrysosporium* and *P. sordida* was obviously observed. The *P. chrysosporium* showed no selectivity to lignocellulose. The wood cell walls were eroded and the ML were degraded by activity of *P. chrysosporium* (Fig $3.4a_2$ and and $3.4c_1$). This is different from *P. sordida* white-rot fungus which preferentially degraded lignin instead of polysaccharides, causing defibrillation of wood (Fig. $3.4d_1$-d_3). These microscopic observations are consistent with previously reported (Schmidt, 2006; Burdsall, 1985; Koyani and Rajput, 2014; Schwanninger et al., 2004). SEM observations revealed that fungi colonized its hyphae in vessel members and then penetrated the neighboring parenchyma cells of *E. fordii* (Fig. $3.4a_3$) or fiber cells of beech wood (Fig. $3.4c_2$) to promote degradation. Furthermore, observations in the radial direction showed the penetration of hyphae from vessel lumen into adjacent cells via vessel pits (Fig. $3.4b_3$), and vessel-ray pits were destroyed by fungal activity (Fig. $3.4c_3$). This observation was supported by findings from previous studies, which reported that hyphae tended to colonize the vessel lumen of infected hardwoods (Wilcox, 1970), then branch through simple or bordered pits to open pits, and resolve the hyphal penetration (Bari et al., 2015; Schwarze, 2007).

3.3.2. Chemical characterization

Lignin monomer composition and distribution among cell types and within different cell layers were the chemical parameters determining wood durability (Skyba et al., 2013). Based on TAPPI T222 om-98 examination, *E. fordii* wood had a higher Klason lignin content than beech wood. These values are 33.4% (0.14) and 20.6% (0.15) for *E. fordii* and beech wood, respectively. The numbers given in the brackets are standard deviation. Fig. 3.5a–f shows the 2D HSQC NMR spectra of the whole control and degraded woods obtained at the solution stage in DMSO-d_6. The main lignin substructures identified are also shown. The different lignin and polysaccharide cross-signals assigned on the spectra are listed in Table 3.1, as previously described (Martínez et al., 2011; Li et al., 2016; Yue et al., 2016). The results of a semi-quantitative analysis of the integrals of the HSQC cross-signal are listed in Table 3.2.

The differences between the spectra of fungal-degraded and control woods were observed. Cross peaks were observed at 106.2/6.47 (G_c) and 107.4/6.26 (G'_c) ppm, which can be assigned to guaiacyl-condensed units. This is due to that correlation around 6.5/110 ppm can be assigned to C_6-H_6 correlation of 4−O−5 structures based on the NMR data of lignin models, as previously report (Li et al., 2016). However, the presence of the equivalent G units could not be unequivocally established. The most significant difference between lignin structures of *E. fordii* wood and beech wood was that the former had a new signal determined as G''_c (Table 3.2). Although, this signal was slightly shifted to 108.5/6.90 ppm, it can be assigned to C_2-H_2 correlations on the aromatic rings of 4−O−5-linked unit (Li et al., 2016; Yue et al., 2016). It is also indicated that the structure of condensed lignin contents a substituent in the C-5 position, e.g., 5-5, β-5, and 4−O−5 structures (Heitner et al., 2010). The G/S-ratios of *E. fordii* were also higher than those of beech wood. Therefore, the main difference in the molecular structures of *E. fordii* and beech wood is the more condensed nature of

E. fordii lignin. The localization and structure of lignin are important wood properties because G are more strongly cross-linked and therefore, more resistant to chemical degradation than lignins with a high S (Nuopponen et al., 2006).

Table 3.1. Assignment of lignin and polysaccharide ^{1}H-^{13}C correlation signals in the HSQC spectra shown in Fig. 3.4.

Labels	δ_C/δ_H (ppm)	Assignment
$S_{2,6}$	103.9/6.69	C_2-H_2 and C_6-H_6 in syringyl units
$S'_{2,6}$	106.4/7.18	C_2-H_2 and C_6-H_6 in C_α-oxidized syringyl units
G_c	106.2/6.47	Condensed-lignin aromatics related to $4-O-5$ structures
G'_c	107.4/6.26	Condensed-lignin aromatics related to $4-O-5$ structures
G_2	111.3/6.95	C_2-H_2 in guaiacyl units
G'_2	111.7/7.39	C_2-H_2 in C_α-oxidized guaiacyl units
G_6	118.9/6.75	C_6-H_6 in guaiacyl units
G'_6	123.0/7.53	C_6-H_6 in C_α-oxidized guaiacyl units
G''_c	108.5/6.90	Condensed-lignin aromatics related to $4-O-5$ structures
$A_{\beta(G)}$	83.5/4.30	C_β-H_β in β-O-4′ substructures linked to a guaiacyl unit
$A_{\beta(S)}$	86.3/4.04	C_β-H_β in β-O-4′ substructures linked to a syringyl unit
C_α	86.9/5.44	C_α-H_α in β-5′ (phenylcoumaran) substructures
B_α	84.8/4.68	C_α-H_α in β-β′ (resinol) substructures
D_α	81.3/5.08	C_α-H_α in β-1′ (spirodienone) substructures
-OMe	55.5/3.74	Methoxyl
Gl_1	103.1/4.30	C_1-H_1 in (1-4) β-D-glucopyranoside
X_1/X'_1	101.5/4.33	C_1-H_1 in β-D-xylopyranoside/3-O-acetyl-β-D-xylopyranoside
M_1	100.5/4.56	C_1-H_1 in (1- 4) β-D-mannopyranoside
X'_2	73.1/4.46	C_2-H_2 in 2-O-acetyl-β-D-xylopyranoside
X'_3	74.8/4.80	C_3-H_3 in β-D-xylopyranoside

Table 3.2. Semi-quantitative analysis of the integrals of the HSQC cross-signal of lignin and carbohydrates.

Labels	E. fordii			Beech		
	Control	P. chrysosporium	P. sordida	Control	P. chrysosporium	P. sordida
$S_{2,6}$	77.0	81.4	81.9	103.9	84.9	103.1
$S'_{2,6}$	11.1	12.0	12.7	15.3	28.5	16.1
G_c	10.3	8.9	10.7	8.5	8.4	8.3
G'_c	8.4	6.8	8.8	1.8	1.2	1.4
G_2	47.1	44.8	44.3	33.1	31.1	32.6
G'_2	8.8	8.5	8.4	7.3	12.2	7.8
G_6	52.9	48.8	54.4	32.3	31.6	32.9
G'_6	3.3	3.0	3.4	3.1	7.3	3.2
G''_c	7.0	3.9	3.4	0.0	0.0	0.0
$A_{\beta(G)}$	21.8	22.2	19.2	27.9	18.8	26.2
$A_{\beta(S)}$	30.2	33.0	30.6	29.7	16.4	27.6
C_α	5.5	5.6	5.7	3.8	2.5	3.5
B_α	9.5	10.8	10.6	7.1	5.7	7.4
D_α	1.2	1.6	1.7	3.8	2.5	3.7
-OMe	537.6	581.0	597.5	650.0	658.6	648.9
Gl_1	25.9	28.2	29.6	65.3	187.3	78.8
X_1/X'_1	48.5	49.5	49.1	64.5	78.8	73.5
M_1	11.8	9.7	10.3	14.2	17.5	13.2
X'_2	21.4	20.9	22.4	46.5	62.0	52.6
X'_3	16.3	15.2	16.4	41.7	49.2	43.5

Analysis of the 2D HSQC NMR spectra of *E. fordii* wood (Fig. 3.5a–c) before and after fungal exposure revealed similar signals for lignin and polysaccharide moieties, including cellulose and hemicelluloses. The lignin intensities of degraded woods with their characteristic one-bond δ_C/δ_H correlation at 108.5/6.90 (G''_c) was lower than those of control samples. On the other hand, the polysaccharide signals at 100.5/4.56 (M_1), 73.1/4.46 (X'_2), and 74.8/4.80 (X'_3) ppm of degraded and control samples were substantially less significant. Besides, these lignin and polysaccharide intensities of *E. fordii* wood exposed to *P. chrysosporium* were slightly lower than those of *P. sordida*.
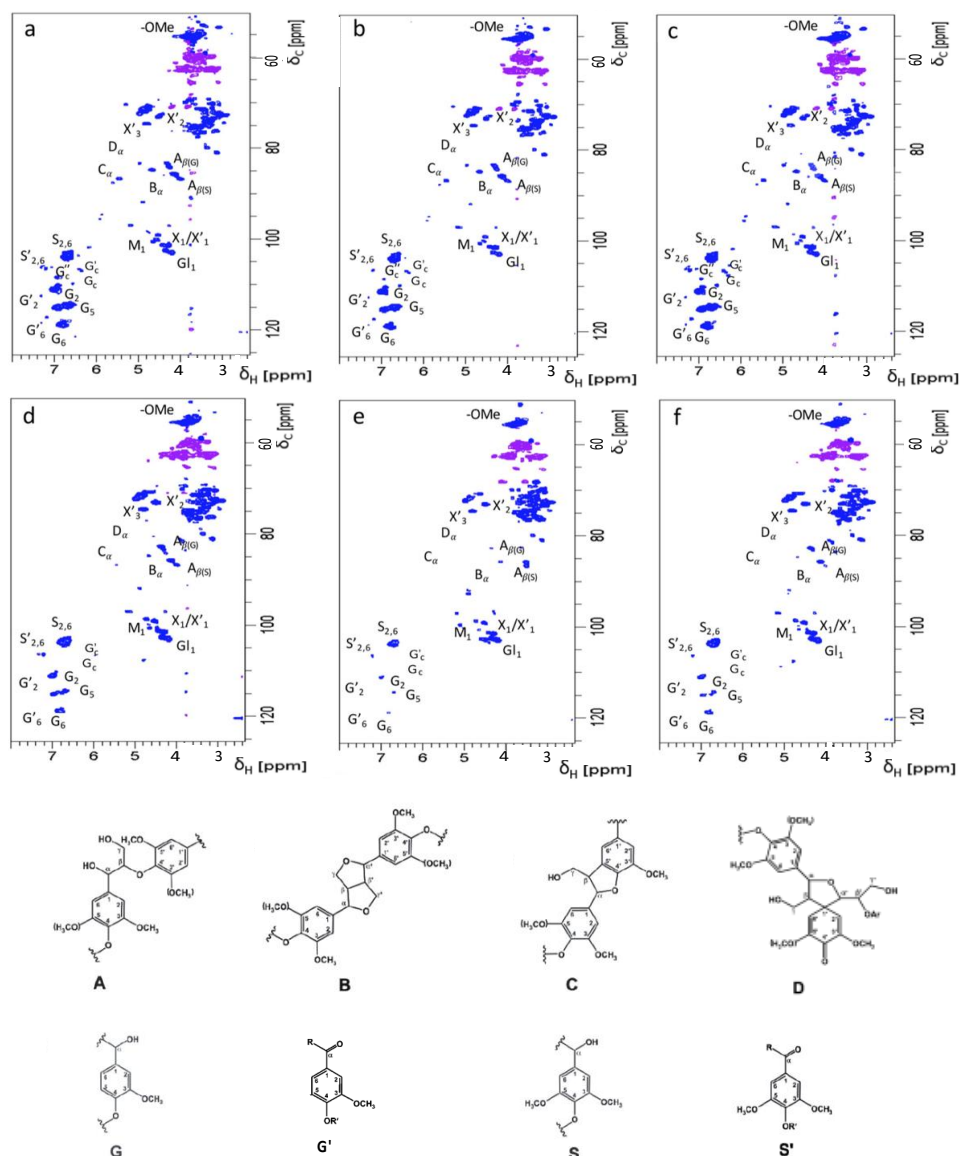
Fig. 3.5. 2D HSQC NMR experiments in the solution state of: (a) control *E. fordii* wood; (b) *E. fordii* wood degraded by *P. chrysosporium*; and (c) *E. fordii* wood degraded by *P. sordida*; (d) control beech wood; (e) beech wood degraded by *P. chrysosporium*; and (f) beech wood degraded by *P. sordida*. The main lignin structures identified are also shown: (A) β-*O*-4′ substructure; (B) resinol substructure; (C) phenylcoumaran substructure; (D) spirodienone substructure; (G) guaiacyl unit; (G') C_α-oxidized G unit; (S) syringyl unit; (S') C_α-oxidized S unit (R, lignin or OH; R′, H or lignin). See Table 1 for signal assignment.

In contrast to *E. fordii* wood, analysis of the 2D HSQC NMR spectrum of beech wood revealed a significant decrease in both lignin and polysaccharide signals (Fig. 3.5d–f). The C_2-H_2 and C_6-H_6 in syringyl units were lower in treated woods because of fungal activity. The C_β-H_β correlation in β-*O*-4′ substructures (A_β) was observed at δ_C/δ_H 83.5/4.30 for β-*O*-4′ substructures linked to S units, at δ_C/δ_H 86.3/4.04 for β-*O*-4′ substructures linked to G units, which decreased after the fungal test. Decreasing signals of other lignin substructures were also identified in the HSQC spectra. A strong signal for resinols (B_α), phenylcoumaran (β-5′) substructures (C_α) and spirodienone (D_α) decreased in the wood treated with *P. chrysosporium*, while those values were relatively unchanged in the wood exposed to *P. sordida*. In addition to lignin removal, the NMR spectrum of the white rotted wood also revealed a simultaneous increase in polysaccharide signals, especially for wood treated with *P. chrysosporium*. This may because *P. chrysosporium* produced more extracellular slime called sheath, composed of β-glucan, in the sample analyzed and that the signal was observed at δ_C/δ_H 103.1/4.30 for β-D-glucopyranoside. While variations do exist concerning wood species, *P. chrysosporium* is well known to be a simultaneous white rot fungus causing decay of lignin, cellulose, and hemicelluloses at the same rates. The *P. sordida* exhibited preferential delignification, as reported previously (Schmidt, 2006; Skyba et al., 2013; Li et al., 2016; Yue et al., 2016). These findings are consistent with microscopic observation.

Wooden cultural properties are degraded by fungi (brown-rot, white-rot, and soft-rot fungi) and bacteria (erosion, tunneling, cavitation, etc.). These processes, at the same time are driven by different environmental factors which have not been explicitly explored within this study. Although further examinations are needed, *E. fordii* wood exhibited significant resistance to fungal degradation. Morphological

investigation and chemical analysis revealed that its excellent natural durability is probably due to the unique structure of fibers and the highly-condensed lignin content.

3.4. Summary

The rationale for the traditional selection of *E. fordii* wood was suggested from its morphological and chemical properties. Although, *E. fordii* wood was unable to inhibit fungal growth, it exhibited marked resistance to degradation by wood decay fungi evaluated. The characteristic of a fungi-resistance *E. fordii* wood presented in this study is of particular relevance to the highly-condensed lignin content as well as the compactness of wood fibers. This explains why *E. fordii* wood can survive underground for centuries, even for a millennium. The internal part of excavated *E. fordii* wood is sometimes intact and does not need to be preserved. In such cases, conservation of the degraded outer layer with an appropriate consolidation agent may be sufficient for this particular wood species.

Chapter 4. Evaluation of chemical treatments on dimensional stabilization of archaeological waterlogged hardwoods

4.1. Introduction

Archaeological WW is often subject to extreme levels of shrinkage and drastic changes in shape upon drying due to its high degree of wood tissue deterioration (Bugani, 2009; Christensen, 2012). The wood structure resembles a sponge, absorbing a large amount of water. The waterlogged wooden objects will retain their shape as long as they remain wet (Broda and Mazela, 2017; Rowell and Barbour, 1990; Jiachang et al., 2009). If such a wood is exposed to air, the weakened cell walls are unable to withstand the stresses imposed by the surface tension of receding columns of liquid water, leading to a collapse of the wood structure (Pearson, 1987). Therefore, the first step in WW conservation involves the use of an appropriate consolidation agent to replace the water that fills the WW structure. The conservation treatment will protect wooden objects against shrinkage, collapse, and loss of shape upon drying (Broda and Mazela, 2017; Rowell and Barbour, 1990; Pearson, 1987). Water contained in the WW structure can be replaced only in the lumen of cells, but it is usually necessary to also replace the water in the wood cell walls (Bugani, 2009). The dimensional stabilization of WW depends on the amount of impregnation agent in the treated wood, in particular its penetration in the wood cell walls (Reinprecht, 2016).

Currently, the most widely used consolidation method involves PEG, which is freely soluble in alcohols (ethanol, methanol, and isopropanol) as well as water. Low-molecular PEG is appropriate for the conservation of lightly deteriorated WW, while high-molecular PEG is more suitable for heavily decayed wooden objects (Broda and Mazela, 2017; Babiński, 2015). The PEG treatments are commonly used because of

the low cost of materials and equipment and the satisfactory results obtained. Unfortunately, PEG is not a perfect agent for wood conservation due to its considerable disadvantages (Hocker et al., 2012). PEG leaches from treated wood as the exposure to temperature and humidity changes, causing irreversible shrinkage and structural collapse (Smith, 2013). Moreover, the chemical reaction of PEG with other substances can cause further wood degradation. It has been shown that the reactions of PEG with metal and/or the sulfur compounds present in WW (e.g. ships) produce various low-molecular weight organic acids (formic, glycolic, oxalic), causing further wood degradation (Hocker et al., 2012; Mortensen, 2009; Sandström et al., 2002; Unger et al., 2001).

Because of the many adverse effects of PEG, conservators are now exploring additional treatment options to conserve WW. Among them, the use of carbohydrates as a conservation material has been investigated (Babiński, 2015; Babiński et al., 2017; Horie, 2010; Morgós et al., 2015; Unger et al., 2001). Carbohydrates have many advantages such as non-toxic, non-corrosive, and low hygroscopic properties. The conservation of WW with sucrose, mannitol, and recently lactitol and trehalose was reported Babiński, 2015; Babiński et al., 2017; Morgós et al., 2015; Unger et al., 2001). The impregnation processes could be accomplished with or without heating because of the small molecular sizes of chemical. The wood thus conserved has a natural color and carbohydrates can also be easily extracted from treated wood so the treatment can be reversed (Morgós et al., 2015).

Interest in further seeking green materials (such as keratin (Kawahara et al., 2002; Endo et al., 2008; Endo and Sugiyama, 2013; Endo et al., 2015)) for the consolidation of wood has been increasing in recent years (Walsh et al., 2017; Mchale et al., 2017). The dimensional stability of the WW treated with keratin was excellent.

The treatment involving feather keratin enhanced the mechanical properties of WW (Endo et al., 2010). The low molecular weight of keratin resulted in its fast diffusion into the WW. The color of the keratin-treated wood was quite similar to that of normal wood (Babiński et al., 2014). Additionally, feather keratin-treated wood had antimicrobial activity. However, there are few reports on the conservation of tropical WWs.

The purpose of this chapter was to compare general preservation treatment methods using PEG, trehalose, and feather keratin on Vietnamese WWs. Finding an effective consolidation agent for WW conservation will facilitate the preservation of such historic resources for future generations.

4.2. Materials and methods

4.2.1. Materials

Archaeological WW samples were collected from the Thang Long Imperial Citadel excavation site. Based on microscopic observations, the samples were identified as *Albizia* sp., *Afzelia* sp., *Bouea* sp., *Dysoxylum* sp., *Elaeocarpus* sp., *Garcinia* sp., and *Syzygium* sp. The samples were cut into $20 \times 20 \times 10$ mm blocks (radial × tangential × longitudinal dimensions).

Polyethylene glycol 4000 ($C_{2n}H_{4n+2}O_{n+1}$, PEG4000) were purchased from Wako Pure Chemical Industries, Japan. Trehalose ($C_{12}H_{22}O_{11}$, TREHA®) was obtained from Hayashibara Co. Ltd, Japan and feather keratin powder (KERATIDE®) was purchased from Toyo Feather Industry Co. Ltd., Japan. All the chemicals were used without further purification.

4.2.2. Methods

Treatment

The samples were saturated in distilled water at a low pressure of 0.1 MPa for 40 min and the weight of each specimen was measured. The specimens ($n = 5$) were immersed in a 50% (w/w) aqueous solution of keratin at 60 °C for 2 weeks. The WW specimens were then removed from the keratin solution and immersed in a 4M Magnesium sulfate heptahydrate aqueous solution at 60 °C for 2 weeks. The samples were subsequently removed from the solution and dried in ambient temperature.

For the PEG and trehalose ($n = 5$ for each treatment) impregnations, the fully water saturated blocks were immersed in 20% (w/w) solutions at 60 °C, and the concentration of the PEG or trehalose solution was increased every two weeks in steps of 10%. Finally, the samples were treated with a 70% solution and dried in air at room temperature for a week.

After drying, all the specimens were seasoned to a constant weight in air at a relative humidity (RH) of about 60% and temperature 20 °C. The equilibrated samples were imaged and the shrinkage or swelling rates were calculated from the sample images obtained using the Image-J software (https://imagej.nih.gov).

Dimensional stability tests

To evaluate the efficiency of chemical treatment, the dimensional stability of WWs was determined by measuring the shrinkage or swelling rates, anti-shrink/swell efficiency, and increase in the weight of wood after treatment.

The anti-shrink/swell efficiency (*ASE*) denotes the percentage of shrinkage or swelling of the untreated wood that has been suppressed by a stabilizing treatment. It was calculated from the sample images obtained using the Image-J software according to Eq. (4.3):

$$ASE = \frac{\beta_0 - \beta_1}{\beta_0} \text{ x } 100$$

$$(4.3)$$

where *ASE*: anti-shrink/swell efficiency (%), β_0: linear shrinkage or swelling of the untreated wood [%], and β_1: linear shrinkage or swelling of treated wood (%).

Linear wood shrinkage or swelling in the tangential, radial, and longitudinal directions was calculated using Eq. (4.4):

$$\beta = \frac{l_0 - l_1}{l_0} \text{ x } 100$$

$$(4.4)$$

where β: linear wood shrinkage or swelling [%]; l_0: initial sample dimension (at the maximum moisture content; waterlogged) [mm]; l_1: final sample dimension (after drying and seasoning) [mm].

The weight percent gained (*R*) was calculated on the basis of an increase in the mass of the treated wood sample relative to the mass of an identical untreated sample according to Eqs. (4.5) and (4.6):

$$R = \frac{m_t}{m_{em}} \text{ x } 100 = \left(\frac{m_{em+i} - m_{em}}{m_{em}} \right) \text{ x } 100$$

$$(4.5)$$

$$m_{em} = \frac{m_w}{U_{max} + 1} \quad ,$$

(4.6)

where R: weight percent gained, m_t: mass of a treatment medium, m_{em}: estimated mass of an oven-dried untreated sample, m_{em+i}: mass of an oven-dried treated sample, m_w: mass of a saturated waterlogged control sample, and U_{max}: the maximum moisture content of the control sample.

SEM observations

The untreated and chemically treated specimens were prepared from internal part of samples. They were freeze-dried for 4 days and then coated with platinum using an auto fine coater (JFC-1600, JEOL, Japan) operated at 30 mA for 90 s. A field emission SEM (JSM-7800F prime, JEOL, Japan) was operated at an accelerating voltage of 2 kV.

4.3 Results and discussion

Figure 4.1 presents the properties of all tested WWs. All the samples corresponding to the different species showed the same behavior. A higher water content is associated with the lower basic density of WW. The maximum moisture content in all WWs ranged between 315% and 612%, while the basic density of wood was between 0.14 and 0.25 g/cm^3.
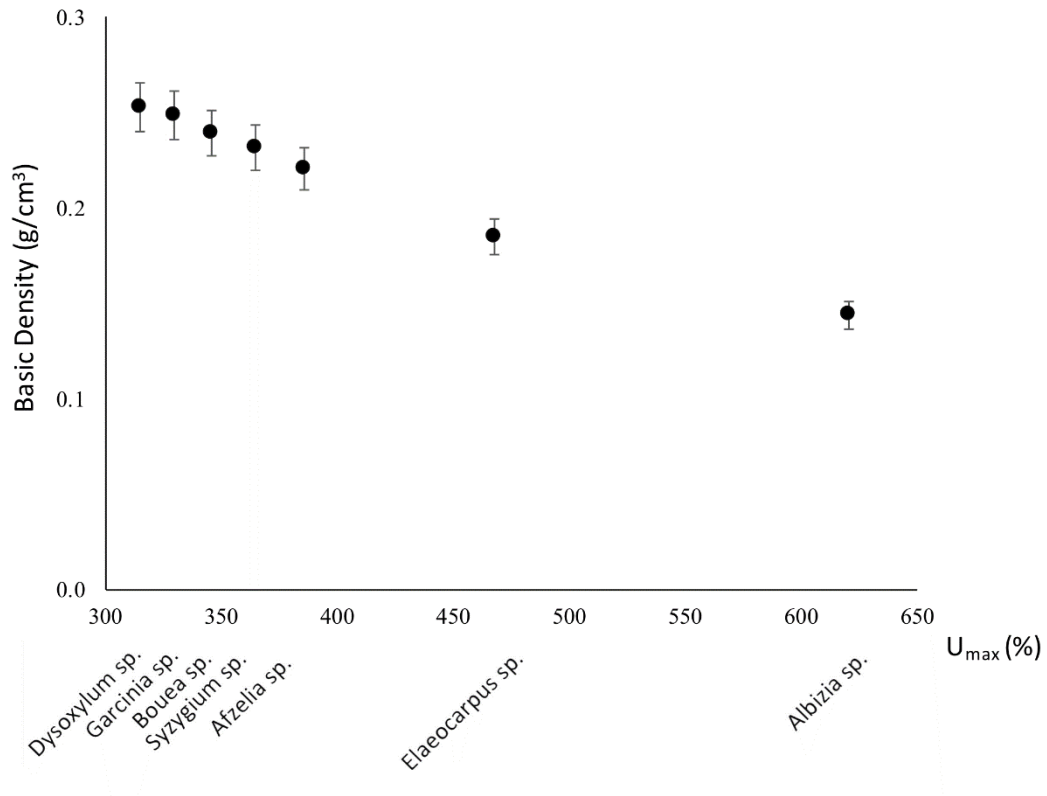
Fig. 4.1. Relationship between basic density and the maximum moisture content.
The bars represent the standard deviations.

The degradation of WW results in the loss of wood substances such as the polysaccharides cellulose and hemicellulose (see Fig. 1.2 in Chapter 1). Such losses are immediately compensated by the filling of woods with water. Therefore, the increase of maximum wood moisture content (U_{max}) and decrease of basic density together indicate increasing wood degradation (Broda and Mazela, 2017; Rowell and Barbour, 1990). Among the samples being researched, two classes of wood degradation can be distinguished, according to U_{max} limit values of 185% and 400% (Rowell and Barbour, 1990). The *Elaeocarpus* sp. and *Albizia* sp. samples evaluated according to the above criterion can be classified as heavily deteriorated (U_{max} from 467% to 621%). The remaining samples were evaluated based on the same criterion, and could be classified as medium-degraded (U_{max} from 315% to 385%).

Chemically degraded WWs showed the extensive changes in dimensions due to wood tissue degradation. The measurement of the shrinkage rate of untreated WWs showed extremely high values in all three directions (Fig. 4.2). Depending on the wood species and its extent of degradation, tangential shrinkage varied between 36.3% and 56.7%, while the radial variation was between 18.1% and 30.6%. The longitudinal shrinkage was between 10% and 15.6%.
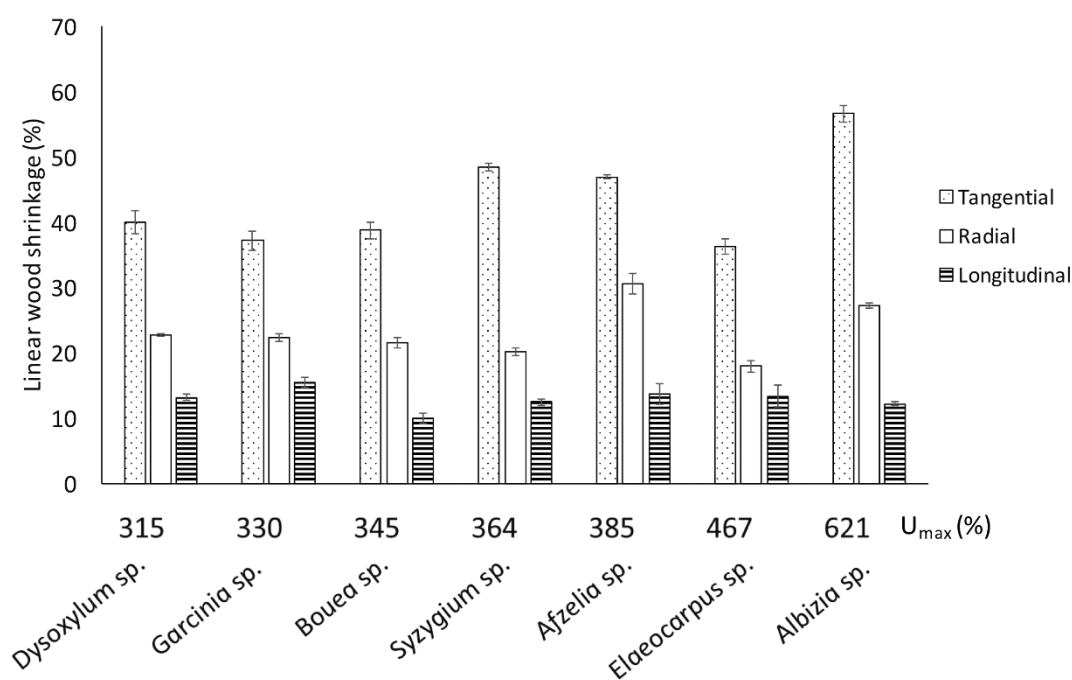
Fig. 4.2 Shrinkage ratios of the untreated WWs. The bars represent the standard deviations.

However, the dimensional stability of WWs was significant improved after chemical treatment (Fig. 4.3). The linear shrinkage value for the tangential direction ranged between 1.1% and 13%, while the variation in the radial direction was between 0.7% and 6.4%. The shrinkage in the longitudinal direction was less than 2%. In particular, the three-dimensional characteristic of PEG-stabilized WWs was well-preserved. After being treated with PEG and subjected to air drying, the shrinkage value in the tangential direction ranged between 1.3% and 6.2%, while it varied

between 0.7% and 3.1% in the radial direction. The smallest shrinkage value (<1.9%) was measured in the longitudinal direction. Similarly, good dimensional stability was achieved in the WWs after trehalose treatment. The shrinkage varied between 1.1% and 6.8% in the tangential direction, 0.7% and 3.6% in the radial direction, and was less than 1% in the fiber direction. After keratin treatment, the dimensions of the WW samples were well preserved. The shrinkage in the tangential direction ranged from 1.7% to 13%, while the contraction in the radial direction varied between 0.7% and 6.4%. Additionally, the longitudinal shrinkage decreased to about 0.2–1.6%.
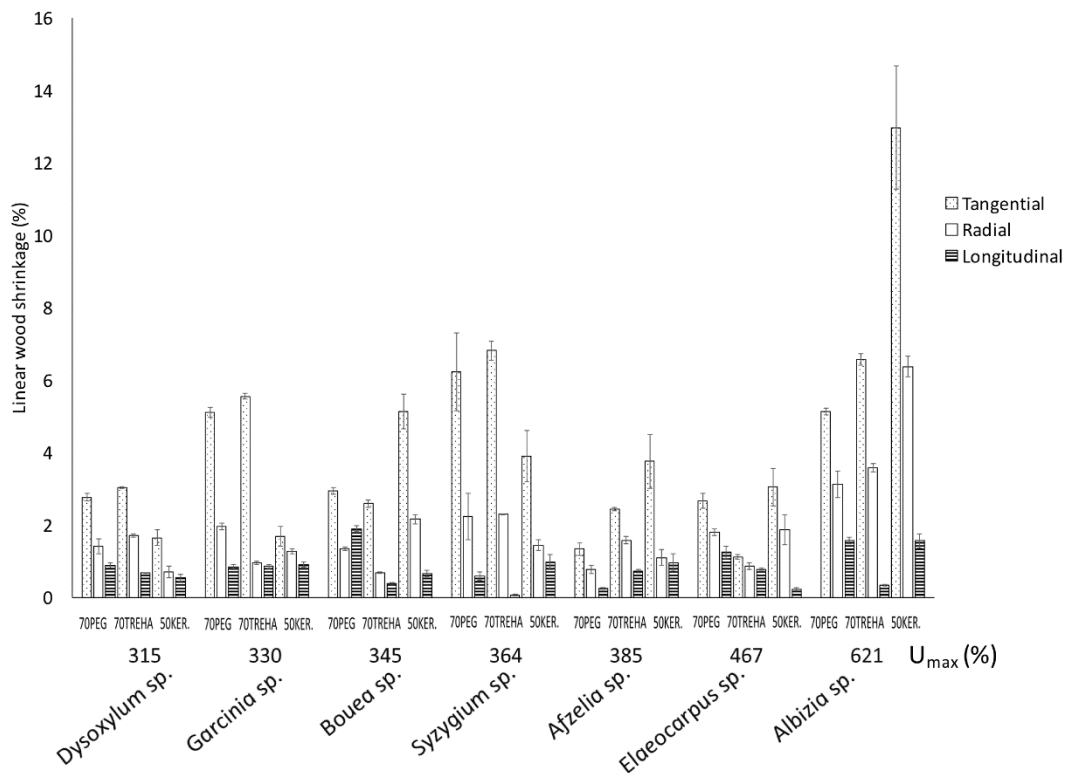
Fig. 4.3 Shrinkage ratios of treated WWs. The bars represent the standard deviations.

The mean value of ASE of different WW species after pretreatment with the tested impregnations, air drying, and equilibrating at 60% RH and 20 °C is presented in Fig. 4.4. The obtained results clearly indicate that PEG, trehalose, and keratin stabilized the WWs effectively. For the WWs treated with trehalose, the ASE values

were about 86.2–96.4%; the corresponding values for PEG treatment were about 87.1–96.9%. After the treatment with keratin, ASE values increased beyond 89%, except for the case of the heavily degraded WW (U_{max} = 612%, ASE value only 72%). According to previous reports (Unger and Unger, 1995), an ASE exceeding 75% is considered as acceptable in conservation science. Therefore, the dimensional stability of heavily degraded WWs after keratin treatment was not sufficient enough.
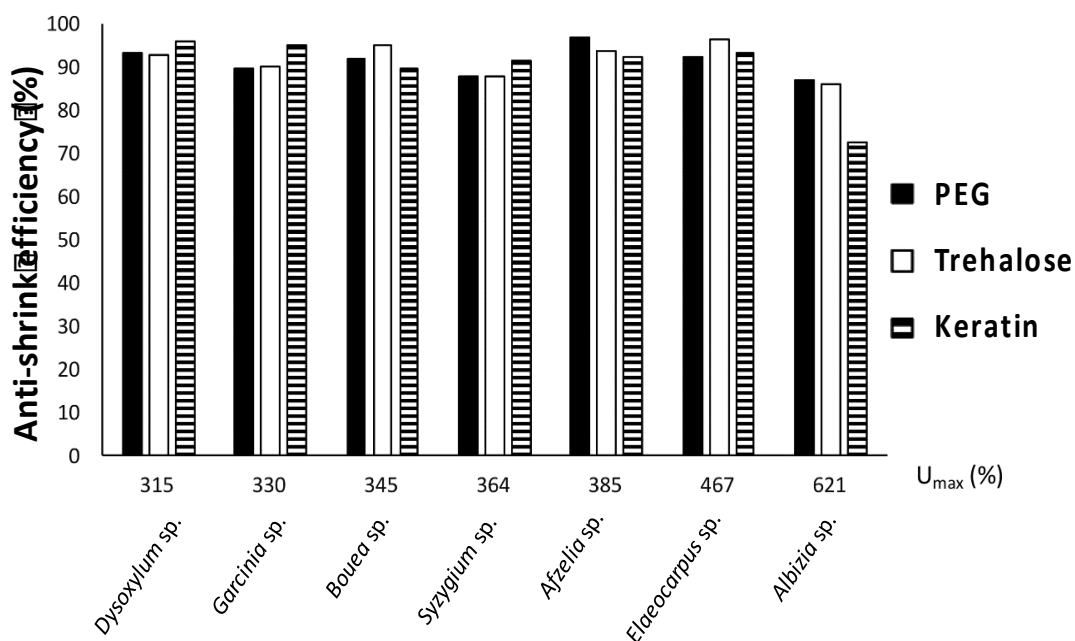
Fig. 4.4 ASE of treated WWs.

The uptake of chemical agents after the consolidation treatment is shown in Fig. 4.5. In general, the amount of chemical uptake increased with increasing U_{max}, except for *Syzygium* sp. The impregnations of keratin and trehalose into WWs were smaller than that of PEG. The weight percent gained after the keratin and trehalose treatments was about twice lower compared to that after the PEG treatment. The weight of PEG-treated WW becomes significantly different in the case of conservation of large wooden objects such as those obtained from the Vasa shipwreck, which are suspended when exhibited (Hocker et al., 2012).
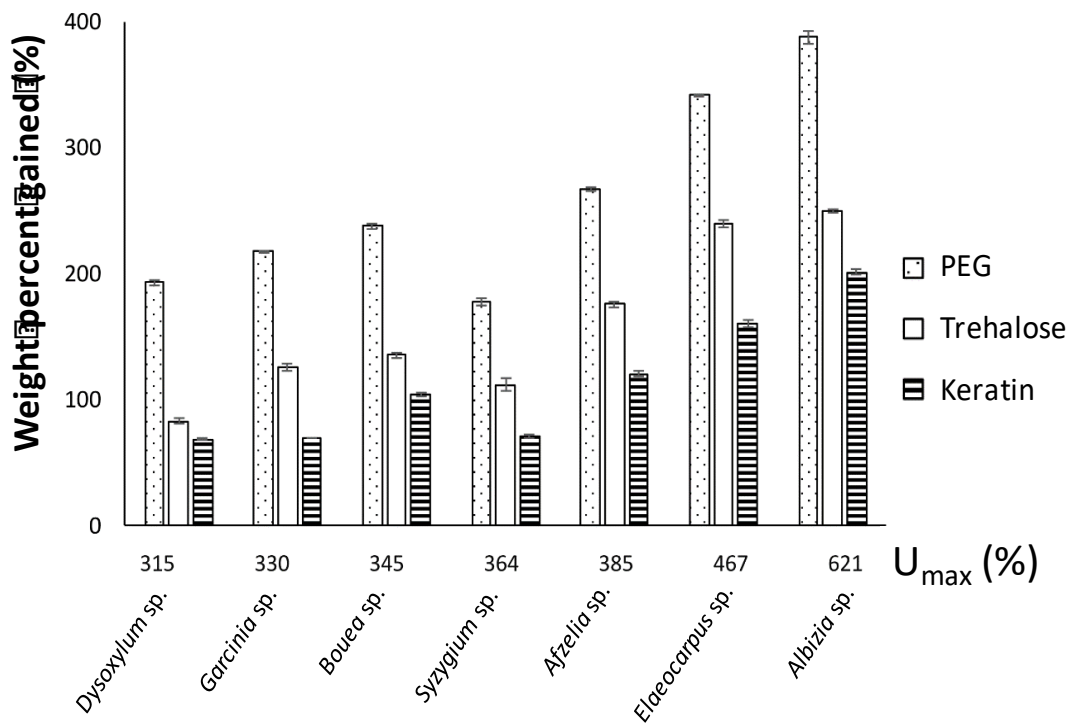
Fig. 4.5 The weight percent gained after chemical treatments for the different specimens. The bars represent the standard deviations.

SEM observation

Microscopic examinations revealed the significant differences in structures between the untreated and treated wood samples (Fig. 4.6). The freeze-dried WW without treatment revealed severe degradation of its cells. Bacterial attack of a WW causes loss of wood strength. Particularly, the S_2 layer of fibers was almost completely destroyed by biological degradation, detached from the ML, and became distorted, as seen in Fig. 4.6a_1-a_2. The parenchyma cells were however still intact (Fig. 4.6a_1). The dimensional stability of WWs involved filling the inside of both cell walls and/or cell lumina. The appearances of the woods treated with PEG and trehalose were similar. Most fibers and parenchyma cells were filled by the impregnation agent, while lumen of the vessels remained empty (Fig. 4.6b_1-b_2 and c_1-c_2). However, in the keratin-treated wood, the lumen of cells was almost empty (Fig. 4.6 d_1). The ML maintained the original structural dimension without the support of fillers such as PEG or trehalose.

This observation indicated that the stabilizing effect of keratin was different from those of PEG or trehalose. Keratin specifically adsorbed on the lignin-rich ML. Keratin also has an affinity for lignin degradation products, as has been previously reported (Endo and Sugiyama, 2013).
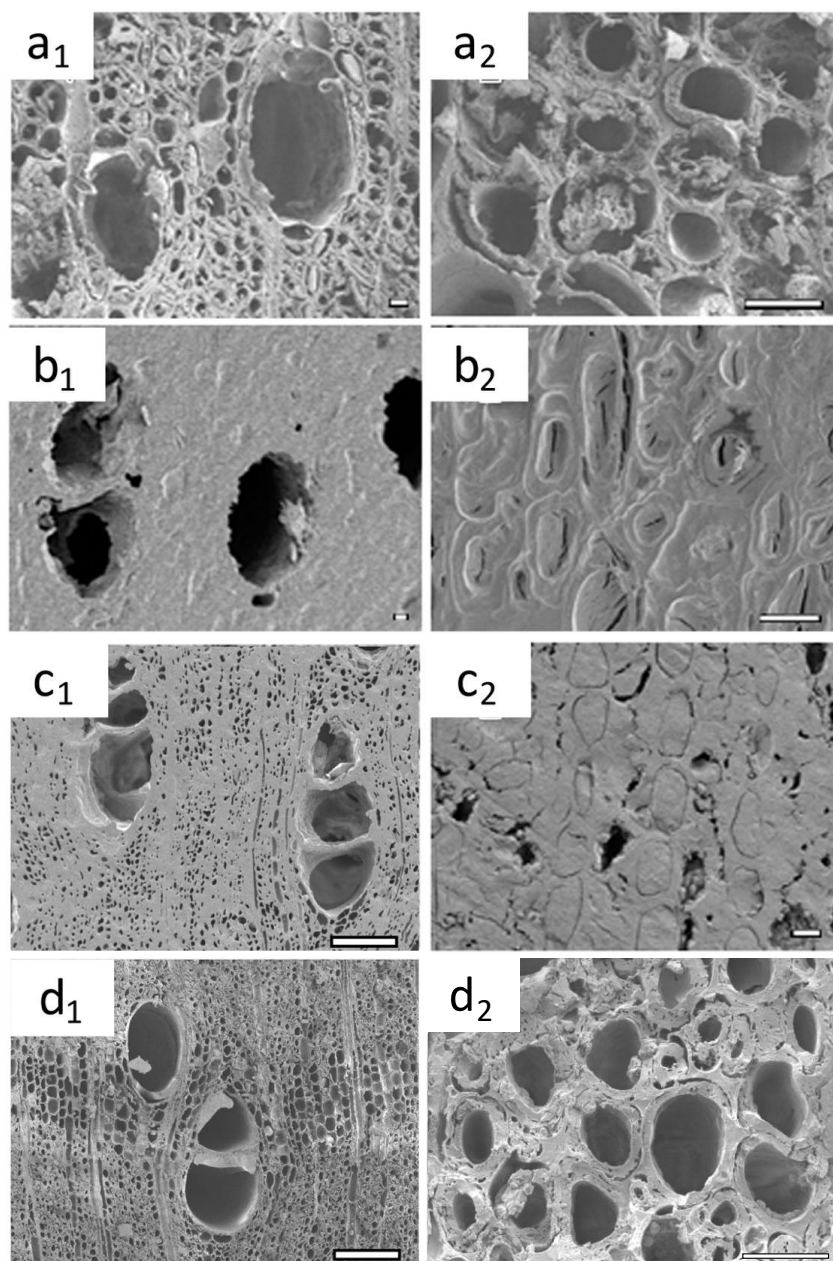
Fig. 4.6 SEM images of waterlogged *Dysoxylum* sp. wood: (a_1-a_2) untreated wood, (b_1-b_2) treated with PEG, (c_1-c_2) treated with trehalose, and (d_1-d_2) treated with keratin. For a_1, b_1, c_1, d_1, the scale bars represent a distance of 100 µm; for a_2, b_2, c_2, d_2, the scale bars represent 10 µm.

Although the stabilization effect of chemical treatment on WWs is one of the most important parameters, the artistic appearance of woods is also a meaningful feature worth considering. The coloration of the as-treated samples is presented in Fig. 4.7. The dimensions of the WWs treated with PEG, trehalose, or keratin were well preserved. The PEG-treated wood samples were unnaturally darker in color, while the trehalose-treated samples appeared slightly lighter. The appearance of feather keratin-treated woods was much more natural. The color of WWs after keratin treatment was similar to that of modern wood.

Fig. 4.7 Post-treatment appearance and coloration of the waterlogged *Dysoxylum* sp. wood after air drying: (a) untreated, (b) treated with PEG, (c) treated with trehalose, and (d) treated with keratin. The solid bar below represents 1 cm.

In summary, all chemical treatment procedures provided satisfactory stabilizing effects. The ASE values reached above 82% except for the case of the heavily-decomposed WW ($U_{max} = 621\%$) treated with keratin, for which it was lower than 75%. Based on the improved dimensional stability of wood, shortened impregnation time, and color of WWs after the treatments, keratin showed as good performance in average as material for WW conservation

4.4. Summary

Treatment with PEG, trehalose, and keratin resulted in sufficient dimensional stabilities of WWs. The ability of keratin treatment to protect the dimensions of severely degraded WW was not as good as those of PEG or trehalose. The main purpose of WW conservation is to prevent dramatic dimensional changes of artefacts caused by the shrinkage and collapse of weakened cell walls upon drying. It is also important to reduce the impregnation time and protect the original appearance of historical wooden objects. Additionally, the reversibility of the treatment processes is also a criterion used in the conservation and restoration of archaeological artefacts. Keratin treatment shortened impregnation time and the good aesthetic results obtained from this treatment. Furthermore, keratin can be removed from treated objects, so such a treatment can be reversed. Due to the inherent limitations of WW materials, this study has investigated the impregnation of WWs with commonly used chemicals. Further examinations based on different experimental setups are also required. Although several further steps remain in the development of this method, the keratin treatment method presented in this study appears to have unique properties that can be applied practically for the conservation of WW.

Chapter 5. Diffusion of chemicals into archaeological waterlogged hardwoods

5.1. Introduction

Archaeological WW often shows extreme levels of shrinkage and deformation upon drying owing to the high degree of wood-tissue degradation (Bugani et al., 2009; Bugani et al., 2012). Chemical hydrolysis and deterioration by microorganisms in the wet underground environment cause microvoids in the wood cell walls to become larger, increasing the porosity of the wood. However, as long as these voids remain filled with water, WW can retain its shape (Jiachang et al., 2009; Uzielli, 2009). Therefore, the water that fills the wood structure must be replaced with an appropriate consolidation agent in order to protect the wooden object against shrinkage, collapse, and deformation during drying (Broda and Mazela, 2017; Rowell and Barbour, 1990; Pearson, 1987). Water in the lumens of a wood sample can be easily replaced, but it is usually also necessary to replace the water in the cell walls of the wood. Thus, the dimensional stability of a treated sample depends upon the amount of conservation agent in the wood and the ability of the agent to penetrate the cell walls of the sample (Reinprecht, 2016).

The diffusional replacement of water in WW has been investigated with a range of different chemical agents, including carbohydrates (saccharose, lactose, trehalose) (Babiński, 2015; Morgós et al., 2015), PEGs of different molecular weights (PEG300 to PEG6000) (Jiachang et al., 2009; Olek et al., 2016; Giachi et al., 2011; Hocker et al., 2012), polymerizable monomers and cross-linkable precondensates (e.g., melamine and phenolic resins) (Horie, 2010), and keratin (Endo et al., 2008). Furthermore, the conservation of WW has been performed using several types of

diffusion technologies, including multi-spraying, long-term immersion, bandaging, panel impregnation, and pressure-diffusion techniques (Reinprecht, 2016).

The diffusion of a conservation agent into a WW sample depends upon several factors, including temperature of the treatment (Dean, 1993; Vinden, 1983). It is well known that an increase in temperature increases solute diffusion coefficients considerably (Christensen, 1951; Tamblyn, 1985). On the other hand, the rate of solute diffusion through a wood sample decreases with increasing solute molecular weight (Fukuyama and Urakami, 1986; Håfors, 2010; Tarkow et al., 1966; Vinden, 1983). The diffusion of chemical depends on the species of wood (e.g., Scots pine, spruce, oak, or birch (Burr and Stamm, 1947; Håfors, 2010; Jacobson, 2006; Tanaka et al., 2017; Tarkow et al., 1966; Vinden, 1983)), direction of diffusion through the wood (Dean, 1993; Jacobson, 2006; Vinden, 1983), and moisture content of the wood (Dean, 1993). Furthermore, in some species (e.g., *Pinus radiata*), differences in diffusion rates between the sapwood and heartwood can occur owing to heartwood formations, tylosis, and/or the deposition of calcareous materials that reduce the diffusion of solutes through the wood (Bamber and Fukazawa, 1985; Becker, 1976).

An important consideration in the treatment of archaeological wood is the period of time taken to impregnate the artefact with the consolidating solution (Rowell and Barbour, 1990; Pearson, 1987). The processes involved in the diffusion of such solutions through fresh timber have been investigated in previous studies (Burr HD, Stamm, 1947; Fukuyama and Urakami, 1986; Tanaka et al., 2015). However, the area of archaeological WW conservation has received little research attention owing to practical and experimental difficulties and the wide variation in the characteristic properties of archaeological wood samples (Rowell and Barbour, 1990; Unger et al., 2001; Kaye, 1995; Jensen and Gregory, 2006).

It will only be possible to confidently predict the durations required for WW treatments when the diffusion rates of consolidating agents into different types of WW are quantitatively established. Consequently, the purpose of the present chapter was to derive the steady-state diffusion rates of PEG4000, trehalose, and keratin through WWs. Identifying diffusion rates of consolidation agents is the necessity of deciding treatment conditions for each tree species.

5.2. Materials and methods

5.2.1. Materials

Archaeological WW samples were obtained from the Thang Long Imperial Citadel site. Based on their diagnostic anatomical features, a total of eight different taxa, i.e, *E. fordii*, *Dysoxylum* spp., *Garcinia* sp., *Syzygium* sp., *Afzelia* sp., *Albizia* spp. were selected. The samples were cut into $40 \times 40 \times 5$ mm blocks and diffusion along the 5-mm dimension was measured. The outer decayed layers of the sample were removed to give a relatively uniform inner core with minimum defects. Samples were cut from the same beam in order to provide specimens with similar properties. The saturated moisture contents (U_{max}) were determined by weighing the wood samples before and after oven drying at 105 °C.

PEG4000 (Mw: 3,350) was purchased from Sanyo Chemical Industries, Japan. Trehalose (TREHA®, Mw: 342) was obtained from Hayashibara, Japan, and feather keratin powder (KERATIDE®, MW: ~750 Da) was purchased from the Toyo Feathers Company, Japan. All chemicals were used without further purification. Silicone rubber (KE 12) was obtained from Shin-Etsu Chemical Co., Ltd., Japan.

5.2.2. Experimental procedures

Diffusion of the chemicals through the WWs was measured using a diffusion cell based on a design used in previous studies (Vinden, 1983; Dean et al., 1997). A wood specimen was held between the two cups of the diffusion cell (Fig. 5.1). In order to eliminate the effect of pressure on transfer, constant head devices (Mariotte bottles) were connected to each side of the cups. Each side of the cup contained 1000ml of liquid. The specimen was saturated in distilled water at a low pressure of 0.1 MPa for 1 h. Then, the sample was fixed in the diffusion cell using silicone rubber (the effective diffusion area: 900mm^2) to allow diffusion to occur along the required direction. Once the diffusion cell was set up, one side of the cell (C_2) was filled with distilled water and the other side (C_1) with a 10% (w/w) PEG, trehalose, or keratin aqueous solution.
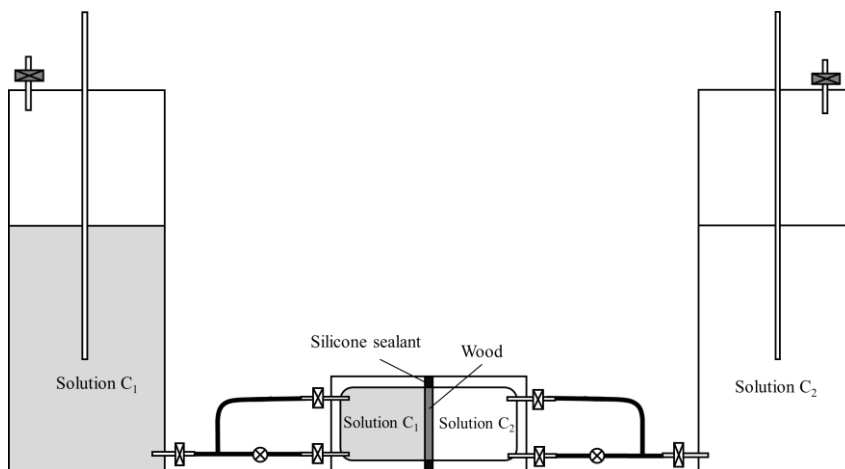
Fig. 5.1. Diffusion apparatus

The apparatus was maintained at a temperature of 28 °C. The chemical agent was allowed to diffuse through the wood sample along the concentration gradient, and the liquid at C_2 was sampled at regular intervals for analysis. 2 ml of liquid samples were taken until a steady-state flow was achieved. The chemical contents were

determined using an oven-dryer (EYALA NDS-450D, Tokyo Rikakikai Co. Ltd., Japan). The liquid samples were dried at 80 °C for 6 h then at 105 °C until a constant weight was achieved.

5.2.3. Determination of diffusion coefficient

In steady-state diffusion, concentration is assumed to be constant with time and, as a result, the flux is constant. The steady-state diffusion coefficient is defined as the quantity of a chemical that diffuses across a particular dimension of a wood sample (A) with time (*dt*) under a concentration gradient ($\partial C/\partial x$), and can be calculated as follows:

$$D = \frac{dQ}{A \, dt \, \frac{\partial C}{\partial x}}$$

The diffusion length is defined as *l*. Within a very short time (namely Δt), the quantity of the diffusing chemical was small enough so it can be considered that the concentration difference between the two sides of the cell is constant and equal to *(C₁ – C₂)/l*. The constant quantity of the chemical diffusing through the wood (*dQ/dt*) is equal to Q_t. Thus, the steady-state diffusion coefficient is simply:

$$D = \frac{Q_t \, l}{A \, (C_1 - C_2)}$$

where *D* is the steady-state diffusion coefficient (m²/s)*, Q_t* is the quantity of solute diffusing through the wood sample (g/s)*, l* is the diffusion length (m), *A* is the effective diffusion area (m²), *C₁* is the concentration of the chemical in the concentrated solution (g/m³), and *C₂* is the concentration of the chemical in dilute solution (g/m³).

5.3. Results and discussion

The specimens examined present different stages of degradation. High U_{max} values, i.e., from 315 to 621%, are typical of medium-to-heavily-degraded wood (Rowell and Barbour, 1990), while U_{max} for *E. fordii* wood is only 68%. The degree of degradation of *E. fordii* wood is limited, despite the artifacts being buried for hundreds of years. The deterioration of WW involves the loss of wood substance, mainly cellulose and hemicellulose (Broda M, Mazela, 2017). An increase in U_{max} as well as a decrease in basic density indicates an increase in the degree of wood degradation (Broda M, Mazela, 2017; Rowell and Barbour, 1990). When a wood sample becomes more porous through the degradation process, the amount of water it contains increases, affecting diffusion rates. The wider channels caused by the loss of cell wall material provide enhanced pathways for the transport of liquids (Robertson and Packer, 1996).

Steady-state diffusion coefficients

Fig. 5.2 presents the mean value of constant mass movement of the chemical diffusing through the wood (Q_t). It was clarified that the mass movement of preservatives depends on wood species. The highest rate of chemical diffusing through the wood was observed in *Afzelia* sp. (U_{max} = 385%), while the lower rate of transfer was found in heavily-degraded samples (*Albizia* sp., U_{max} = 621%). Unsurprisingly, the lowest rate of chemical transfer was determined in *E. fordii* wood (U_{max} = 68%). It is also evidenced that the chemical transfer rate of trehalose was higher than those of keratin or PEG400 in the same direction of wood.
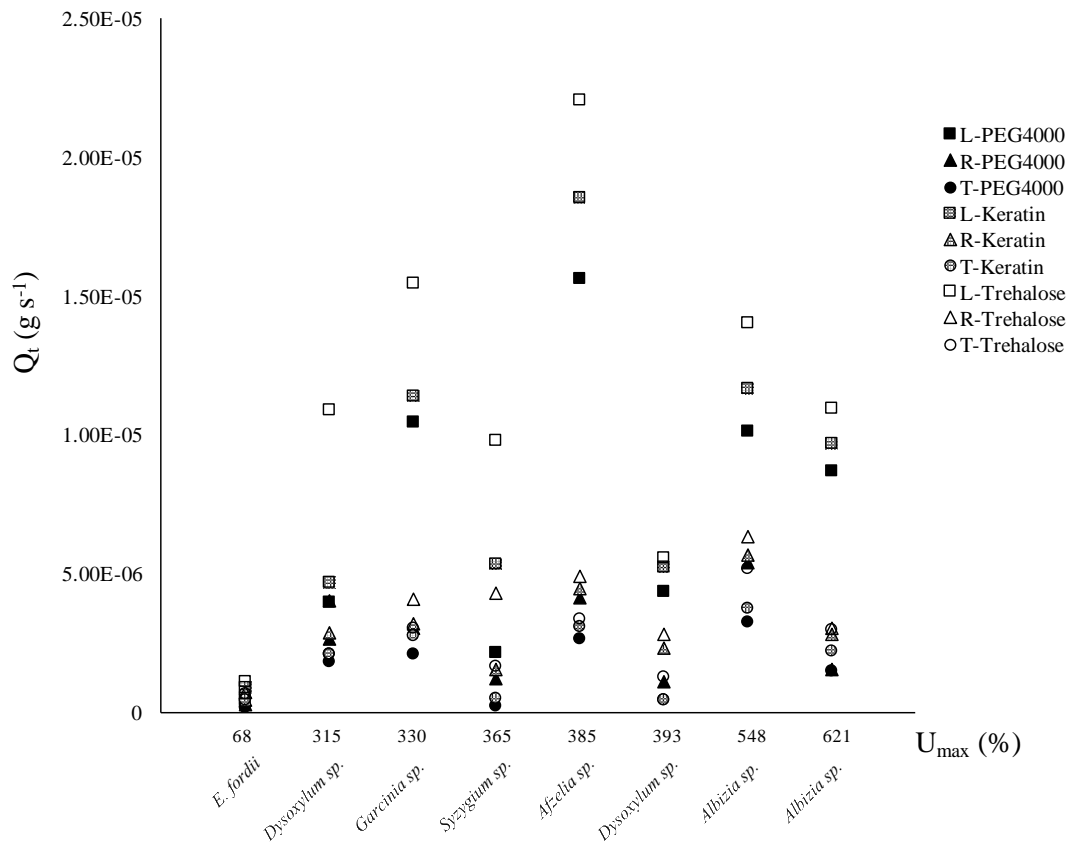
Fig. 5.2. Constant quantity of the chemical diffusing through the wood

L - longitudinal direction, R - radial direction, T - tangential direction

Table 5.1 shows the steady-state diffusion coefficients for the chemicals through the WWs. The values for each species are plotted in Figs. 5.3, 5.4, and 5.5. The variation in the diffusion coefficients is remarkably large owing to the different wood structures. Within the same timber samples, the diffusion coefficients measured in the longitudinal direction are larger than those in the transverse directions. The diffusivity of a chemical depends on its molecular weight. It is clear that the diffusion coefficient of trehalose with a molecular weight of 343 is extremely high. Subsequently, the diffusion of keratin through wood samples with damaged and porous cell walls is high owing to its low molecular weight ~750 Da, while the lowest coefficient is observed for PEG with a molecular weight of 3,350.

Table 5.1. Steady-state diffusion coefficients for trehalose, keratin, and PEG4000

No.	Species	U_{max} (%)	PEG4000			Keratin			Trehalose		
			Longitudinal	Radial	Tangential	Longitudinal	Radial	Tangential	Longitudinal	Radial	Tangential
1	*E. fordii*	68	2.40E-10	1.50E-10	9.00E-11	0.50E-09	0.24E-09	0.23E-09	0.62E-09	0.39E-09	0.36E-09
2	*Dysoxylum* sp.	315	2.27E-09	1.50E-09	1.02E-09	2.70E-09	1.63E-09	1.17E-09	6.29E-09	2.25E-09	1.20E-09
3	*Garcinia* sp.	330	6.07E-09	1.70E-09	1.19E-09	6.66E-09	1.80E-09	1.55E-09	8.93E-09	2.34E-09	1.72E-09
4	*Syzygium* sp.	365	1.22E-09	6.80E-10	1.20E-10	3.07E-09	0.86E-09	0.26E-09	5.72E-09	2.45E-09	0.92E-09
5	*Afzelia* sp.	385	8.96E-09	2.35E-09	1.52E-09	10.80E-09	2.52E-09	1.77E-09	12.70E-09	2.83E-09	1.90E-09
6	*Dysoxylum* sp.	393	2.53E-09	6.10E-10	2.40E-10	3.00E-09	1.29E-09	0.25E-09	3.19E-09	1.59E-09	0.72E-09
7	*Albizia* sp.	548	5.78E-09	3.08E-09	2.00E-09	6.79E-09	3.29E-09	2.13E-09	8.12E-09	3.59E-09	2.95E-09
8	*Albizia* sp.	621	5.02E-09	8.60E-10	8.30E-10	5.61E-09	1.57E-09	1.27E-09	6.40E-09	1.75E-09	1.68E-09

Of all the species evaluated, *E. fordii* presents the lowest rates of diffusion in all directions owing to its low water content and unique structure. The *E. fordii* wood consists of thick-walled fibers with the lumina almost completely closed. Furthermore, the presence of deposits in some vessels is also likely to be responsible for the low permeability values. The small values of diffusion coefficient were also observed in *Syzygium* sp. This may be due to very high extractives content that forms an inhibition for diffusion (Imamura, 1989). The diffusion of chemicals in *Dysoxylum* spp. decreases with increasing U_{max} although they have similar anatomical features and extractive content (see Chapter 2). This phenomenon can be interpreted by considering the different amount of water in the pores, which was available for transfer of chemicals, as reported (Robertson and Packer, 1996). Similarly, the diffusion of heavily degraded *Albizia* sp. (U_{max} = 621%) was lower than that with lower degradation (U_{max} = 548%). This situation is probably due to the higher extractives content in the heavily degraded sample (U_{max} = 621%) that limited the permeability.

The longitudinal diffusion coefficients are shown in Fig. 5.3. Within the same species, the diffusion of trehalose is faster than that of keratin and PEG4000. The diffusivities of keratin are only slightly higher than those of PEG4000, even though they have very different molecular weights. Fig. 5.3 reveals that there is little correlation between longitudinal diffusivity and maximum moisture content in the wood samples. The highest rates of longitudinal diffusion are observed for *Afzelia* sp. (U_{max} = 385%), ranging from 8.96×10^{-9} to 12.7×10^{-9} m^2 s^{-1}. Similar diffusion rates are observed for *Garcinia* sp. (U_{max} = 330%) and *Albizia* sp. (U_{max} =548 and 621%). This may depend on the circumstance that the higher U_{max} in the *Afzelia* sp. wood might have favoured the diffusion of chemical molecules, or that any hindrance to diffusion was present in the *Albizia* sp. wood (higher U_{max} values), depending on the difference in the anatomical structures of the hardwood species (Håfors, 2010).

Because of their similar structures, the diffusion rates of keratin and PEG4000 in *Dysoxylum* spp. are similar. These values are between 2.27×10^{-9} and 3.00×10^{-9} m^2 s^{-1}. The diffusivities of the chemicals are limited in *E. fordii* wood, ranging from 0.24×10^{-9} to 0.62×10^{-9} m^2 s^{-1}.
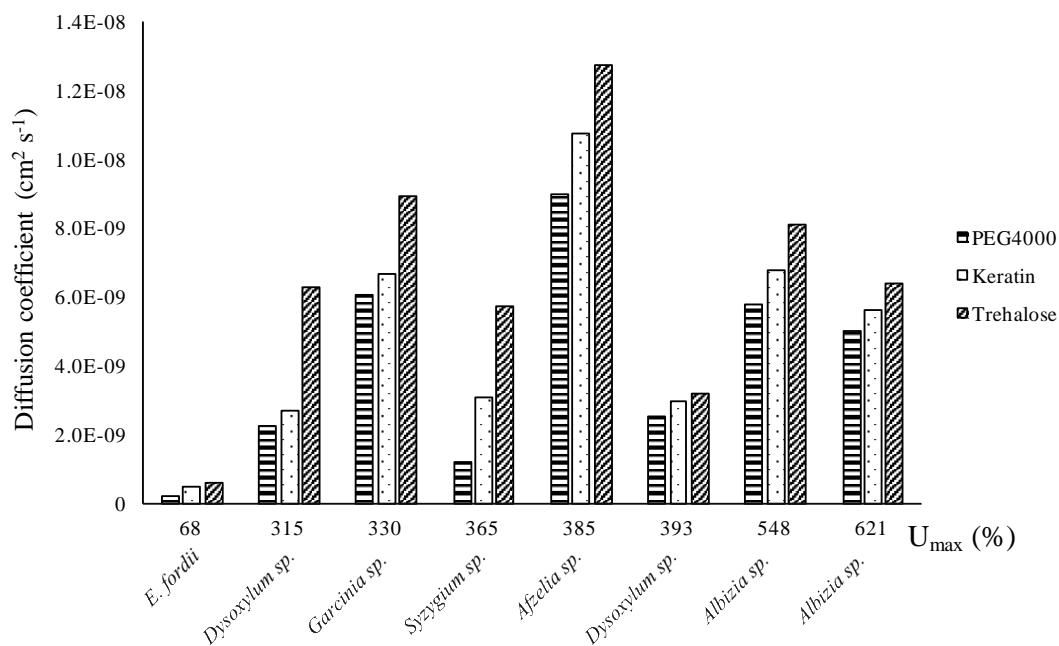
Fig. 5.3. Steady-state diffusion coefficients for the chemicals in the longitudinal direction

Conversely, the diffusion coefficients along the radial direction increase with increasing maximum moisture content, except for *Syzygium* sp. (U_{max} = 365%), *Dysoxylum* sp. (U_{max} = 393%), and *Albizia* sp. (U_{max} = 621%) (Fig. 5.4). This is probably due to the anisotropic structure of wood and the presence of deposits that limit diffusion in the ray cells of those species. The diffusion rate for trehalose is higher than that of the other chemicals. Within the same species (except for *Garcinia* sp. (U_{max} = 330%)), the diffusivity of keratin is higher than that of PEG4000. This may be due to the heterogeneously microporous structures of the specimens.
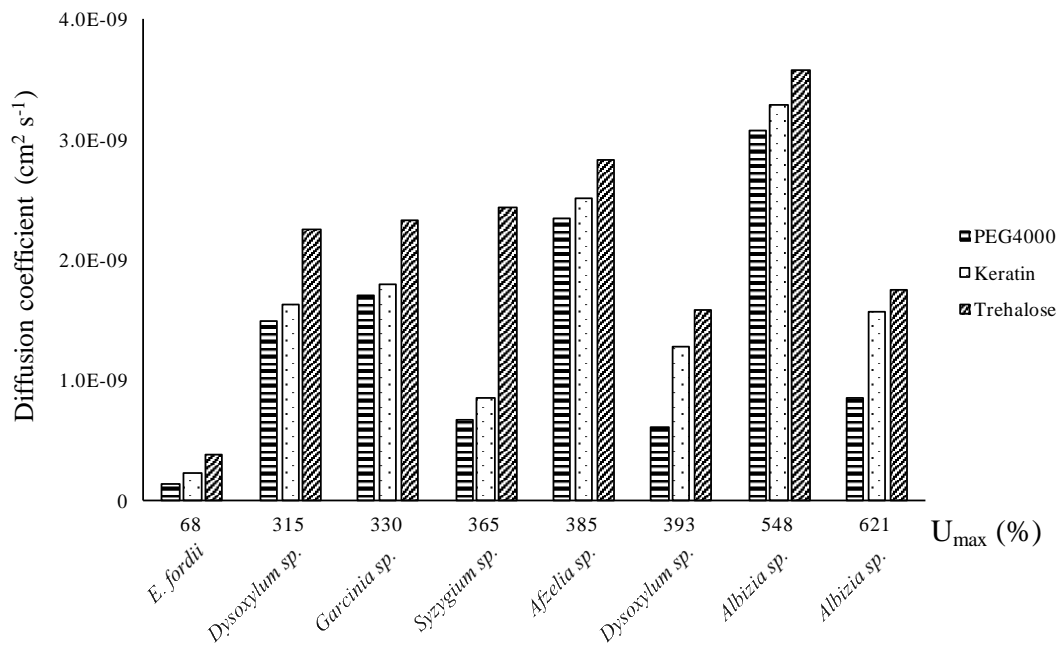
Fig. 5.4. Steady-state diffusion coefficients for the chemicals in the radial direction

Similarly, solute diffusivity along the tangential direction increases with increasing water content except for *Syzygium* sp. (U_{max} = 365%), *Dysoxylum* sp. (U_{max} = 393%), and *Albizia* sp. (U_{max} = 621%) (Fig. 5.5). The anisotropic structure of wood can strongly affect diffusivity. The highest rates of diffusion are observed in *Albizia* sp. (U_{max} = 548%), ranging from 2.00×10^{-9} to 2.95×10^{-9} m^2 s^{-1}. The diffusivities of the chemicals in *E. fordii* wood are significantly low, varying from 0.10×10^{-9} to 0.36×10^{-9} m^2 s^{-1}.
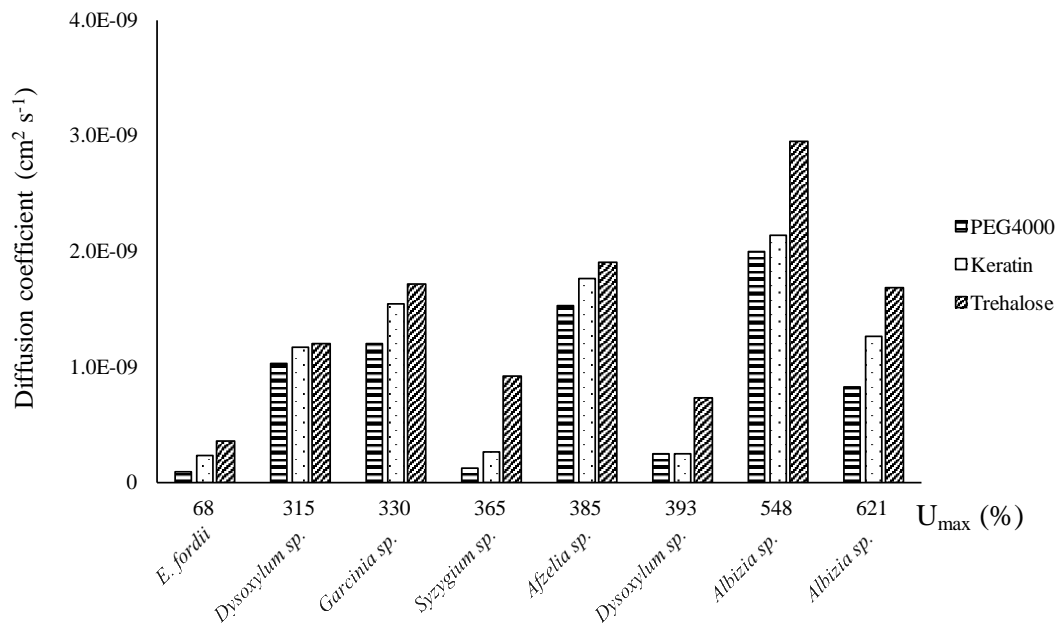
Fig. 5.5. Diffusion coefficients for the chemicals in the tangential direction

Wood exhibits an extremely complex heterogeneously microporous structure, reflecting the photosynthetic apparatus of the tree and its biological development (Butterfiel and Meylan, 1980; Schweingruber, 2007). In practice, the permeability characteristics of archaeological WW are extensively affected by the degradation process (Rowell and Barbour, 1990; Pearson, 1987). The biological degradation of timber also alters its permeability by forming cavities and destroying pit membranes (Robertson and Packer, 1996). In contrast to modern wood, in which the diffusion of chemicals occurs mainly along the cell lumina, the flow paths for diffusing solutes in WW are through the solvent-filled voids, such as the lumen of cell, cell wall voids, and transient capillaries (Dean, 1993). However, not all the water in the pores is available for the diffusion of chemicals (Robertson and Packer, 1996). The diffusion phenomenon into the wood cell wall has been previously investigated (Tarkow et. al., 1966). The result showed that the upper limit of molecular size that could penetrate into the secondary cell wall of green Sitka spruce heart wood was the PEG molecular weight 3000. If the internal voids of the capillary system of the secondary cell wall of the WWs are larger than those of the green Sitka spruce, larger molecules could

penetrate into the cell wall material. Another possibility is that the tertiary cell wall that forms a barrier for diffusion from the cell lumen into the secondary cell wall may be sensitive to temperature and permit larger molecules to pass through at elevated temperature (Tarkow et. al., 1966; Håfors, 2010).

In the transverse direction, wood cells are connected to neighboring cells through numerous intervascular pits. The pits tend to be oriented tangentially to the center of the tree (Pearson, 1987). The type, quantity, and occlusion of the pits have significant effects on the movement of chemicals through them (Vinden, 1983). Transient cell wall capillaries may only play a small part in diffusion processes (Jacobson, 2006; Dean, 1993). Moreover, the presence of wood rays, the abundance of pits on the radial walls, and thicker tangential walls result in the anisotropic structure of wood. Therefore, the variation of diffusion coefficients in this study is probably caused by the anisotropic structure of the WWs. In all the species evaluated, higher rates of diffusion are observed for the radial direction than for the tangential direction.

5.4. Summary

The diffusion of chemicals along the longitudinal direction is between 1.5- and 8.1-times faster than that in the radial direction. Diffusion rates along the radial direction are 1.1- to 5.8-times higher than those in the tangential direction. According to Fick's law, a steady-state diffusion coefficient is independent of the concentration of the bulk solution and the thickness of the wood sample. However, since the degree of deterioration varies widely (even though wood samples are cut from the same beams) diffusion coefficients can be used as references. Future study is required to determine additional coefficients for different WW species and samples with different degrees of wood degradation. Although several further experiments are under

development for this research, the diffusion coefficients calculated in this study along with the measured dimensions of WW samples from the same species can be used to estimate treatment time. Thus, through our research, it will be possible to safely shorten the period of preservation processing, which is currently decided mainly based on intuition and personal experience, by obtaining diffusion coefficients more accurately.

Chapter 6. Shrinkage and swelling behavior of archaeological waterlogged wood preserved with slightly crosslinked sodium polyacrylate

6.1. Introduction

Archaeological WW becomes considerably fragile over time because of chemical hydrolysis and biological deterioration in the wet buried environment (Endo and Sugiyama, 2013; Rowell and Barbour, 1990). Because of the disintegration of cellulose, hemicellulose, and lignin, the microvoids within the wood cell walls become larger, making the wood more porous. As long as the gaps remain filled with water, WW can retain its shape (Jiachang et al., 2009; Uzielli, 2007). In contrast to recent wood, in which drying stresses and changes in shape can be largely sustained by the inherent strength of the material, WW often undergoes extreme levels of shrinkage upon drying, owing to decomposition of the carbohydrates (Rowell and Barbour, 1990; Uzielli, 2007; Unger et al., 2001). As drying proceeds, the weakened cell walls are unable to withstand the stress imposed by the surface tension of the receding columns of liquid water, leading to collapse of the wood structure (Pearson, 1987). The decomposition of cellulose microfibrils cause an increase in longitudinal shrinkage, which can be as large as 10%, can thus be considered an indicator of structure deterioration (Rowell and Barbour, 1990; Uzielli, 2007; Pearson, 1987).

Generally, the shrinkage of WW increases as the residual density decreases. A linear relationship has been observed between the maximum moisture content and volumetric shrinkage (Hoffmann et al., 1986; Unger et al., 2001). During dehydration of the WW cellulose, strong molecular interactions cause cellulosic molecules to hide their hydrophilic surfaces, eliminating moisture and leading to extreme shrinkage

(Hoffmann, 1993). In most cases, the collapse of the structure causes not only volumetric shrinkage, but also irreversible damage associated with distortions and numerous cracks (Rowell and Barbour, 1990; Jiachang et al., 2009; Hoffmann, 1993). Once such shrinkage and deformation has occurred, it is difficult to restore the WW to its original size and shape in common solvents, including water.

So far, several methods have been reported for the restoration of collapsed WW. Early investigations were conducted using low concentration sodium hydroxide (NaOH) solution (Jiachang et al., 2009; Hoffmann, 1988). However, NaOH solution, a strong alkali agent, accelerates the degradation of the remaining wood. Furthermore, the restoration performance is limited to a maximum of about 10% recovery (Rowell and Barbour, 1990; Jiachang et al., 2009). Another method using mechanical swelling achieved by rapid decompression of supercritical CO_2 fluid was also studied, and enabled partial or sometimes total recovery of the initial volume of the objects. However, sufficient viscosity of the treatment solution is of prime necessity to obtain effective swelling of very degraded collapsed wood, and therefore total recovery of the initial shape was not obtained for heavily degraded collapsed wood (Chaumat et al., 1999). More recently, treatment with lactic acid appeared to be effective in the re-swelling of once-dried WW for oak wood. However, based on visual inspection, this treatment is not free from degradation of the wall components, particularly lignin, due to acid-induced hydrolysis (Jensen et al., 2007). Additionally, an active alkali-urea treatment was developed to achieve total recovery of the initial shape; however, the degraded secondary wall was completely removed in the recovered WW (Jiachang et al., 2009). This was the context in which a novel and mild method for the restoration of WW was studied.

Recently, a unique behavior was reported for bacterial cellulose (BC) in which acrylic acid and sodium acrylate were copolymerized and cross-linked *in situ* (Xiang et al., 2016). This cross-linked BC gel had excellent shape recovery after multiple drying and rewetting cycles because of the superabsorbent nature of sodium polyacrylate (PAANa) (Shim et al., 2016; Ahmed, 2015). This phenomenon can be interpreted by considering the high osmotic pressure of PAANa gel, which absorbs a large amount of water in its three-dimensional networks and retains the absorbed water even under compression, drying, and shrinkage. The PAANa gel has high durability and stability in the swelling environment and during the storage (Ahmed, 2015). Therefore, in this chapter, the applicability of this technique to WW as a potential tool for preservation from unexpected drying was investigated.

6.2. Materials and methods

6.2.1. Sample preparation

Archaeological sample was collected from the Thang Long Imperial Citadel excavation site in Hanoi, Vietnam, which is recognized on the UNESCO World Heritage list. The specimen was identified as *Afzelia* sp. based on microscopic anatomical observations. All the samples were taken from the same piece of wood. The saturated moisture content (U_{max}) was determined to be 385% based on weighing the wood samples before and after oven drying at 105 °C. The basic wood density was calculated to be 0.22 g/cm^3 based on the oven-dried weight of wood sample and its maximum water saturation volume. The WW determined to be in a medium state of degradation (Rowell and Barbour, 1990). The specimen was then cut into $20 \times 20 \times 5$ mm blocks (tangential $\times$ radial $\times$ longitudinal dimensions).

Acrylic acid (AA), 4,4´-azobis (4-cyanopentanoic acid) (V-501) catalyst and *N*,*N*´-methylenebisacrylamide (MBA) crosslinking agent were purchased from Wako Pure Chemical Industries, Ltd., Japan. Sodium acrylate (AANa) monomer was obtained from Sigma Aldrich, USA. All chemicals were used without further purification.

6.2.2. Impregnation, *in situ* polymerization and crosslinking

Figure 6.1 presents a flowchart of the process for the impregnation, *in situ* polymerization and crosslinking PAANa.

Preparation of impregnation solution

AA 98% (1.2 g, 16 mmol), AANa 97% monomer (0.50 g, 5.3 mmol), and MBA (0.10 g, 0.6 mmol) crosslinking agent were solubilized in 10 g of distilled water under stirring in a test tube. Then, a given amount of the catalyst (V-501, 0.06 g, 0.2 mmol) was added to the stirred solution and fully dissolved by stirring.

Vacuum impregnation of wood

In the next step, the WW samples ($n = 7$ specimens) were placed in the test tube, which had been filled with impregnation solution. The test tube was equipped with a nitrogen inlet adapter. Impregnation was performed by impregnation under a low pressure of 0.1 MPa for about 20 min.

PREPARATION OF IMPREGNATION SOLUTION • Acrylic acid • Sodium acrylate • *N,N'*-methylenebisacrylamide • Distilled water • Catalyst V-501	**WW SAMPLES** *Afzelia* sp., medium degraded: $U_{max} = 385\%$, size: $20 \times 20 \times 5$ mm (tangential × radial × longitudinal)

VACUUM IMPEGNATION OF WOOD
vacuum (0.1 MPa), 20 min

NITROGEN BUBBLING AND BLANKET

***IN SITU* SIMUTANEOUS POLYMERIZATION AND CROSSLINKING RESULTING PARTIALLY CROSSLINKED PAANa**
at 40 °C and 6 h

MANUAL REMOVAL
of surplus hydrogel covering wood surface

EXTRACTION OF UNREACTED CHEMICALS
from wood structure with acetone overnight

DRYING OF TREATED WOOD
at room temperature

Fig. 6.1. Block diagram for the separate conservation steps of WW completed with slightly crosslinked PAANa

Nitrogen bubbling and blanket

In the next step, nitrogen gas was purged for 10 min to remove oxygen dissolved in the impregnation solution. The nitrogen blanket is necessary for many polymerizations because oxygen radical itself may stop polymerization or monomer radical formation. Hence, it is necessary to maintain an inert atmosphere.

In situ *simultaneous polymerization and crosslinking of impregnations resulting partially crosslinked PAANa*

For *in situ* temperature polymerization and crosslinking, the reactor was immersed in a thermo-controlled water bath and kept at 40 °C for 6 h. The synthesis scheme for partially crosslinked PAANa is shown in Fig. 6.2.
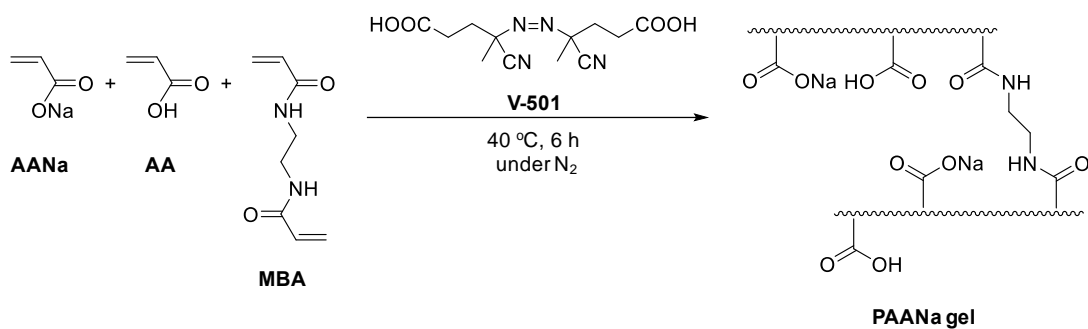
Fig. 6.2. Synthesis scheme for partially crosslinked PAANa

Manual removal

The samples were removed from the obtained hydrogels. The surplus crosslinked polymer gel was removed manually from surface of the samples.

Extraction of unreacted chemicals from wood structure

In the next step, treated samples were immersed in acetone overnight in order to remove unreacted monomers and catalyst.

Drying of treated wood

The treated WW containing slightly crosslinked PAANa was dried at room temperature.

6.2.3. Fourier-transform infrared microscopy

For further investigation, it was essential to confirm the polymerization of the acrylic monomers inside the WW. Fifteen μm cross-sections from untreated and PAANa-treated samples were prepared. Fourier-transform infrared microscopy (FTIR) was performed using a Spotlight 200 Frontier FTIR (PerkinElmer, USA) spectrometer connected to a microscope operated in transmission mode. The spectra from a section with an area of 30 × 30 μm were acquired in the range of 4000–400 cm^{-1} with a resolution of 4 cm^{-1}. For each spectrum, 64 scans were collected.

6.2.4. Shape recovery tests

The shape recovery properties were investigated based on two drying-rewetting cycles. In the first cycle, the untreated and treated samples, which were extracted from water and acetone, respectively, were air-dried for 3 days. Both samples were then immersed in distilled water at room temperature until the dimensional changes reached a plateau. In the second cycle, the recovered samples were again air-dried for 3 days and then re-immersed in distilled water to reach swelling equilibrium. The shrinkage and swelling ratios were calculated from sample images using Image-J software (https://imagej.nih.gov). The shrinkage and swelling along the longitudinal, radial, and tangential axes were quantified and evaluated by the restoration degree (R_c),

$$\%R_c = (a_i/a_0) \times 100$$

where a_0 are the dimensions of original untreated sample and a_i is the sample's dimensions after the 1st drying, 1st rewetting, 2nd drying, 2nd rewetting, respectively.

6.2.5. Scanning electron microscopy

The untreated and PAANa-treated specimens were prepared from internal part of samples. They were freeze-dried for 4 days and then coated with platinum (JFC-1600, JEOL, Japan). A field emission SEM (JSM-7800F prime, JEOL, Japan) was operated at an accelerating voltage of 1.5 kV.

6.2.6. Transmission electron microscopy

The wood blocks, $1 \times 1 \times 3$ mm (tangential × radial × longitudinal dimensions), were prepared from the fully waterlogged condition of untreated and PAANa-treated samples. The treated sample was extracted from swelling equilibrium condition. Both samples were then substituted with acetone using the freeze substitution method (Feder and Sidman, 1958). The blocks were then embedded in Spurr resin (EM S024, TAAB, England) (Spurr, 1969). Ultrathin sections with a 90 nm thickness were cut with an ultramicrotome (Ultracut E; Leica, Berks, England) equipped with a diamond knife. The sections were stained with uranyl acetate and lead citrate (Reynolds, 1963) and observed using a transmission electron microscopy (TEM, JEM 1400, JEOL, Japan) operated at 120 kV.

6.3. Results and discussion

6.3.1. *In situ* polymerization and crosslinking

The FTIR spectra of the treated and untreated WW are shown in Fig. 6.3. Generally, the main characteristics of the treated wood were similar to those of untreated sample. The most significant difference between the two spectra is the band at 1707 cm^{-1}, which is the absorption band corresponding to C=O stretching of the polymer (Dong et al., 1996). The presence of this critical absorption band indicated that PAANa was successfully polymerized inside the WW.
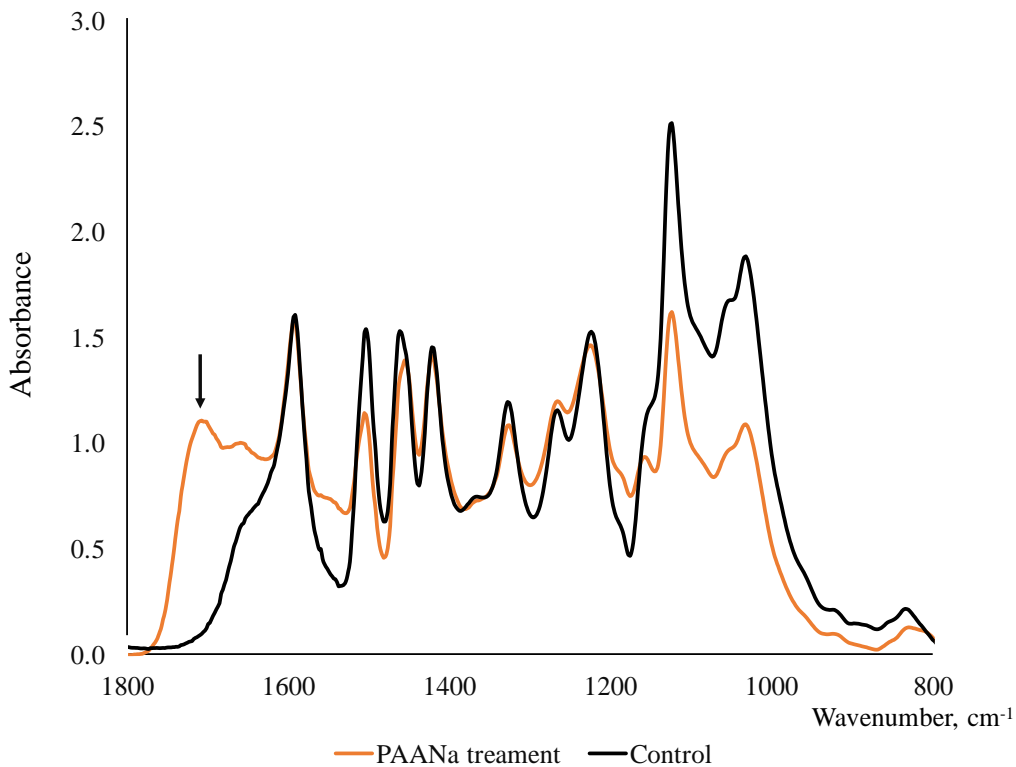
Fig. 6.3. FTIR spectra of PAANa-treated and untreated WW. Note that the C=O absorbance at 1707 cm^{-1} is clearly observed in the spectrum of the PAANa-treated sample (arrow).

6.3.2. Shrinkage and swelling behavior

The changes in the shape of the PAANa-treated and untreated specimens during repeated drying-rewetting experiments are shown in Fig. 6.4. A significant difference between the shrinkage-swelling behaviors of the treated and untreated specimens was clearly observed. Although the specimens treated with PAANa recovered nearly their original volume even after two drying-rewetting cycles, the untreated samples could not recover their original shape and size after being dried once. The shrinkage-swelling behavior was monitored carefully along the three anisotropic axes.
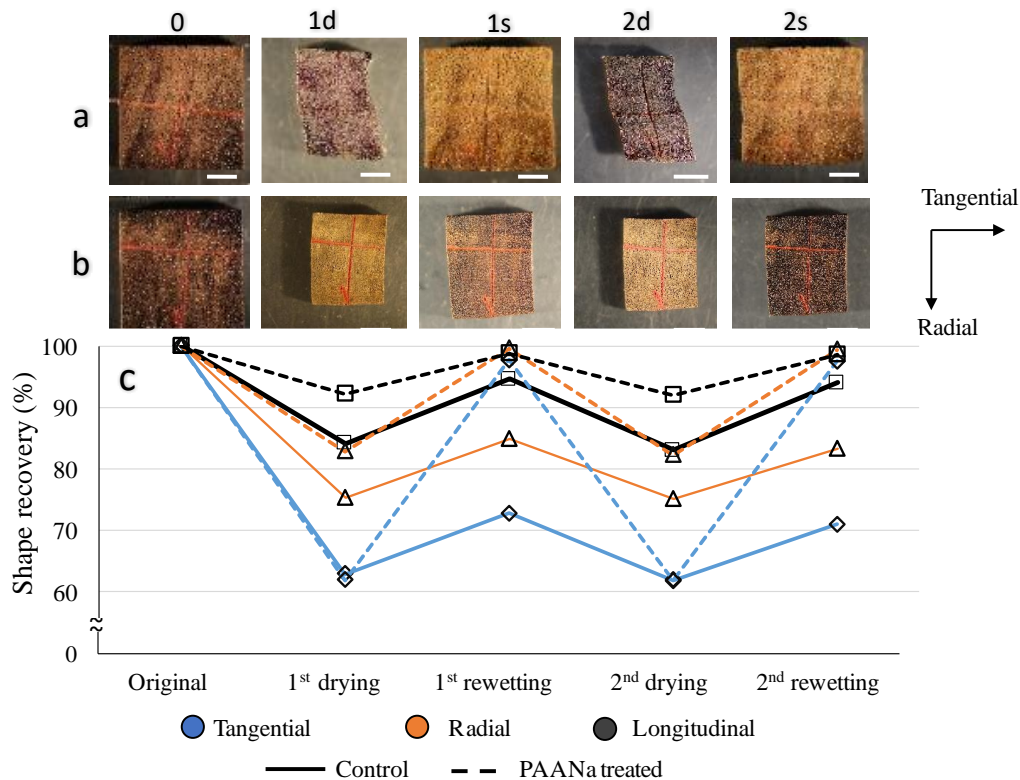
Fig. 6.4. Repeated shrinkage-swelling cycles of WW samples. a_0–a_{2s}: PAANa-treated WW; b_0–b_{2s}: untreated WW; c_0–c_{2s}: shape recovery rate (%); a_0, b_0, c_0: original samples; a_{1d}, b_{1d}, c_{1d}: the first air-drying cycle; a_{1s}, b_{1s}, c_{1s}: the first swelling cycle; a_{2d}, b_{2d}, c_{2d}: the second air-drying cycle; a_{2s}, b_{2s}, c_{2s}: the second swelling cycle; scale bar: 5 mm.

During the first drying-rewetting cycle, the dimensions of the PAANa-treated and untreated samples shrank after air-drying (Fig. 6.4a_{1d} and 6.4b_{1d}). The results showed that the tangential shrinkage of untreated sample was approximately 1.5 times as great as the radial shrinkage; these values were about 37.16% and 24.68%, respectively, while the longitudinal shrinkage reached 15.97% (Fig. 6.4c_{1d}). On the other hand, less deformation was observed in the PAANa-treated samples after the first natural drying process, especially in the radial and longitudinal directions, which showed shrinkage values of 17.23 % and 7.79%, respectively. However, shrinkage along the tangential direction was similar. This extreme radial, tangential, and longitudinal shrinkage could suggest that the cellulose underwent severe degradation (Berti et al., 2002).

After the first immersion in water, the PAANa-treated samples were almost 100% restored (Fig. 6.4a_{1s} and 6.4c_{1s}) in all three dimensions, while the recovery rate was limited to around 10% in in all directions in untreated samples (Fig. 6.4b_{1s} and 6.4c_{1s}). This suggested that the irreversible adhesion of cell wall components, pores and degradation cavities of cell wall layers, occurs during the first drying process unless WW is treated with PAANa.

In the second drying-rewetting cycle, the PAANa-treated and untreated samples were air-dried for 3 days. The dimensions of the PAANa-treated samples were similar to those observed after the first drying process (Fig. 6.4a_{2d} and 6.4b_{2d}), while the untreated samples were slightly smaller than those after the first drying (Fig. 6.4c_{2d}). Surprisingly, even after the second re-wetting process, the PAANa-treated samples exhibited perfect recovery to their original dimensions (Fig. 6.4c_0 and 6.4c_{2s});

however, only limited recovery was observed in the untreated samples; the recovery rates were even smaller than those observed after the first rewetting process.

According to a previous study (Ling, 2009), repeated drying and rewetting of degraded WW will lead to even greater shrinkage. Because of the degradation of polysaccharide substances in WW, the cellulose chains move closer together during the drying process, allowing the hydroxyl groups to form hydrogen bonds. When the collapsed ancient wood reabsorbs water, the newly formed hydrogen bonds can no longer accept water molecules, making the wood unable to swell to its original size (Jingran, 2014).

At the end of the second rewetting cycle, the WW samples treated with PAANa regained 96% of their original volume, while the recovery rate was limited to 56% in the untreated samples. In other words, PAANa provided elasticity to the hygroscopic nature of the WW, and therefore allowed the treated WW to recover its shape.

Although the recovery effect of the chemicals used on WW is of the greatest importance, the aesthetic features are important aspects as well. The swollen PAANa is a transparent polymer, therefore the natural color of treated wood was preserved (Fig. 6.4a$_{1s}$ and 6.4a$_{2s}$).

6.3.3. Morphological investigations

To clarify how the treatment affected the wood structure at the cellular level, SEM observation was carried out, and the results are shown in Fig. 6.5. The image clearly indicated the severe degradation of the cells, which were slightly shrunken due to the lack of cell wall integrity. Particularly, the inner secondary cell wall layers were

almost completely destroyed by biological degradation and detached from the ML as seen in Fig. 6.5a.
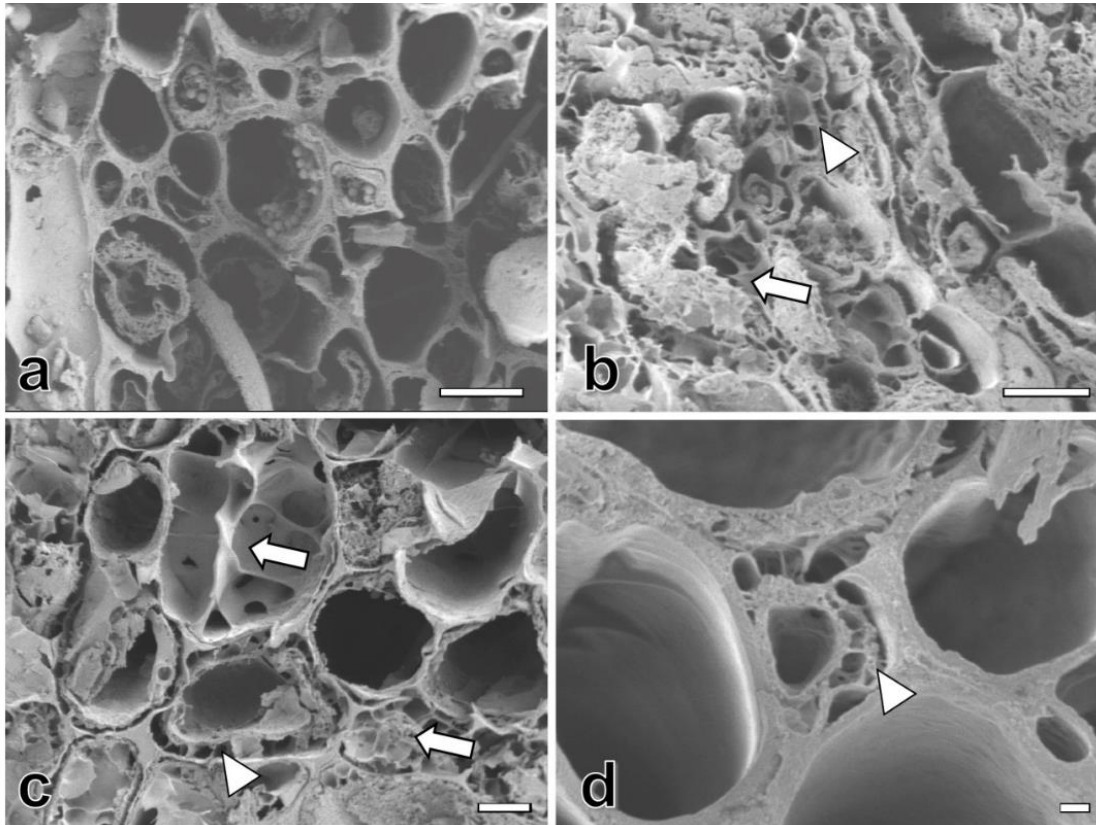

Fig. 6.5. The morphological features of the waterlogged, collapsed wood and re-swelled wood. (a) Freeze-dried WW without treatment, (b) air-dried WW treated with PAANa, (c) re-swelling of the PAANa-treated wood, (d) localization of PAANa in inter-cellular space. Arrows: PAANa located in cell lumina. Arrowhead: PAANa located near the ML. a–c: Scale bar 10 µm; d: scale bar 1 µm.

The PAANa-treated WW samples showed severe shrinkage during the natural drying process. Fig. 6.5b shows a transverse view of the PAANa-treated WW samples in which the fiber cells became elliptical. However, after immersion in water, the PAANa-treated WW exhibited obvious re-swelling of its wood tissues, in which the collapsed fiber cells were restored to a round shape (Fig. 6.5c). In the swollen treated wood, the crosslinked PAANa was found to be fully impregnated into WW samples

investigated. This is due to the small molecular size of chemicals which enhances chemicals penetrate easily into the WW through the diffusion and permeation processes. The PAANa was clearly observed to be localized in the cell lumina and near the ML, as shown in Fig. 6.5c. The intercellular space was well preserved (Fig. 6.5d). After repetition of the shrinkage-swelling processes, the final morphology of the swollen PAANa-treated WW was almost the same as its original shape.

Fig. 6.6 shows the TEM images of the PAANa-treated and untreated cell layers. In the treated samples, the cell lumina and the area around the ML were relatively electron dense. Since uranyl acetate and lead citrate stains are known to deposit in areas where water is miscible, the high density of the PAANa-treated WW may be interpreted as evidence of the presence of the superabsorbent polymer PAANa, which increased the concentration of this staining agent.
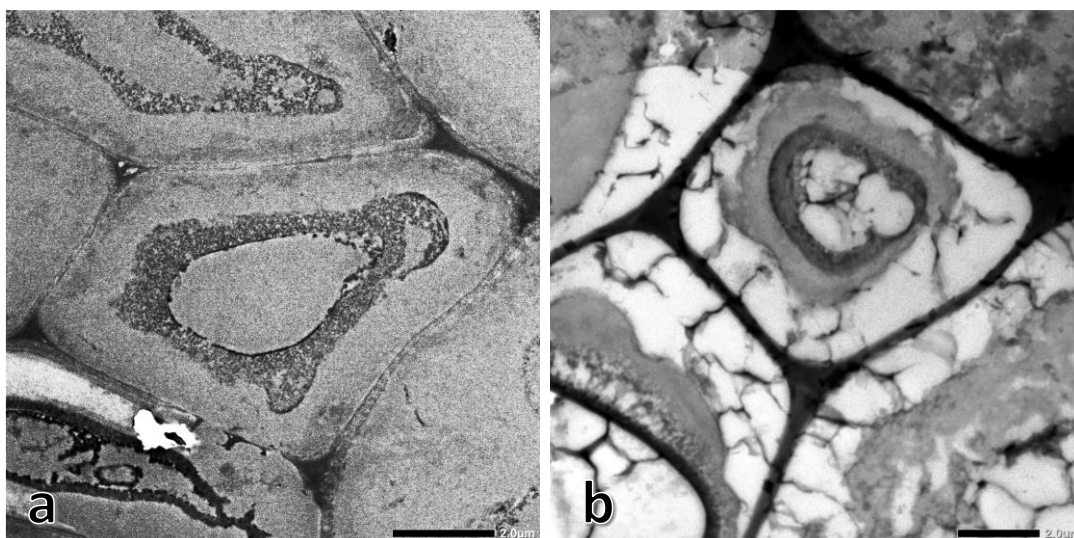
Fig. 6.6. TEM images of WW transverse sections. (a) WW cell wall and (b) PAANa-treated WW cell wall. Scale bar: 2 μm.

In summary, the recoverability of WW was greatly enhanced by impregnation with PAANa. During the shrinkage-swelling processes, the final dimensions of the

treated WW were almost restored to the initial dimensions. This regeneration cycle could be reproduced repeatedly. Because of superabsorbent properties of PAANa, the elasticity in the hygroscopic nature of the WW was improved, and therefore shape recovery properties were achieved. Additionally, the PAANa is well-known for its high structure stability in the polymer field, therefore, the presence of sodium in polymer treated wood would not cause the future danger for wood degradation in long term.

6.4. Summary

Treatment with PAANa resulted in excellent shape recovery of WW after multiple drying-rewetting cycles, while the recovery was not complete in the untreated samples. This unique behavior is probably due to the restoration of the elasticity of the WW after PAANa treatment. In conservation and restoration of archaeological artifacts, the reversibility of the treated materials is one of criteria. Therefore, a method to remove slightly crosslinked PAANa without damaging the wooden objects would also be a subject for further research. For suitably sized archeological objects that fit the requirements of the proposed method, PAANa treatment could be used to provide resistance and recovery after unexpected drying, and may be used either as the primary conservation method or as a pretreatment in conjunction with other established conservation methods. However, when the samples are large and unwieldly, impregnation of acrylic monomers as a first step would be difficult and potentially problematic. In such cases, a method of surface treatment should be considered, as the deterioration of the WW is most severe in a limited area near the surface. This chapter has investigated on medium degraded WW, further examinations on different classes of wood degradation are also needed. Although several further steps remain in the

development of this method, the PAANa treatment presented in this chapter seems to have unique properties that can be applied practically for the conservation of WW.

Chapter 7. General conclusions

Conservation of archaeological WW is often a difficult subject in Vietnam. This is because general preservation methods cannot be applied for Vietnamese tropical WWs, therefore, appropriate preservation treatment is required. This study aimed to establish appropriate preservation technology for the WW obtained from the Thang Long Imperial Citadel site, Hanoi, Vietnam. Chapter 1 presents the current situation and research background of WW in Vietnam. Chapter 2 summarizes the species identification and physicochemical properties of 15 waterlogged hardwood samples. The anatomical features showed that those samples belonging to 10 different taxa. The wood identification reaches in common the genus level. However, two of timber samples were identified to the species level owing to its historical and traditional revelance, i.e., *Erythrophleum fordii* Oliv. and *Vatica tonkinensis* A. Chev. The measurements on physical and chemical characteristics of WW showed different levels of wood degradation. Chemical analysis also confirmed the degree of wood degradation. A very high lignin content was determined in wood with U_{max} from 315% to 864%. Interestingly, the degradation of *E. fordii* and *V. tonkinensis* was very limited even after several hundred years of burial. The maximum moisture content of these two species was less than 70% and they have similar properties comparing to those of modern woods.

In Chapter 3, the natural durability of the *E. fordii* wood against white rot fungi was performed to elucidate the good stage of preservation of this timber in soil, and for determining appropriate procedures to conserve this timber. The results showed that fungi caused less than 2% mass loss. Microscopic observations revealed high structural rigidity of *E. fordii* timber. The *E. fordii* wood fiber consisted of heavily lignified thick-walled fibers with the fiber lumina almost completely closed. 2D HSQC

NMR evaluation revealed the *E. fordii* wood to have a heavily condensed lignin structure that reflected by the durability classes.

General preservation treatment methods using PEG4000, trehalose, and keratin was tested (Chapter 4). The results showed that the dimensional stability of WWs was significantly improved after the treatments. The anti-shrink efficiency (ASE) values of the WWs treated with keratin ranged between 72.5% and 96.2% depending on the species and degree of wood degradation. These values varied from 82.4% to 96.9% for the WWs treated with PEG4000 or trehalose. Microscopic observations showed that the chemically treated woods maintained their original cell structures, forms, and shapes. It was also revealed that the reinforcement of cell walls by the feather keratin treatment was different from those observed for the PEG4000 or trehalose treatments. It was observed that PEG4000 and trehalose primarily filled the wood voids, while keratin predominantly absorbed on the cell walls and ML. Based on the improved dimensional stability of wood, shortened impregnation time, removability of chemical, and aesthetic results obtained from the treatment, keratin showed a good performance in average as a preservation agent.

In order to determine the suitable treatment condition for WW, determination of steady-state diffusion coefficients of PEG4000, trehalose, and keratin through eight WW species were carried out (Chapter 5). The diffusion coefficients were strongly affected by wood species and the anatomical structures of wood. Within the same species of wood, the highest diffusion rates were measured in the longitudinal direction, followed by those in the radial and tangential directions. The longitudinal diffusion coefficients were 1.5- to 8.1-times higher than the radial diffusion coefficients, which were in turn approximately 1.1- to 5.7-times higher than the tangential diffusion coefficients. The diffusion rates were found to be inversely

proportional to the molecular weight of the diffusing chemical. The diffusivity of trehalose through the WWs was found to be higher than those of keratin and PEG4000. A potential method to easily estimate chemical diffusion coefficients for dip-diffusion treatments was suggested.

A new method utilizing the *in-situ* crosslinking reaction of the hydrophilic polymer to enhance recoverability of WW from unexpected drying was developed (Chapter 6). The results showed that treatment with cross-linked PAANa resulted in excellent shape recovery of WW after multiple drying-rewetting cycles, while the recovery was not complete in the untreated samples. The cross-linking PAANa treatment could be used to provide resistance and recovery after unexpected drying, and may be used either as the primary conservation method or as a pretreatment in conjunction with other established conservation methods.

In conclusion, the species identification and physicochemical properties of 15 WW samples were examined. It is revealed that the *E. fordii* (called as Lim wood) commonly excavated from the site is extremely resistant to degradation. The condensed type lignin is abundant, and the wood is made from the thick wall wood fibers with fibers lumina were completely closed. General preservation treatment methods using PEG, trehalose, and feather keratin was applied for conservation of small WW samples. Based on the improved dimensional stability of wood, shortened impregnation time, color, and removability of material, keratin exhibited high performance in average as a preservation material. It was clarified that the diffusion coefficient of preservatives depends on wood species, and pointed out the necessity of deciding treatment conditions for each tree species. Finally, a new method of protecting excavated wood from unexpected drying by utilizing the *in-situ* crosslinking reaction of the hydrophilic polymer was developed. The preservation of

small WW with cross-linked PAANa can be applied practically for the conservation of WW. However, inherent limitations of WW materials, several species have not been explicitly explored within this study. Moreover, since the anisotropic structure of wood and the degree of deterioration varies widely (even though wood samples are cut from the same beams), future study is required to examine additional tests for different WW species and samples with different degrees of wood degradation.

References

Ahmed EM (2015) Hydrogel: Preparation, characterization, and applications: A review. J Adv Res 6:105–121

Anagnost SE (1998) Light microscopic diagnosis of wood decay. IAWA J 19:141–167

Babiński L (2015) Dimensional changes of waterlogged archaeological hardwoods pre-treated with aqueous mixtures of lactitol/trehalose and mannitol/trehalose before freeze-drying. J Cult Herit 16:876–882

Babiński L, Fabisiak E, Dąbrowski HP, Kittel P (2017) Study on dimensional stabilization of 12,500-year-old waterlogged subfossil Scots pine wood from the Koźmin Las site, Poland. J Cult Herit 23:119–127

Babiński L, Izdebska-Mucha D, Waliszewska B (2014) Evaluation of the state of preservation of waterlogged archaeological wood based on its physical properties: Basic density vs. wood substance density. J Archaeol Sci 46:372–383

Babiński L (2011) Investigations on pre-treatment prior to freeze-drying of archaeological pine wood with abnormal shrinkage anisotropy. J Archaeol Sci 38:1709–1715

Babiński L (2012) Research on dimensional stability in waterlogged archaeological wood dried in a non-cooled vacuum chamber connected to a laboratory freeze-dryer Drewno Pr Nauk Doniesienia Komun 55:5–19

Babiński L (2015) Dimensional changes of waterlogged archaeological hardwoods pre-treated with aqueous mixtures of lactitol/trehalose and mannitol/trehalose before freeze-drying. J Cult Herit 16:876–882

Bamber RK, Fukazawa F (1985) Sapwood and heartwood: A review. For Abstr 46:567–580

Bari E, Nazarnezhad N, Kazemi SM, Ghanbary MAT, Mohebby B, Schmidt O, Clausen CA (2015) Comparison between degradation capabilities of the white rot fungi Pleurotus ostreatus and Trametes versicolor in beech wood. Int Biodeterior Biodegrad 104:231-237

Becker G (1976) Treatment of wood by diffusion of salts. Jour Inst Wood Sci 7:30-36

Berti S, Bettazzi F, Chimichi S, De Capua E, Gambetta A, Giachi G, Lazzeri S, Machioni N, Martena F, Paci S, Staccioli G (2002) Il legno ed il suo degrado nei manufatti recuperati nel porto antico di Pisa (in French). In: Proc 1 Congresso di Chimica dei beni Culturali "La scienza dell' Arte", pp 400–409

Bich DTN, Phuong LX, Nguyet NTM, Thu PTT, Nam NQ, Chuong PV (2011) Fundamental properties of some wooden objetcs excavated in Thang Long Imperial Citadel (in Vietnamese). Vietnam National University of Forestry, Vietnam

Bich DTN, Phuong LX, Thu PTT, Phuoc LN, Thang NT, Dien LQ (2013) Characteristics of archaeological woods excavated in Doan Mon gate (in Vietnamese). Vietnam National University of Forestry, Vietnam

Blanchette RA (1984) Screening wood decayed by white rot fungi for preferential lignin degradation. Appl Environ Microbiol 48:647-653

Blanchette RA (1984) Selective delignification of eastern hemlock by *Ganoderma tsugae*. Phytopathology 74:153-160

Blanchette RA, Nilsson T, Daniel G, Abad A (1990) Biological degradation of wood. In: Rowell, R.M., Barbour, R.J. (Eds.), Archaeological Wood. Advances in Chemistry Series, No. 225. American Chemical Society, Washington, DC, pp. 141–192

Blanchette RA (2000) A review of microbial deterioration found in archaeological wood from different environments. Int Biodeterior Biodegrad 46:189–204.

Braovac S, Kutzke H (2012) The presence of sulfuric acid in alum-conserved wood - Origin and consequences. J Cult Herit 13:S203–S208

Broda M, Mazela B (2017) Application of methyltrimethoxysilane to increase dimensional stability of waterlogged wood. J Cult Herit 25:149-156

Bugani S, Modugno F, Łucejko JJ, Giachi G, Cagno S, Cloetens P, Janssens K, Morselli L (2009) Study on the impregnation of archaeological waterlogged wood with consolidation treatments using synchrotron radiation microtomography. Anal Bioanal Chem 395:1977–1985

Burdsall HH (1985) A contribution to the taxonomy of the genus Phanerochaete (Corticiaceae, Aphyllophorales). J. Cramer Publisher, Braunschweig, Germany

Burr HD, Stamm AJ (1947) Diffusion in wood. J Phys Colloid Chem 51:240–261

Butterfiel BG, Meylan BA (1980) Three-dimensional structure of wood. An ultrastructural approach. Chapman and Hall, London New York

Cesar, T, Danevčič, T, Kavkler, K, Stopar, D, 2016. Melamine polymerization in organic solutions and waterlogged archaeological wood studied by FTIR spectroscopy. J Cult Herit 23:106–110

Chau NV (2005) Historical Rice and Fall of Thang Long Royal Citadel – Advantages and Challenges in the Conservation and Development Context of Hanoi, in: The 2nd Asian Academy Heritage Management Field School, Hanoi, Vietnam

Chaumat G, Tran QK, Perre C, Lumia G (1999) Trials of shape recovering from collapsed waterlogged wood by treatment with CO_2 supercritical fluid. In: Proc 7th ICOM-CC Work Gr Wet Org Archaeol Mater, pp 137–142

Chaumat G, Albino C, Blanc L (2007) Development of new consolidation treatments from fatty acid resin solution. In Proc ICOM–WOAM Conference, Amsterdam.

Chen T (1988) Flora of China. Science Press, Beijing, China

Cheng JS, Zhen S (1987) Chinese virose plant. Science Press, Beijing, China

Christensen GN (1951) Diffusion in wood. II. The temperature coefficient of diffusion through wood. Aust J Appl Sci 2 (4): 430-439

Christensen M, Kutzke H, Hansen FK (2012) New materials used for the consolidation of archaeological wood-past attempts, present struggles, and future requirements. J Cult Herit 13S:S183–S190

Christensen M, Frosch M, Jensen P, Schnell U, Shashoua Y, Nielsen OF (2006) Waterlogged archaeological wood – chemical changes by conservation and degradation. J Raman Spectrosc 37:1171–1178

Christensen M, Kutzke H, Hansen FK (2012) New materials used for the consolidation of archaeological wood-past attempts, present struggles, and future requirements. J Cult Herit 13S:S183–S190

Cowling EB (1961) Comparative biochemistry of the decay of sweetgum sapwood by white-rot and brown-rot fungi. USDA Forest Service, Washington, DC

Dean LR (1993) The conservation and stabilization of ancient waterlogged woods and the diffusion of water-borne polymers through wood. PhD Thesis, University of Portsmouth, England

Dean LR, Jones AM, Jones EBG (1997) Diffusion rates of PEG into wet archaeological oak. In Proc 6th ICOM Work Gr Wet Org Archaeol Mater Conf York, pp 435–448

Dong J, Ozaki Y, Nakashima K (1996) FTIR Studies of Conformational Energies of Poly (acrylic Acid) in Cast Films. J Polym Sci 507–515

Du D, Qu J, Wang JM, Yu SS, Chen XG, Xu S, Ma SG, Li Y, Ding GZ, Fang L (2010) Cytotoxic cassaine diterpenoid-diterpenoid amide dimers and diterpenoid amides from the leaves *of Erythrophleum fordii*. Phytochemistry 71:1749-1755

Endo R, Hattori T, Tomii M, Sugiyama J (2015) Identification and conservation of a Neolithic polypore. J Cult Herit 16:869–875

Endo R, Kamei K, Iida I, Kawahara Y (2008) Dimensional stability of waterlogged wood treated with hydrolyzed feather keratin. J Archaeol Sci 35:1240–1246

Endo R, Kamei K, Iida I, Yokoyama M, Kawahara Y (2010) Physical and mechanical properties of waterlogged wood treated with hydrolyzed feather keratin. J Archaeol Sci 37:1311–1316

Endo R, Sugiyama J (2013) Evaluation of cell wall reinforcement in feather keratin-treated waterlogged wood as imaged by synchrotron X-ray microtomography (µ XRT). Holzforschung 67:795–803

Eriksson KEL, Blanchette RA, Ander P (1990) Microbial and enzymatic degradation of wood and wood components. Springer-Verlag, Germany

Feder N, Sidman RL (1958) Methods and principles of fixation by freeze-substitution. J Biophys Biochem Cytol 4(5):593–600

Faix O (1991) Classication of lignins from different botanical origins by FT-IR spectroscopy. Holzforschung 45: 21–27

Fang XF, Fang BZ (2007) Wood physical and mechanical properties of *Erythrophleum fordii* in southern Fujian (In Chinese). J Fujian Forest Sci Technol 34:146–147

Fengel D, Wegener G (1984) Wood: chemistry, ultrastructure, reactions. Walter De Gruyter, Berlin, pp. 132–181

Fukuyama M, Urakami H (1986) Diffusion of Nonelectrolytes through Wood Saturated with Water III. Diffusion rates of polyethylene glycols. Mokuzai Gakkaishi 32(3):147–154

Giachi G, Capretti C, Donato ID, Macchioni N, Pizzo B (2011) New trials in the consolidation of waterlogged archaeological wood with different acetone-carried products. J Archaeol Sci 38:2957–2967

Giachi G, Bettazzi F, Chimichi S, Staccioli G (2003) Chemical characterisation of degraded wood in ships discovered in a recent excavation of the Etruscan and Roman harbour of Pisa. J Cult Herit 4:75–83

Goodell B, Nicholas DD, Schultz TP (2003) Wood Deterioration and Preservation. American Chemical Society, Washington, DC

Ha MT, Tran MH, Phuong TT, Kim JA, Woo MH, Choi JS, Lee S, Lee JH, Lee HK, Min BS (2017) Cytotoxic and apoptosis-inducing activities against human lung cancer cell lines of cassaine diterpenoids from the bark of *Erythrophleum fordii*. Bioorganic Med Chem Lett 27:2946-2952

Håfors B (2010) Conservation of the wood of the Swedish warship Vasa of A.D. 1628. Evaluation of polyethylene glycol conservation programmes. PhD thesis, University of Gothenburg, Sweden

Heitner C, Dimmel D, Schmidt JA (2010) Lignin and lignans: advances in chemistry. CRC Press, London

Hocker E, Almkvist G, Sahlstedt M (2012) The Vasa experience with polyethylene glycol: A conservator's perspective. J Cult Herit 13:175–182

Hoffmann P (1988) Zur Ruckformung mittelalterlicher Drechslerware. In: Tl. II. Holzer mit Schwindungsschaden. Arbeitsbl Restaur Grup 8, pp171–185

Hoffmann P (1993) Restoring deformed fine medieval turned woodware. In Proc. ICOM Comm Conserv l0th Trienn Meet. Washington, DC, pp 257–261

Hoffmann P, Peek R-D, Puls JSE (1986) Das Holz der Archäologen (in German). Holz als Roh-und Werkst 44:241–247

Hoffmann P (1986) On the Stabilization of Waterlogged Oakwood with PEG. II. Designing a Two-Step Treatment for Multi-Quality Timbers. Stud Conserv 31:103–113

Horie V (2010) Materials for Conservation, Organic consolidants, adhesives and coatings. Butterworth-Heinemann, London

Hung TM, Cuong TD, Kim JA, Tae N, Lee JH, Min BS (2014) Cassaine diterpene alkaloids from *Erythrophleum fordii* and their anti-angiogenic effect. Bioorganic Med Chem Lett 24:168-172

Imamura H. (1989) Contribution of extractives to wood characteristics. In: Rowe JW (eds) Natural products of woody plants. Springer series in wood science. Springer, Berlin, Heidelberg, pp 843-860

Jacobson A (2006) Diffusion of chemicals into green wood. PhD Thesis. Georgia Institute of Technology, Atlanta, USA

Jensen P, Gregory DJ (2006) Selected physical parameters to characterize the state of preservation of waterlogged archaeological wood: A practical guide for their determination. J Archaeol Sci 33:551–559

Jensen RL, Botfeldt K, Jensen, JB, Lanchot VJ, Stratkvern K (2007) On treatments for swelling of dried-up waterlogged archaeological wood. In: Proc 10th ICOM Work Gr Wet Org Archaeol Mater, Amsterdam, pp 639–651

Jiachang C, Donglang C, Jingen Z, Xia H, Shenglong C (2009) Shape recovery of collapsed archaeological wood ware with active alkali-urea treatment. J Archaeol Sci 36:434–440

Jingran G, Jian L, Jian Q, Menglin G (2014) Degradation assessment of waterlogged wood at Haimenkou site. Frat ed Integrita Strutt 30:495–501

Jingran G, Jian Q, Menglin G (2014) Degradation assessment of waterlogged wood at Haimenkou site. Frat. ed Integrita Strutt. 30, 495–501

Jones D, Brischke C (2017) Performance of bio-based building Materials. Woodhead Publishing Series in Civil and Structural Engineering. United Kingdom

Kawahara Y, Endo R, Kimura T (2002) Conservation Treatment for Archaeological Waterlogged Woods using Keratin from Waste. J Text Eng 48:107–110

Kaye B (1995) Conservation of waterlogged archaeological wood. Chem Soc Rev 24:35–43

Kim H, Ralph J, Akiyama T (2008) Solution-state 2D NMR of ball-milled plant cell wall gels in DMSO-d_6. Org Biomol Chem 1:56-66

Kim JS, Singh AP, Wi SG, Koch G, Kim YS (2008) Ultrastructural characteristics of cell wall disintegration of *Pinus* spp. in the windows of an old Buddhist temple exposed to natural weathering. Int Biodet Biodeg 61: 194–198

Kim NH (2005) An investigation of mercerization in decayed oak wood by a white rot fungus (*Lentinula edodes*). J Wood Sci 51:290-294

Kohdzuma Y (2004) Characteristics of waterlogged woods. National Research Institute for Cultural Properties, Nara, Japan

Koshijima T, Watanabe T (2003) Association between lignin and carbohydrates in wood and other plant tissues. Springer-Verlag Berlin Heidelberg

Koyani RD, Rajput KS (2014) Light microscopic analysis of Tectona grandis L.f. wood inoculated with *Irpex lacteus* and *Phanerochaete chrysosporium*. Eur J Wood Wood Prod 72:157-164

Labbé D (2011) A short history of urban and regional development in the Red river delta, University of British Columbia, Canada

Li Y, Akiyama T, Yokoyama T, Matsumoto Y (2016) NMR assignment for Diaryl ether structures (4−O−5 structures) in Pine wood lignin. Biomacromolecules 17:1921–1929

Ling L (2009) Unearthed archaeological wooden relics: generation, reply and permanent fixture. Scientific Res. China's Cult Reli 2:53–55

Macchioni N (2003) Physical characteristics of the wood from the excavations of the ancient port of Pisa J Cult Herit 4:85–89

Mahajan S (2011) Characterization of the white-rot fungus *Phanerochaete carnosa* through Proteomic methods and compositional analysis of decayed wood fibre. PhD thesis, University of Toronto, Canada

Martínez AT, Rencoret J, Nieto L, Jiménez-Barbero J, Gutiérrez A, Del Río JC (2011) Selective lignin and polysaccharide removal in natural fungal decay of wood as evidenced by in situ structural analyses. Environ Microbiol 13:96-107

Mchale E, Steindal CC, Kutzke H, Benneche T, Harding S.E (2017) *In situ* polymerisation of isoeugenol as a green consolidation method for waterlogged archaeological wood. Sci Rep 7:46481

Morgós A, Imazu S, Ito K (2015) Sugar conservation of waterlogged wood archaeological finds in the last 30 years. In: Conserv Digit. National Maritime Museum in Gdańsk, pp 15–20

Mortensen, M.N., 2009. Stabilization of polyethylene glycol in archaeological wood. PhD thesis, Technical University of Denmark, Denmark

Mtui W, Nokes SE (2014) Lignocellulolytic enzymes from tropical fungi: Types, substrates and applications. Sci Res Essays 7(15):1544-1555

Nan LI, Fang YU, Shi-shan YU (2004) Triterpenoids from *Erythrophleum fordii*. Acta Bot Sin 46:371-374

National Research Institute of Cultural Heritage (2012) Conservation of Wooden Objects. National Research Institute of Cultural Heritage, Daejeon, Korea

Nilsson T, Rowell R (2012) Historical wood - structure and properties. J Cult Herit 13S:S5–S9

Nishimura H, Sasaki M, Seike H, Nakamura M, Watanabe T (2012) Alkadienyl and alkenyl itaconic acids (ceriporic acids G and H) from the selective white fungus *Ceriporiopsis subvermispora*: A new class of metabolites initiating ligninolytic lipid peroxidation. Org Biomol Chem 10:6432-6442

Nishimura H, Yamaguchi D, Watanabe T (2017) Cerebrosides, extracellular glycolipids secreted by the selective lignin-degrading fungus *Ceriporiopsis subvermispora*. Chem Phys Lipids 203:1-11

Nuopponen MH, Wikberg HI, Birch GM, Jääskeläinen AS, Maunu SL, Vuorinen T, Stewart D (2006) Characterization of 25 tropical hardwoods with Fourier transform infrared, ultraviolet resonance raman, and ^{13}C-NMR cross-polarization/magic-angle spinning spectroscopy. J App Pol Sci 102:810–819

Olek W, Majka J, Stempin A, Sikora M, Zborowska M (2016) Hygroscopic properties of PEG treated archaeological wood from the rampart of the 10th century stronghold as exposed in the Archaeological Reserve Genius loci in Poznań (Poland). J Cult Herit 18:299–305

Oliveira LS, Santana ALBD, Maranhão CA, Miranda RDCM, Lima VLAG, Silva SI, Nascimento MS, Bieber L (2010) Natural resistance of five woods to *Phanerochaete chrysosporium* degradation. Int Biodeterior Biodegrad 64:711-715

Onuorach EO (2000) The wood preservative potentials of heartwood extracts of *Milicia excelsa* and *Erythrophleum suaveolens*. Bioresour Technol 75:171–173

Pandey KK, Pitman AJ (2003) FTIR studies of the changes in wood following decay by brown-rot and white-rot fungi. Int Biodeterior Biodegradation 52:151–160

Pearson C (1987) Conservation of marine archaeological objects. Butterworth Co Ltd., London

Pelit H, Yalçın M (2017) Resistance of mechanically densified and thermally post-treated pine sapwood to wood decay fungi. J Wood Sci 63:514–522

Phuong DQ, Faylona MGPG, Parry D (2009) A conservation perspective on the Ba Dinh archaeological Site. Bull. Indo-Pacific Prehistory Assoc. 29, 61–67.

Phuong DQ, Groves D (2004) Hanoi's built environment: Village culture and external imprints - some observations by a local and a tourist, in: The 2nd international conference on Vietnamese studies, Ho Chi Minh city, Vietnam.

QD 2198-CN (1997) Classification of Vietnamese timber (in Vietnamese). Ministry of Agriculture and Rural Development, Vietnam

Qu J, Hu YC, Yu SS, Chen XG, Li Y (2006) New cassaine diterpenoid amides with cytotoxic activities from the bark of *Erythrophleum fordii*. Planta Medica 72:442-449

Ralph J, Marita JM, Ralph SA, Hatfield RD, Lu F, Ede RM, Peng J, Quideau S, Helm RF, Grabber J, Kim H, Jimenez-Monteon G, Zhang Y, Jung HJG, Landucci L, MacKay J, Sederoff R, Chapple C, Boudet A (1999) Solution-state NMR of lignins. In: Argyropoulos DS (ed) Advances in lignocellulosics characterization. TAPPI Press, Atlanta, pp 55–108

Reinprecht L (2016) Wood deterioration, protection and maintenance. Wiley Blackwell, London

Rencoret J, Marques G, Gutiérrez A, Nieto L, Santos JI, Jiménez-Barbero J, Martínez AT, Río JC (2009) HSQC-NMR analysis of lignin in woody (*Eucalyptus globulus* and *Picea abies*) and non-woody (*Agave sisalana*) ball-milled plant materials at the gel state. Holzforschung 63:691-698

Reynolds ES (1963) The use of lead citrate at high pH as an electron-opaque stain in electron microscopy. J Cell Biol 17:208–212

Robertson MB, Packer KJ (1996) Diffusion of D_2O in archaeological wood measured by ^{1}D NMR Profiles. Appl Magn Reson 17:49–64

Rodgers BA (2004) The archaeologist's manual for conservation, A guide to non-toxic, minimal intervention artifact stablization. Kluwer Academic Publishers, New York

Rowell RM, Barbour RJ (1990) Archaeological wood: Properties, chemistry and preservation. Adv Chem Series 225. Am Chem Soc, Washington DC

Rowell R (1984) The chemistry of solid wood, American Chemical Society. Washington DC

Rowell RM (2005) Handbook of wood chemistry and wood composites, CRC Press Taylor & Francis Group

Salanti A, Zoia L, Tolppa EL, Giachi G, Orlandi M (2010) Characterization of waterlogged wood by NMR and GPC techniques. Microchem. J. 95, 345–352

Sandström M, Jalilehvand F, Persson I, Gelius U, Frank P, Hall-Roth I (2002) Deterioration of the seventeenth-century warship Vasa by internal formation of sulphuric acid. Nature 415, 893–897

Schindelholz E, Blanchette R, Held B, Jurgens J, Cook D, Drews M, Hand S, Seifert B (2009) An evaluation of supercritical drying and PEG/freeze drying of waterlogged archaeological wood. In Proc. 10th ICOM Gr Wet Org Archaeol Mater Conf Amsterdam, pp 399–416

Schmidt O (2006) Wood and tree fungi: Biology, damage, protection, and use. Springer-Verlag, Germany

Schwanninger M, Rodrigues JC, Pereira H, Hinterstoisser B (2004) Effects of short-time vibratory ball milling on the shape of FT-IR spectra of wood and cellulose. Vib Spectrosc 36:23-40

Schwarze FWMR (2007) Wood decay under the microscope. Fungal Biol Rev 21:133-170

Schweingruber FH (2007) Wood structure and environment. Springer-Verlag Berlin

Schweizer F, Houriet C, Mas M (1984) Controlled air drying of large Roman timber from Geneva. In Proc. 2nd ICOM Waterlogged wood working Gr. Conf.; Centre d'Etude et de Traitement Les Bios Gores d'Eau Waterlogged Wood; Grenoble. pp. 327–346

Shaozhi Z, Yu P, Dongp L, Youming Z, Guangming C, Heng L (2016) A thermophysical study on the freeze drying of wooden archaeological artifacts. J Cult Herit 17:95–101

Shim H, Xiang X, Karina M, Indrarti L, Yudianti R and Uyama H (2016) One-dimensional shrinkage and swelling of crosslinked bacterial cellulose gel. Chem Lett 45:253–255

Sjostrom E, Alen R (1999) Analytical methods in wood chemistry, pulping, and papermaking. Springer-Verlag Berlin Heidelberg

Skyba O, Douglas CJ, Mansfield SD (2013) Syringyl-rich lignin renders poplars more resistant to degradation by wood decay fungi. Appl Environ Microbiol 79(8):2560-2571

Smith CW (2003) Archaeological conservation using polymers. Texas A&M University Press, USA

Spurr AR (1969) A low-viscosity epoxy resin embedding medium for electron microscopy. J Ultrastruct Res 26:31-43

Takano M, Hayashi N, Nakamura M, Yamaguchi M (2009) Extracellular peroxidase reaction at hyphal tips of white-rot fungus *Phanerochaete crassa* WD1694 and in fungal slime. J Wood Sci 55:302–307

Takayasu K (2004) An introduction to the conservation science of archaeological relics. National Research Institute for Cultural Properties, Nara, Japan

Tamblyn NE (1985) Treatment of wood by diffusion. In: Findlay W.P.K. (eds) Preservation of timber in the tropics. Forestry Sci, vol 17. Springer, Dordrecht

Tanaka S, Seki M, Miki T, Shigematsu I, Kanayama K (2015) Solute diffusion into cell walls in solution-impregnated wood under conditioning process I: Effect of relative humidity on solute diffusivity. J Wood Sci 61:543–551

Tanaka S, Seki M, Miki T, Umemura K, Kanayama K (2017) Solute diffusion into cell walls in solution-impregnated wood under conditioning process III: effect of relative humidity schedule on solute diffusion into shrinking cell walls. J Wood Sci 63: 263–270

TAPPI (1998) Standard methods for Acid-insoluble lignin in wood and pulp. T222 Om-98. TAPPI Press, Atlanta, USA

TAPPI (1998) Acid-insoluble lignin in wood and pulp. T222 om-98. TAPPI Press, Atlanta, USA

TAPPI (1999) Water solubility of wood and pulp. T207cm-99. TAPPI Press, Atlanta, USA

TAPPI (1999) Alpha-, beta- and gamma-cellulose in pulp. T203C. TAPPI Press, Atlanta, USA

TAPPI (2007) Solvent extractives of wood and pulp. T204C. TAPPI Press, Atlanta, USA

TAPPI (2011) Holocellulose in wood. T9m-54. TAPPI Press, Atlanta, USA

Tarkow H, Feist WC, Southerland CF (1966) Interaction of wood with polymeric materials penetration verus molecular size. Forest Prod J 16 (10): 61-65

Tejedor CC (2010) Re-conservation of wood from the seventeenth-century swedish warship the Vasa with alkoxysilanes: a re-treatment study applying thermosetting elastomers. PhD Thesis. Texas A&M University.

Thang NX, Tri BM (2016) Archaeological findings under excavation of the Parliament building (in Vietnamese). Social Sciences Publishing House, Hanoi

Thompson R, 2005. The chemistry of wood preservation. Woodhead publishing limited, England

Tri BM (2005) Thang Long Imperial Citadel Site, An archaeological report (in Vietnamese). In the 2nd Asian academy heritage management field school, Hanoi

Tri BM, Tin TT (2006) The Imperial Citadel of Thang Long (in Vietnamese). The Cultural and Information publishing house, Hanoi

Tri BM, Tin TT (2010) Thang Long - History of the thousand years (in Vietnamese). The Cultural and Information publishing house, Hanoi

Tsao CC, Shen YC, Su CR, Li CY, Liou MJ, Dung NX, Wu TS (2008) New diterpenoids and the bioactivity of *Erythrophleum fordii*. Bioorganic Med Chem Lett 16:9867-9870

Tsujiyama S (2001) Differential scanning calorimetric analysis of the lignin-carbohydrate complex degraded by wood-rotting fungi. J Wood Sci 47:497-501

UNESCO (2013) Preservation of the cultural heritage complex of Thang Long-Ha Noi

Unger A, Schniewind A, Unger W (2001) Conservation of wood artifacts. Springer-Verlag, Berlin Heidelb

Unger W, Unger A (1995) On the bioresistance of waterlogged wood impregnated with sucrose. Mater und Org 29:231–240

Uzielli L (2007) Wood science for conservation of cultural heritage. Proc Int Conf held by COST Action IE0601 Florence, Italy

Vinden P (1983) Preservation treatment of wood by diffusion processes. PhD Thesis. University of London, England

Vuong TQ, Long NV (1977) Hanoi from prehistory to the 19th century (in Vietnamese). Vietnamese Stud 48:9–57

Walsh Z, Janeček ER, Jones M, Scherman OA (2017) Natural polymers as alternative consolidants for the preservation of waterlogged archaeological wood. Stud Conserv 62(3):173–183

Wilcox WW (1970) Anatomical changes in wood cell walls attacked by fungi and bacteria. Bot Rev 36:1-28

Wittköpper M (1998) Der aktuelle Stand der Konservierung archäologischer Naßhölzer mit Melamin/Aminoharzen am Römisch-Germanischen Zentralmuseum (in German). Arbeitsblätter für Restaur Grup 8 Holz H, pp 277–282

Xiang X, Shim H, Uyama H (2016) Dimensionally heterogeneous swelling-shrinkage behaviors of bacterial cellulose-crosslinked poly (acrylic acid) nanocomposite sheet. In: 23rd Annu Meet Cellul Soc Japan, p 143

Yue F, Lu F, Ralph S, Ralp J (2016) Identification of $4{-}O{-}5$-Units in softwood lignins via definitive lignin models and NMR. Biomacromolecules 17:1909–1920

Zabell RA, Morrell JJ (1992) Wood Microbiology, Decay and its Prevention. Academic Press, New York, USA

Zhigang Z, Junjie G, Er S, Jie Z, Jianmin X (2012) Natural distribution, endangered mechanism and conservation strategy of an endangered tree species,

Erythrophleum fordii Oliv. In: Asia and the Pacific workshop - Multinational and transboundary conservation of valuable and endangered forest tree species. IUFRO Headquarters, Vienna, Austria, pp. 113–116

Zoia L, Salanti A, Orlandi M (2015) Chemical characterization of archaeological wood: Softwood Vasa and hardwood Riksapplet case studies. J Cult Herit 16:428–437

Acknowledgments

members of Research Institute of Forest Industry, Vietnamese Academy of Forest Sciences for giving valuable supports during my overseas study.

I would like to express my sincere thanks to the Ministry of Education, Culture, Sports, Science and Technology of Japan (MEXT) for providing the scholarship. The study would not have been possible without appropriate sample material, and I would like to thank the Thang Long Research Center, Hanoi and the Institute of Archaeology, Vietnam Academy of Science and Technology for providing the archaeological wood materials.

Last but not least, I would like to thank my wonderful family for going through this with me; who have continued encouragement and endured far more than should have been necessary during my overseas study./

To all, again, my sincerest thanks.

List of Publications

1. **Nguyen Duc Thanh**, Keita Sakakibara, Yoshinobu Tsujii, Yohsei Kohdzuma, Junji Sugiyama (2017) Shrinkage and swelling behavior of archaeological waterlogged wood treated with crosslinked sodium polyacrylate, Journal of Wood Science, Volume 64, Issue 3, pp 294–300.

2. **Nguyen Duc Thanh**, Hiroshi Nishimura, Tomoya Imai, Takashi Watanabe, Yohsei Kohdzuma, Junji Sugiyama (2018) Natural durability of the culturally and historically important timber - *Erythrophleum fordii* wood against white-rot fungi, Journal of Wood Science, Volume 64, Issue 3, pp 301–310.

3. **Nguyen Duc Thanh**, Yohsei Kohdzuma, Rie Endo, Junji Sugiyama (2018) Evaluation of chemical treatments on dimensional stabilization of archaeological waterlogged hardwoods obtained from the Thang Long Imperial Citadel site, Vietnam, Journal of Wood Science. Volume 64, Issue 4, pp 436–443.

4. **Nguyen Duc Thanh**, Soichiro Wakiya, Kazutaka Matsuda, Bui Duy Ngoc, Junji Sugiyama, Yohsei Kohdzuma (2018) Diffusion of chemicals into archaeological waterlogged hardwoods obtained from the Thang Long Imperial Citadel site, Vietnam, Journal of Wood Science, Volume 64, Issue 6, pp 836–844.